Simulating the effects of land-surface change on southern Africa's climate

Neil Campbell MacKellar

Thesis Presented for the Degree of

DOCTOR OF PHILOSOPHY

in the Department of Environmental and Geographical Science

UNIVERSITY OF CAPE TOWN

November 2007

ABSTRACT

Regional Climate Model (RCM) experiments, using the MM5 model, are undertaken to investigate the potential climatic impacts of land-surface change in southern Africa. Simulations are first run to assess the RCM's sensitivity to perturbed initial soil moisture conditions. Following a disturbance in initial soil moisture, it is found that latent heat fluxes in the subsequent months are significantly affected in certain regions, but there is little effect on sensible heat flux and near-surface temperature. There is also no noticeable impact on regional circulation or precipitation. This implies that, for the magnitude of the initial soil moisture disturbance, soil moisture-rainfall coupling in the model is weak.

Further MM5 integrations are performed to assess potential climatic impacts of altering the vegetation of southern Africa from an estimated natural state to present-day conditions. Contemporary vegetation cover is given by the United States Geological Survey land surface classification, and an estimated pristine state is simulated using the Sheffield Dynamic Global Vegetation Model. For three simulated periods: 1 Aug - 28 Feb 1988/89, 1991/92 and 1995/96, significant impacts on mean Sep-Nov (SON) and Dec-Feb (DJF) surface climate arise from the change in vegetation. The most notable result is cooling over large parts of the continent in SON, which gives rise to increased large-scale subsidence and decreased moisture convergence. Resultant decreases in rainfall cause a hydrological feedback through reduced latent heat flux which mitigates the initial cooling and weakens the subsidence anomaly in DJF. The subsidence anomalies extend as high 500 hPa, which has important implications for regional moisture transport over southern Africa.

The role of synoptic forcing in modifying the atmosphere's response to land surface change is explored using a self-organizing map (SOM). The SOM is used to identify archetypal patterns in the large-scale 850 and 500 hPa geopotential height and precipitable water fields in the reanalysis data that cover the same domain and force the RCM at its lateral boundaries. For each of the patterns (nodes) identified in these variables by the SOM, the mean RCM-simulated response to vegetation change is evaluated. Conditions characterized by strong sub-tropical anticyclones and low atmospheric moisture show the greatest temperature and geopotential height changes and are most sensitive to changes in radiative fluxes, whereas precipitation and surface hydrological processes are more sensitive under conditions of weak subsidence and high levels of atmospheric moisture.

PREFACE

Although a large volume of research has been directed towards understanding how changes in land-surface characteristics can affect atmospheric processes, southern Africa has received little attention in this regard. Knowledge of the extent to which vegetation and soil moisture influence the climate of the region can lead to an improved understanding of the causes of inter-annual and intra-seasonal variability. This will in turn contribute towards improved seasonal forecasting and further insight into the impacts of long term climatic change. This thesis therefore aims to advance understanding of land-atmosphere interactions in southern Africa by undertaking a series of numerical simulations using a Regional Climate Model (RCM).

Part I of the thesis gives a review of the literature relevant to this topic and defines the aims of the study. The experimental work that forms the basis of this thesis is presented as three manuscripts that have been submitted to journals for peer review. Part II is a paper entitled "Effects of perturbed initial soil moisture conditions on MM5 simulations of southern African climate", which has been submitted to *Theoretical and Applied Climatology*. This aims to address how strongly the climate of southern Africa as simulated by an RCM responds to a disturbance in initial soil moisture. This gives an indication of potential biases that may be introduced to subsequent model simulations from uncertainties in soil moisture initialization. Part III consists of a paper entitled "Simulated effects of anthropogenic vegetation change on southern Africa's summer climate", which has been submitted to the *International Journal of Climatology*. It firstly presents a procedure to estimate a pristine vegetation state for southern Africa based on simulations by a dynamic vegetation model. A set of RCM simulations is then undertaken aimed at exploring the potential atmospheric response to a shift in vegetation from the estimated pristine state to present-day conditions. Part IV is a manuscript entitled "Synoptic-based evaluation of climatic response to vegetation change over southern Africa", also submitted to *International Journal of Climatology*. This extends the analysis of the model simulations of Part III by evaluating the results in terms of prevailing large-scale circulation. Part V summarizes and synthesizes the findings of the three experimental sections.

In keeping with the requirements of a Ph.D. thesis, the contribution of the second and third authors to the three submitted journal articles is of a supervisory nature. All model simulations, data analysis and generation of figures were done by the first author. The manuscripts were written entirely by the first author, except where comments and clarifications suggested by the other authors have been incorporated.

ACKNOWLEDGEMENTS

There are many people to thank for their assistance and support in carrying out this work. I am most grateful to Bruce Hewitson for endless ideas, enthusiasm and encouragement and Mark Tadross for invaluable input and criticism. For their assistance with the SDGVM model and for useful discussions, I thank Gill Drew, Ian Woodward, Mark Lomas and Guy Midgley. I thank Filippo Giorgi and the Abdus Salaam International Centre for Theoretical Physics for facilitating my participation in regional climate modelling workshops. The Water Research Commission, National Research Foundation and BIOTA Southern Africa are credited for financial support.

The staff and students at the Climate Systems Analysis Group at the University of Cape Town have provided an exceptionally enjoyable environment in which to work. In particular Chris Jack and Jeremy Main must be thanked for their help with all computer-related issues, and Sharon Barnard for making sure I could always pay the rent on time.

And finally, for patience, support and understanding, I'd like to thank Leoné.

CONTENTS

PART I

BACKGROUND

1.1 Introduction

Vegetation and soil water content are two key factors affecting energy and moisture exchange at the earth's surface. Vegetation modifies the reflectance (albedo) of the surface to incoming solar radiation, determines the aerodynamic roughness of the surface and acts as a conduit for transferring water from sub-surface soil layers to the atmosphere. Similarly, the availability of water in the soil profile is a limiting factor in determining plant transpiration and direct evaporation from the soil surface, which controls how available energy is partitioned into latent and sensible heat components. Soil moisture can also affect the albedo of soil surfaces, as wet soil tends to be darker than dry soil. Such effects on surface properties have implications for radiation, heat, momentum and moisture budgets, which in turn exert forcing on local atmospheric processes and can potentially influence regional and large-scale circulation.

The close association between vegetation and soil moisture, and their effects on climate, makes the study of these two factors intimately linked. In nature, however, it is practically impossible to decouple fully the components of the land-atmosphere system for isolated examination, and thereby gain an in-depth understanding of the complex interplay between these components. To address this problem, numerical models provide an indispensable research tool in which individual parameters or processes can be perturbed to investigate their role in the system. Highly sophisticated atmospheric models have been developed over the past few decades in the form of General Circulation Models (GCMs) and Regional Climate Models (RCMs). In addition, detailed representations of land-surface hydrology and biospheric processes have evolved and have been coupled to these atmospheric models. However, although these models are extremely useful, they are by no means perfect, and experimental results are often greatly influenced by choice of model and its configuration. There is therefore still considerable uncertainty regarding land surface-climate interaction, leading to ongoing research in this field.

Although the topic of land-atmosphere interaction has received much global attention recently, very little work has focussed on southern Africa. Many gaps still exist in current understanding of the region's climate, but the role of the land surface has been

1.1 Introduction

Vegetation and soil water content are two key factors affecting energy and moisture exchange at the earth's surface. Vegetation modifies the reflectance (albedo) of the surface to incoming solar radiation, determines the aerodynamic roughness of the surface and acts as a conduit for transferring water from sub-surface soil layers to the atmosphere. Similarly, the availability of water in the soil profile is a limiting factor in determining plant transpiration and direct evaporation from the soil surface, which controls how available energy is partitioned into latent and sensible heat components. Soil moisture can also affect the albedo of soil surfaces, as wet soil tends to be darker than dry soil. Such effects on surface properties have implications for radiation, heat, momentum and moisture budgets, which in turn exert forcing on local atmospheric processes and can potentially influence regional and large-scale circulation.

The close association between vegetation and soil moisture, and their effects on climate, makes the study of these two factors intimately linked. In nature, however, it is practically impossible to decouple fully the components of the land-atmosphere system for isolated examination, and thereby gain an in-depth understanding of the complex interplay between these components. To address this problem, numerical models provide an indispensable research tool in which individual parameters or processes can be perturbed to investigate their role in the system. Highly sophisticated atmospheric models have been developed over the past few decades in the form of General Circulation Models (GCMs) and Regional Climate Models (RCMs). In addition, detailed representations of land-surface hydrology and biospheric processes have evolved and have been coupled to these atmospheric models. However, although these models are extremely useful, they are by no means perfect, and experimental results are often greatly influenced by choice of model and its configuration. There is therefore still considerable uncertainty regarding land surface-climate interaction, leading to ongoing research in this field.

Although the topic of land-atmosphere interaction has received much global attention recently, very little work has focussed on southern Africa. Many gaps still exist in current understanding of the region's climate, but the role of the land surface has been

largely neglected by efforts to address this. There is therefore a need to investigate land-atmosphere interaction in southern Africa in order to gain a more complete understanding of the region's climate. The contribution of the land surface to intra-seasonal and inter-annual variability in southern Africa is not yet known, but antecedent land-surface conditions are potentially useful predictors in seasonal forecasting applications. This is particularly relevant in a region that is heavily dependant on agriculture. Furthermore, the land surface can also have a modulating effect on long-term climatic change, which is an important consideration when assessing both historical and projected future climate changes.

The following section presents a review of previous modelling studies of land-atmosphere interaction. Given the vast amount of research that has been conducted, this review is by no means exhaustive, but it provides an overview of the major themes that have been explored and what important results have emerged. This puts into context the objectives and aims of this thesis, which are presented thereafter.

1.2 Simulation of land-atmosphere interaction

1.2.1. Desertification and deforestation

The pioneering work in simulating land surface-atmosphere interactions is largely attributed to J.G. Charney, who undertook a number of numerical studies in the 1970s to investigate the effect of surface albedo change on atmospheric circulation and precipitation. The region of interest for this work is the West African Sahel, which had been experiencing a protracted drought since the late 1960s. With a 2-dimensional, zonally-symmetric model of the atmosphere over West Africa, Charney (1975) suggested that if a lack of rainfall reduces vegetation cover, the albedo of the land surface will be increased, thereby upsetting the radiation balance of the region. More incoming shortwave radiation will be reflected, thus cooling the surface and promoting subsidence in the overlying atmosphere. This increase in stability will inhibit convective activity and cause a further reduction in rainfall. In this way a positive feedback loop is established, thus contributing to the severity of the drought. Employing a more complex GCM, Charney *et al.* (1977) extended this theory by taking into consideration the effects of atmospheric moisture transport and cloud formation.

Here the albedo-induced cooling was to some degree compensated for by an increase in incident shortwave solar radiation caused by reductions in moisture convergence, convective activity and cloud formation. Another consequence of reduced cloud cover, however, is a reduction in the downward flux of longwave radiation, so the net change in radiation absorbed at the surface was still found to be negative.

Subsequent GCM simulations have supported this albedo feedback mechanism (eg. Sud and Fennessey, 1982; Laval and Picon, 1986), but these early experiments are limited by numerous caveats. For example, the only land surface parameter examined is albedo. Factors such as roughness length and plant transpiration were not considered and the land surface representation in the models used was highly simplified. Furthermore, the magnitude of the enforced albedo change tends to be considerably greater than observed change (Fuller and Ottke, 2002). Given these limitations, the early experiments nevertheless provided a base on which more comprehensive studies have been built.

Following the development of more complex land surface models, Xue and Shukla (1993) studied the sensitivity of the Sahel to desertification. In addition to albedo, other vegetation parameters such as roughness length, leaf area index and minimum stomatal resistance were altered simultaneously. Surface temperature was shown to increase by 0.5 °C on average and rainfall decreased by 22%. In addition to direct local effects of the land-surface change, it was established that the African Easterly Jet and West African monsoon were also affected, which has important implications for rainfall in the region. Similar results were obtained by specifying the same land-surface perturbation, but applying longer simulations (Xue, 1997). The increase in surface temperature and decrease in summer precipitation in this case were comparable to observed climate changes from the 1950s to the 1980s, although the simulated land-surface change did not necessarily represent true land-surface degradation for the period. For a more accurate estimate of observed changes in the Sahelian land surface, Taylor *et al.* (2002) employed a detailed model to estimate past and future vegetation change due to human land use practices. GCM simulations were run using three land-surface states, representing the years 1961, 1996 and 2015. Relative to the 1961 simulation, rainfall

was shown to decrease by 4.6% (0.15 mm day^{-1}) in 1996 and 8.7% (0.28 mm day^{-1}) in 2015. The simulated changes were smaller than the recently observed rainfall decrease, indicating that vegetation change is not the primary driver of precipitation change in the region, but can, however, significantly modify variability induced by sea surface temperatures (SSTs).

Whilst Taylor *et al.* (2002) forced a GCM with land-surface changes due to anthropogenic causes, Claussen (1997) investigated a two-way interaction between climate and natural vegetation. Rather than applying a persistent forcing, this approach tests the coupled climate-vegetation system to perturbations in the initial distribution of vegetation. Applying a large and unrealistic disturbance in initial vegetation (i.e. exchanging desert with tropical vegetation and vice versa) led to a new equilibrium vegetation state in which vegetation cover over certain desert regions was enhanced compared to current conditions. The mechanisms responsible for maintaining these conditions were consistent with Charney's hypothesis. Further studies of interactive coupling were done by Wang and Eltahir (2000a,b). A zonally symmetric atmospheric model was synchronously coupled to a dynamic vegetation model and was used to investigate multiple equilibrium states in the land-atmosphere system of West Africa. The theory proposed that if the biosphere-atmosphere system is disturbed from an equilibrium state, the system may respond in one of three ways: a negative feedback leading to full recovery; a positive feedback leading to an enhancement of the original disturbance; or a negative feedback leading to partial recovery. The latter two situations hence result in new equilibrium states. It was shown that a one-off reduction in forests would at first cause a large decrease in precipitation, but the system would eventually return to the original equilibrium. Desertification simulations in the grassland region showed more sensitivity. Depending on the magnitude of grassland removal, the system would either return to its original state, or tend towards one of two new equilibria. An initial increase in grass density would always result in a return to the control state, regardless of the magnitude of the perturbation. Although these studies explore the dynamic climate-vegetation system, they do not take into account persistent perturbations, such as those resulting from human disturbance. Furthermore they do not account for internal climate variability driven by SSTs, which may inhibit the transition between vegetation states. The question of inter-annual variability was investigated by

Zeng and Neelin (2000), who established that feedbacks resulting from land surface change resulted in a strong spatial gradient between desert and forest regions. However, when inter-annual SST variations were included, this gradient was smoothed out, creating an intermediate grass-like vegetation state. This can be seen as an important factor in the distribution of the African savannas.

As well as desertification in semi-arid regions such as the Sahel, tropical deforestation has received much attention in land-atmosphere sensitivity studies, particularly for the Amazon Basin. Expansion of grassland and cropland at the expense of trees increases surface albedo, greatly reduces roughness length and decreases plant rooting depth. The climatic effects of such changes have been investigated in numerous modelling studies. Dickinson and Henderson-Sellers (1988) undertook a GCM sensitivity study whereby the Amazon tropical forest was uniformly replaced by grassland. The simulations showed decreases in total evapotranspiration (ET) and canopy interception. Surface temperatures increased by up to 4 °C, but there was no systematic change in rainfall. A similar experiment done by Nobre *et al.* (1991) resulted in a 2.5 °C increase in mean surface temperature, 30% decrease in ET, 25% decrease in precipitation and a 20% decrease in runoff for the region. In a follow-on experiment to Dickinson and Henderson-Sellers (1988), Pitman *et al.* (1993) highlighted how choice of GCM, experimental configuration and length of simulation can yield quite different results. For example, compared to the results of Dickinson and Henderson-Sellers (1988), Pitman *et al.* (1993) showed a temperature increase of only 0.7 °C and a large precipitation decrease of 603 mm yr^{-1}. Other tropical deforestation experiments showing reduced precipitation and increased temperature of varying magnitude include those of Lean and Warrilow (1989), Lean and Rowntree (1993) and Hahmann and Dickinson (1997).

Some studies have investigated the relative importance of selected vegetation parameters in deforestation. For example, Polcher and Laval (1994) ran a GCM experiment in which the tropical forests of the Amazon, Africa and Indonesia were replaced by grassland, but roughness length was not altered. The experiment produced reduced evaporation and increased soil temperature. An increase in moisture

convergence, and hence precipitation, was also found. This is in contrast to similar experiments (eg. Lean and Warrilow, 1989; Shukla *et al.*, 1990; Hoffman and Jackson 2000), which indicate a reduction in moisture convergence resulting from decreased roughness length. Dirmeyer and Shukla (1994) performed simulations of Amazon deforestation with different prescribed albedos. Four-year control and deforestation experiments were run, with albedo given as unchanged, increased by 0.06 and increased by 0.09. As the albedo anomaly increased, the precipitation was seen to decrease. Relatively small changes in ET suggested moisture convergence was a controlling factor for the precipitation anomalies. Considering the impact of deforestation on large-scale circulation, Zeng *et al.* (1996) proposed a feedback mechanism analogous to El Niño-Southern Oscillation (ENSO). It was hypothesized that deforestation of the Amazon basin could weaken the Walker circulation over the Amazon-Atlantic region and result in reductions in moisture convergence and precipitation. A model sensitivity experiment showed that an increase in albedo of 0.05 would support this hypothesis.

More recent studies have revisited the deforestation issue with the benefit of improved models (particularly land-surface schemes) and increased computing capacity to run longer simulations. Voldoire and Royer (2004) took a similar approach to the previous work and, although similarities exist, the results differed in many respects to previous experiments. An interesting outcome of the study is that mean annual surface temperature showed no significant change between the control and deforested states, but changes in the diurnal temperature range were apparent: minimum daily temperature decreased while maximum daily temperature increased. Relationships with inter-annual variability were also evident, particularly an enhanced atmospheric response to deforestation during dry El Niño events. Semazzi and Song (2001) ran a GCM deforestation experiment for Africa, whereby tropical rainforest was replaced by savanna grassland. Over the deforested region rainfall decreased by 2-3 mm day^{-1} for the dry season (July-September) and less than 1 mm day^{-1} for the wetter seasons. Surface and ground temperatures changed by up to 2.5 and 5 °C respectively. Of further interest is a teleconnection to regions in southern Africa. Rainfall decreased over Mozambique and increased over Botswana, Zambia and parts of the DRC and South Africa. This was explained by the alteration of trapped Rossby wave trains formed by mid-tropospheric latent heat release over the tropical forest region.

Atmospheric response to the conversion of tropical savanna to grassland was investigated by Hoffman and Jackson (2000). Five regions of moist (i.e. greater than 600-700 mm annual rainfall) savanna were considered: the llanos (northern South America), the Brazilian cerrado, and the savannas of northern Africa, southern Africa and northern Australia. The result of the changed land surface was to reduce mean annual precipitation by 8-13% in all but the northern African regions. Mean annual ET was reduced by 8-10% in all regions. Since rainfall in the northern African savanna was largely unaffected, the reason for the decrease in ET was attributed to energy availability, rooting depth and conductance, rather than moisture availability. For all regions except northern Africa, a reduction in moisture convergence was implied. From an intra-seasonal perspective, dry-spell frequency in the middle of the wet season was shown to increase in the Southern Hemisphere regions for the grassland scenario. Mean annual surface air temperature increased by 0.4-1.0 °C for most of the affected area. Additional sensitivity experiments for albedo, roughness length and rooting depth were carried out to determine the relative importance of each of these parameters. It was found that albedo and roughness length played approximately equal roles in the reduction of rainfall, whereas rooting depth had little effect. Overall, a positive feedback loop between reduced vegetation cover and reduced precipitation was supported.

1.2.2. Historical land cover change

The intention of experiments such as those reviewed above is primarily to test the sensitivity of the climate to large, uniform changes in land surface conditions. In most cases the changes applied are of unrealistic magnitude and homogeneity. This approach is useful for identifying the important atmospheric processes associated with land surface change, but the magnitude of the response is typically overestimated. This is illustrated by the different results obtained by Xue (1997) and Taylor *et al.* (2002). The former study used an idealized land-surface change and the magnitude of the climate response was found to be comparable to observed change for the period considered. The latter, however, used more realistic representations of the Sahelian land surface, which produced a much smaller climatic response.

Evaluation of the likely atmospheric impact of historical changes in vegetation distribution has been the subject of a number of modelling studies. For the conterminous United States, Copeland *et al.* (1996) tested the difference between RCM simulations using a current land-surface state versus a potential natural vegetation distribution. They note that since the change is not uniform, the response of surface energy and moisture balances differs according to location. Regional temperature changes were of the order of 1-2 °C warmer or cooler, whilst the average for the domain was a slight increase (0.05 °C) for current versus natural conditions. Rainfall showed a general increase of 5-10% in the present-day scenario. A similar experiment, this time using a GCM, was conducted by Bonan (1997). In contrast to the results of Copeland *et al.* (1996), Bonan (1997) found temperature to decrease significantly (up to 2 °C in magnitude) over the central United States. This was attributed in part to the coarse GCM resolution being unable to resolve important local scale processes over the Great Plains. Cooling over the Great Plains was also found by Baidya Roy *et al.* (2003), who investigated three land cover scenarios, representing the years 1700, 1910 and 1990. It was noted that local effects on climate could not be explained by changes in the land-surface parameters alone, and advective processes were important considerations. A more localized RCM study was done by Marshall *et al.* (2004), who simulated climatic changes induced by land-use change in the Florida peninsula. It was found that altered surface energy fluxes caused an increase in the diurnal temperature range, and regional circulation was disrupted such that the sea breeze circulation was weakened. This resulted in an overall decrease in rainfall associated with the sea breeze fronts. The simulated changes in rainfall and daily maximum temperature were shown to be comparable to observed historical changes.

In RCM simulations for Australia, Narisma and Pitman (2003) show significant changes in surface heat fluxes and temperature, as well as alteration of surface winds and precipitation, resulting from land cover change. It is argued that such effects have contributed to regional temperature increases observed in the 20th century. Narisma *et al.* (2003) extended this work by evaluating the importance of biospheric feedbacks in land cover change experiments. Here the RCM used incorporated a dynamic vegetation component that simulated plant response to changes in CO_2 and climate factors. It was concluded that the inclusion of biospheric feedbacks significantly moderated the effects

of land-surface change.

Maynard and Royer (2004a) compared the relative impacts of vegetation change in tropical Africa and climate change due to increased greenhouse gas (GHG) concentrations. They found that GHG-induced climate change was locally modified by altered vegetation state and that GHG forcing and land surface forcing tended to have the opposite effect on ET. They also concluded that the vegetation changes were of insufficient magnitude to induce any significant changes in large-scale circulation.

1.2.3. Soil moisture

Early numerical studies of the influence of soil moisture on subsequent rainfall were undertaken by Shukla and Mintz (1982), Rind (1982) and Yeh *et al.* (1984). The consensus from these is that large, uniform reductions in soil moisture, and hence ET, resulted in increased surface temperatures and decreased rainfall. This supports a positive feedback mechanism between soil moisture and rainfall.

The role of soil moisture in modulating the Asian summer monsoon was investigated by Meehl (1994). A number of different GCMs and different combinations of parameterization schemes were used to simulate the respective roles of external forcing (manifested in this case by changes in albedo) and internal feedback mechanisms (i.e. soil moisture). In all the model experiments it was found that a strong monsoon, initiated by strong land-sea temperature contrast, was further strengthened by a positive soil moisture feedback. Conversely, weaker monsoons were further weakened by a dry land surface. In contrast, Douville *et al.* (2001) found that persistently elevated soil moisture in the Indian sub-continent led to some local enhancement of rainfall, but in general this positive feedback was compensated for by reduced large-scale moisture convergence. The Sahel, however, was shown to be highly sensitive to soil moisture conditions and a positive feedback was demonstrated.

In contrast to the positive feedback found in the majority of soil moisture sensitivity studies, New *et al.* (2003) and Cook *et al.* (2006) demonstrated with different models

that a negative feedback may exist between soil wetness and precipitation over southern Africa. The most important consequence of disturbed soil moisture was a change in horizontal moisture convergence initiated by changes in surface heating. For a wet soil state, increased latent and decreased sensible heat flux caused the overlying air to cool, thus creating large scale subsidence and surface divergence. This anomalous divergence caused a reduction in moisture flux convergence which resulted in decreased rainfall.

The ability of soil moisture to enhance extreme hydrological conditions has received much attention. Two events that have been of particular interest are the severe drought experienced by much of the central United States in 1988, and widespread flooding in the Upper Mississippi Basin in 1993. Atlas *et al.* (1993) investigated the respective roles of SSTs and soil moisture anomalies on the 1988 drought. They found that SSTs alone for that year caused a reduction in rainfall, but no significant change in temperature. When the observed soil moisture deficit for that year was included, the rainfall reduction was enhanced and surface temperature was significantly increased. Paegle *et al.* (1996) used an RCM to evaluate the role of surface evaporation in the flood of 1993. It was concluded that the low-level jet, transporting large amounts of moisture into the Mississippi Basin from the Gulf of Mexico, was enhanced not by increased local evaporation from a wet soil, but by increased buoyancy induced by sensible heating over a dry soil. RCM simulations carried out for both the drought and flood events by Giorgi *et al.* (1996) showed that soil moisture feedbacks were minor when compared to large-scale forcing. Their results were in agreement with Paegle *et al.* (1996) and showed that increased surface heating caused by reduced evaporation resulted in more buoyant air, which supported convection and led to a negative feedback. A similar experiment by Pal and Eltahir (2001), however, showed contrasting results by supporting a positive soil moisture-precipitation feedback. They showed that the magnitude of precipitation anomalies was proportional to the magnitude of the initial soil moisture disturbance. It was also concluded that a dry initial soil state resulted in a greater rainfall response than a wet initial soil. This suggests that soil moisture will have a more pronounced effect during a drought than for a flood event. Focusing on the 1998 Oklahoma-Texas drought, Hong and Kalnay (2000) showed that dry soil contributed to the persistence of the drought through a positive feedback.

Seneviratne *et al.* (2006) demonstrated the important contribution of soil moisture-atmosphere interaction to climate variability over Europe. Comparing RCM simulations in which the hydrological cycle was fully interactive to simulations whereby soil moisture was a prescribed boundary condition revealed that as much as two-thirds of the variance in summer precipitation over parts of Europe was due to land-atmosphere coupling. Given this high sensitivity, soil moisture has been implicated as an important mechanism contributing to the European summer heatwave of 2003. Fischer *et al.* (2007) indicated that the 2003 spring soil moisture was well below the climatological mean, and RCM simulations suggested that the extreme summertime temperature anomalies could have been reduced by about 40% if soil moisture was close to climatological values.

Recent work has been undertaken to determine whether improved soil moisture initialization in GCM seasonal predictions can improve forecast skill. Ensembles of multi-year GCM simulations by Koster and Suarez (2003), Dirmeyer (2005) and Kanae *et al.* (2006) agree that improved initial soil wetness only increases the potential predictability of rainfall over small parts of the globe. These regions tend to be semi-arid, where the sensitivity of precipitation to local evaporation is high. One of the reasons why these experiments revealed weak responses when compared to other sensitivity studies is that the magnitude of the initial soil moisture anomalies in the former tends to be relatively small. For instance, the difference between a "poor" and an "improved" estimate of soil moisture is likely to be considerably smaller than an observed state versus uniform saturation or desiccation. However, during extreme events, soil water content may indeed approach the extreme values used in sensitivity studies, so the effects are more pronounced. As suggested by Hong and Kalnay (2000) and Ferranti and Viterbo (2006), it therefore seems that in the case of predicting persistent drought conditions, soil moisture becomes a critical factor.

1.3 Aims of the thesis

From the reviews above it is clear that both vegetation and soil moisture can significantly influence climatic processes. There is good consensus between modelling experiments that increased albedo causes surface cooling and subsequent decreases in moisture convergence and precipitation. Less clear, however, are the impacts of ET, as influenced by both plant transpiration and soil moisture; experimental results support both positive and negative feedback loops between ET and rainfall. It is clear that surface roughness is an important control of turbulent exchanges at the surface, but its regional-scale effects are still uncertain, with both positive and negative influences on moisture convergence being demonstrated. Results vary as a function of experimental design, choice of modelling system, magnitude of the land-surface perturbation and region of interest.

The uncertainties that remain ensure that there are many avenues for further research. The climatic impacts of historical land-surface change present a particularly relevant theme. Whether or not land-use change can alter the climate of southern Africa is a critical question in understanding the mechanisms responsible for climatic change and variability in the region. Even if not a primary driver of such change, land-atmosphere interaction can significantly modify climate variations forced by such factors as changes in ocean circulation and atmospheric chemistry. This has implications for inter-annual and intra-seasonal variability and improved understanding of this can contribute to seasonal forecasting efforts in the region. Studies addressing the impacts of historical land-cover change have been undertaken for the United States, Australia and tropical and west Africa, but no such work has evidently been done for southern Africa. The primary objective of this thesis is therefore to take an initial step towards quantifying the likely response of southern African climate to a change in vegetation from a pristine state to present-day conditions. This will provide a first-order estimate of the magnitude of any regional climatic changes brought about by anthropogenic land-surface modification.

The steps taken to address this involve producing a representation of potential natural

vegetation using a dynamic vegetation model and incorporating this into an RCM. RCM simulations are then performed using this natural land surface and also for a present-day land surface to reveal how seasonal and monthly mean climate may respond to altered land cover. A further consideration that has been alluded to in some land-atmosphere studies, but not addressed fully, is the role of synoptic forcing. An extension of the analysis of the modelling experiments therefore aims to evaluate how large-scale circulation may influence the climate's sensitivity to land-surface change. This will give an indication of how land-atmosphere interactions may be influenced by inter-annual variability and long-term climatic change.

Although vegetation change is the dominant theme here, soil moisture is an important consideration as it can result in feedbacks that contribute to the RCM's internal variability. Further simulations are therefore undertaken to reveal how sensitive the modelling system is to perturbations in initial soil moisture. This can give an indication of biases that may affect the outcome of the land-surface change experiments. Although this is a secondary theme, it is presented first (Part II) as it provides a background to how sensitive the model is to hydrological feedbacks.

The specific aims of the thesis can therefore be summarized as follows:

- evaluate the sensitivity of an RCM to initial soil moisture and consequent hydrological feedbacks;
- produce an estimate of pristine vegetation using a dynamic vegetation model and incorporate this into the RCM;
- compare RCM simulations for the natural vegetation and for present-day vegetation to establish a) whether or not this change in land surface has a noticeable impact on southern Africa's climate and b) if so, what are the dominant mechanisms responsible for this;
- compare atmospheric response to the land-surface change under different synoptic conditions to establish how climate sensitivity to land-surface change differs under different large-scale circulation.

These four points provide the basis for the work presented in this thesis. Part II addresses the role of soil moisture and hydrological feedbacks, Part III describes the simulations of potential natural vegetation and investigates the climate's response to vegetation change, and Part IV extends the analysis of Part III by exploring the role of large-scale circulation in land-atmosphere interaction. Part V summarizes and synthesizes the outcomes of these experiments.

PART II

MODEL SENSITIVITY TO SOIL MOISTURE

Effects of perturbed initial soil moisture conditions on MM5 simulations of southern African climate

Neil C. MacKellar and Mark A. Tadross

Abstract: MM5 simulations of the 1991/92 austral summer are undertaken to evaluate the sensitivity of southern Africa's climate to a disturbance in initial soil moisture. A perturbation in soil moisture of a magnitude and spatial variability that is within the bounds of uncertainty in soil moisture representation for the region is applied to the initial conditions of a series of MM5 simulations. For simulations initialized at the beginning of November 1991, it is found that latent heat fluxes in subsequent months are significantly affected in certain regions, but there is little effect on sensible heat flux and near-surface temperature and no noticeable impact on regional circulation or precipitation. This implies that soil moisture-rainfall coupling in the model is weak. Regional differences in the persistence of the soil moisture anomaly and its impact on surface climate are apparent, but the disturbances typically dissipate within the first one to two months of the simulations. Spatial correlations between the initial soil moisture anomaly and subsequent monthly mean rainfall further suggest weak coupling between antecedent soil moisture and local precipitation. Compared to the November-initialized simulations, runs initialized at the beginning of August 1991 show a stronger persistence in the effects of the soil moisture anomaly because of lower rainfall rates in the late-winter early-summer months.

2.1 Introduction

Variability in near-surface climate is influenced substantially by soil moisture-atmosphere interaction (Seneviratne *et al.*, 2006). Accurate initialization of soil moisture in climate modelling studies is therefore necessary to reduce potential biases that may result from an over- or underestimation of initial soil water content. Positive or negative feedbacks can result from a perturbed initial soil moisture state, which will respectively enhance or mitigate the initial disturbance. These feedbacks may impact on the model's simulation of surface energy and moisture fluxes, which can in turn affect near-surface temperature and precipitation. An understanding of the potential feedbacks that may result from uncertainties in initial soil wetness is necessary when engaging in climate model experiments.

Numerous modelling studies undertaken for North America and Europe support a positive feedback mechanism linking soil moisture and rainfall (eg. Atlas *et al.*, 1993; Schär *et al.*, 1999; Hong and Kalnay, 2000; Pal and Eltahir, 2001; Kim and Wang, 2007). This feedback operates in such a way that increased moisture availability at the surface causes increased evaporation, which raises the moisture content of the planetary boundary layer (PBL). This acts to increase moist static energy (MSE) within the PBL, which promotes the formation of deep convective systems, hence increasing precipitation and enhancing the initial soil moisture anomaly. An increase in evaporation at the surface will also lead to reduced sensible heat flux, which reduces PBL temperature and MSE. However, this effect tends to be outweighed by the increase in MSE due to increased latent heat flux (Pielke and Zeng, 1989; Pal and Eltahir, 2001). Furthermore, since reduced sensible heat flux reduces the depth of the PBL, MSE per unit mass within the PBL increases (Eltahir, 1998; Pal and Eltahir, 2001). The opposite processes operate for a dry initial soil state, but the response is asymmetric, with a stronger feedback associated with negative soil moisture anomalies (Pal and Eltahir, 2001; Kim and Wang, 2007). Confirming the results of theoretical modelling studies with observational evidence is, however, difficult due to a lack of extensive soil moisture measurements and the inability to accurately separate soil water and precipitation measurements in the real world. Nevertheless, some empirical linkages have been shown to support the positive feedback theory (eg. Findell and

Eltahir, 1997; Taylor, *et al.*, 1997).

Alternatively, a negative feedback may occur whereby surface cooling caused by high soil moisture and consequent reduction in sensible heat flux promotes increased atmospheric stability. This acts to suppress convection and reduce precipitation. Conversely, dry soil and increased sensible heating leads to more buoyant air, which promotes convective activity. In the presence of sufficient moisture, this will increase precipitation, as was shown for the Mississippi Basin by Peagle *et al.* (1996) and Giorgi *et al.* (1996). Furthermore, the surface cooling associated with anomalously wet soil can result in large-scale subsidence and anomalous anticyclonic circulation, which inhibits large-scale moisture convergence. This has been demonstrated for southern Africa by New *et al.* (2003) and Cook *et al.* (2006). Both hypotheses therefore imply changes in atmospheric circulation, either through convergence and uplift, or through divergence and subsidence. A negative feedback was also demonstrated by Georgescu *et al.* (2003) in response to an anomalous spatial gradient in initial soil moisture across the Mississippi Basin. In this case, changes in precipitation were attributed to alterations in circulation and atmospheric moisture transport, which acted to restore the imposed surface wetness gradient.

It has been shown that both the magnitude and timing of an initial soil moisture perturbation will affect the resulting atmospheric response. Pal and Eltahir (2001) note a non-linear relationship between the magnitude of the initial anomaly and latent heat flux, with the highest sensitivity occurring between 25% and 50% of soil saturation. Below and above this range, wilting point and potential evaporation become respective limiting factors. Another factor affecting feedbacks is timing in the seasonal cycle. Conditions favourable for convective activity (i.e. summer) often exhibit greater responses to perturbations (Findell and Eltahir, 1997; Pal and Eltahir, 2001; Kim and Wang, 2007), but initial anomalies in early spring can persist and induce a precipitation response in later months (Kim and Wang, 2007). Regional climatic characteristics also affect atmospheric sensitivity to soil moisture. There is a weak relationship between latent heat flux and precipitation in arid regions because of low MSE and a high lifting condensation level (Guo *et al.*, 2006). Humid regions, where moisture availability is not a limiting factor and evaporation is controlled more by radiation, also exhibit weak responses to changes in soil moisture. It is therefore the transitional zones, typically

semi-arid regions that are characterized by relatively humid, but conditionally unstable conditions that are most sensitive (Schär *et al.*, 1999; Guo *et al.*, 2006; Kanae *et al.*, 2006). The persistence of anomalously dry soils, however, is greatest in arid regions because low input of water limits the extent to which such a deficit can be mitigated (Dirmeyer, 2005, 2006).

A further consideration for numerical experiments is the choice of model used to simulate the hydrological cycle. The strength of coupling between land and atmosphere varies according to the climate model used (Koster *et al.*, 2006; Guo *et al.*, 2006). Different parameterization approaches, particularly for PBL processes and moist convection will contribute to these discrepancies.

Given current understanding of soil moisture-climate interactions, this paper explores specific questions concerning soil moisture initialization in regional climate simulations over southern Africa. It is known that large changes in soil moisture can affect surface energy fluxes and precipitation, but it is unclear how uncertainties in the initialization of soil moisture affect the seasonal evolution of the simulated climate. Global observations of soil moisture are generally sparse, with those in southern Africa being particularly poor. Gridded reanalysis products present estimates that are often used to initialize Regional Climate Model (RCM) experiments, but accurately portraying soil moisture is directly affected by large biases in precipitation as well as inaccuracies in modelling regional hydrology. Furthermore, reanalysis soil moisture fields do not necessarily represent the same sub-surface levels or ranges of soil wetness as the RCM. In the context of RCM experiments, an important consideration is how this uncertainty in soil moisture initialization is likely to affect the outcome of the simulations.

This study investigates the sensitivity of southern Africa's summer climate to perturbed antecedent soil moisture conditions, as simulated by an RCM. The initial perturbation applied represents the difference between a reanalysis soil moisture field and one that is simulated by the RCM for that same time. This is therefore within the scope of uncertainty in representing soil moisture within the region. This paper seeks to understand whether such uncertainty may potentially have a significant impact on climate modelling and seasonal forecasts in the region. Furthermore, since the perturbation is not artificially uniform, it gives an indication of what feedbacks may

result from a "realistic" disturbance in soil moisture conditions at the beginning of the summer season.

2.2 Method

2.2.1 Model configuration

The RCM used in this study is the fifth-generation Pennsylvania State University-National Center for Atmospheric Research Mesoscale Model (MM5; Grell *et al.*, 1994). The model domain covers sub-equatorial Africa, including Madagascar, at a horizontal grid resolution of 50 km and 23 vertical sigma-levels. PBL physics are represented by the MRF PBL scheme (Hong and Pan, 1996) and precipitation by the Betts-Miller convective adjustment scheme (Betts and Miller, 1993). This configuration was shown by Tadross *et al.* (2005) to be appropriate for the current domain and resolution. Atmospheric initial conditions, lateral boundary conditions and sea-surface temperatures are taken from the National Centers for Environmental Prediction-National Center for Atmospheric Research (NCEP-NCAR) reanalysis (Kalnay *et al.*, 1996). The atmospheric model is coupled to the NOAH land-surface scheme (Chen and Dudhia, 2001a,b). NOAH consists of 4 soil layers and a single plant canopy layer. Three layers occupy the upper 1 m of the soil profile and represent the root zone, and a deep storage layer extends below this to a depth of 2 m.

2.2.2 Model simulations

MM5 simulations are run to test the sensitivity of the model to the same perturbation in initial soil moisture at a) the beginning of Nov and b) the beginning of Aug. Two sets of simulations are carried out, named NOV_INIT and AUG_INIT. Each set consists of 3 pairs of MM5 integrations. Each pair consists of 2 simulations initialized on the same date, but using different initial soil moisture conditions. For NOV_INIT, the three pairs are initialized on 1, 2 and 3 Nov 1991 and run through to 28 Feb 1992. The differences in atmospheric fields between the initial dates introduce perturbations that can contribute to the RCM's internal variability (see Giorgi and Bi, 2000; Christensen *et al.*, 2001; Caya and Biner, 2004), so by using these different starting dates we account for some of the noise associated with the RCM's internal variability. For the NOV_INIT

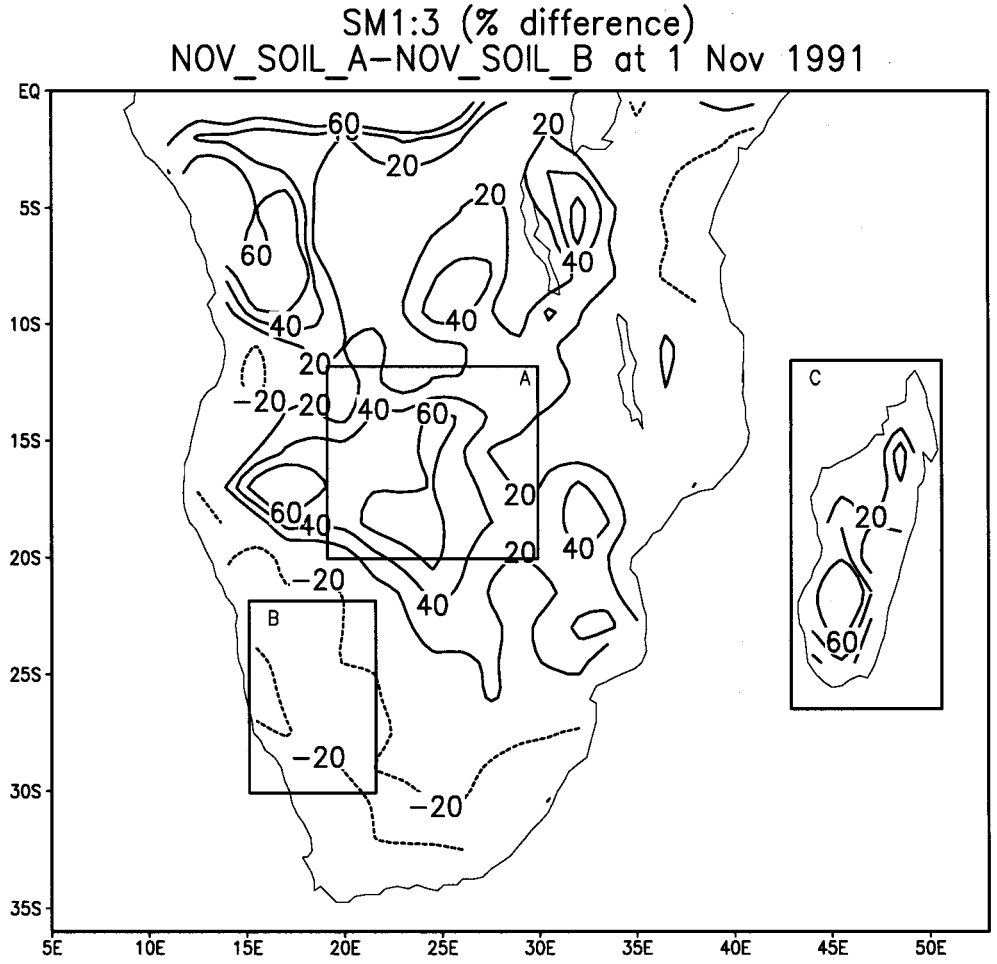

Figure 2.1: Percentage difference in initial soil moisture in layers 1 to 3 between NOV_SOIL_A and NOV_SOIL_B. Boxes denote regions discussed in Section 3.2: CENT (A), SW (B) and MAD (C).

simulations the first member of each pair, irrespective of starting date, takes its initial soil moisture from the NCEP-NCAR reanalysis as at 1 Nov 1991, whereas the second member takes initial soil moisture from the 1 Nov conditions of a separate MM5 integration initialized on 1 Aug 1991. These two initial soil moisture fields are named, respectively, NOV_SOIL_A and NOV_SOIL_B. For AUG_INIT, three pairs of simulations are initialized on 1, 2 and 3 Aug 1991 and run through to 28 Feb 1992. Once again, three pairs of simulations are run to account for internal variability. The first member of each pair, irrespective of starting date, takes its soil moisture initial conditions from the NCEP-NCAR reanalysis at 1 Aug 1991 (hereafter AUG_SOIL_A).

The initial soil moisture conditions of the second pair (AUG_SOIL_B) represent the volumetric difference between NOV_SOIL_A and NOV_SOIL_B, imposed on AUG_SOIL_A. In this way the same volumetric soil moisture anomaly is applied at the start of both the NOV_INIT and AUG_INIT sets of simulations.

The 1991/92 summer season was characterized by strong El Niño conditions and widespread drought throughout much of southern Africa. Following previous work highlighting the role of land surface wetness in exacerbating drought conditions (eg. Hong and Kalnay, 2000; Pal and Eltahir, 2001), these dry conditions are likely to show a pronounced sensitivity to perturbed soil moisture. Test simulations for a season that experienced above average rainfall (1988/89) show that the 1991/92 period does indeed display a stronger response to perturbed soil moisture. Soil moisture-precipitation feedbacks tend to be strongest in mid-summer, when convective activity is at a maximum (Findell and Eltahir, 1997; Pal and Eltahir, 2001; Kim and Wang, 2007), but a soil moisture perturbation occurring in late winter or spring may persist into summer and cause a delayed feedback (Kim and Wang, 2007). The AUG_INIT set of simulations is run to test whether or not this is likely to occur in the chosen model configuration.

Figure 2.1 shows the percentage difference between NOV_SOIL_A and NOV_SOIL_B. Most of the central and northern parts of the continental domain and Madagascar show increased soil moisture in layers 1 to 3 (SM1:3) of over 20%, reaching up to and over 60% in places. The south-west and north-eastern regions show reduced SM1:3 of over 20%. Note the dry-wet gradient when moving from the arid south-western regions to the more humid central parts of the domain. This anomaly amplifies the existing climate gradients and its effects are discussed in Section 2.3.3. Also shown on the figure are boxes A, B and C which indicate archetypal regions of change from which data are extracted in later analyses.

2.2.3 Spatial anomaly correlations

As a simple measure of the influence of the initial soil conditions on the evolution of climate variables, spatial correlations r between the initial soil moisture anomaly and subsequent monthly anomalies are computed as

$$r = \frac{\sum_{i=1}^{imax}\sum_{j=1}^{jmax}\left|x_{i,j}-\bar{x}\right|\left|y_{i,j}-\bar{y}\right|}{\sqrt{\left[\sum_{i=1}^{imax}\sum_{j=1}^{jmax}\left|x_{i,j}-\bar{x}\right|^2\right]\left[\sum_{i=1}^{imax}\sum_{j=1}^{jmax}\left|y_{i,j}-\bar{y}\right|^2\right]}} \qquad (1)$$

where i, j, $imax$ and $jmax$ are the horizontal grid dimensions and their respective maxima; x is the monthly ensemble mean difference (between runs initialized with different soil moisture) of a selected variable, with the spatial mean of this difference for that month $\bar{x}$; and y is the difference between the two initial soil moisture fields in layers 1 to 3, with its spatial mean $\bar{y}$. This computation is applied to land-surface grid points only. The explained variance r^2 gives a measure of the degree to which a variable's monthly mean difference and the initial soil moisture anomaly share common spatial variance. This measure is useful for identifying the strength of the local effects of the initial soil moisture perturbation, but does not account for any changes in surface variables that result from circulation changes. In the latter case, spatial variability is not expected to be similar to that of the initial soil moisture disturbance. Furthermore, this only evaluates whether the pattern of the initial perturbation persists in the spatial form it started, it does not allow that it may change over time and still persist, but in a different spatial form.

2.3 Results

2.3.1 Mean monthly response

Monthly averages of the ensemble mean difference of NOV_SOIL_A-NOV_SOIL_B are shown in Figures 2.2-2.4, illustrating how spatial patterns of selected variables respond to the initial soil moisture perturbation. A *t*-test was performed on the ensemble mean daily time series for each grid point to give a measure of the strength of the anomaly compared to day-to-day variability. The test statistic was modified to account for serial correlation following the method of Zwiers and Von Storch (1996). Positive (negative) differences that are significant at the 95% level are shaded in light (dark) grey.

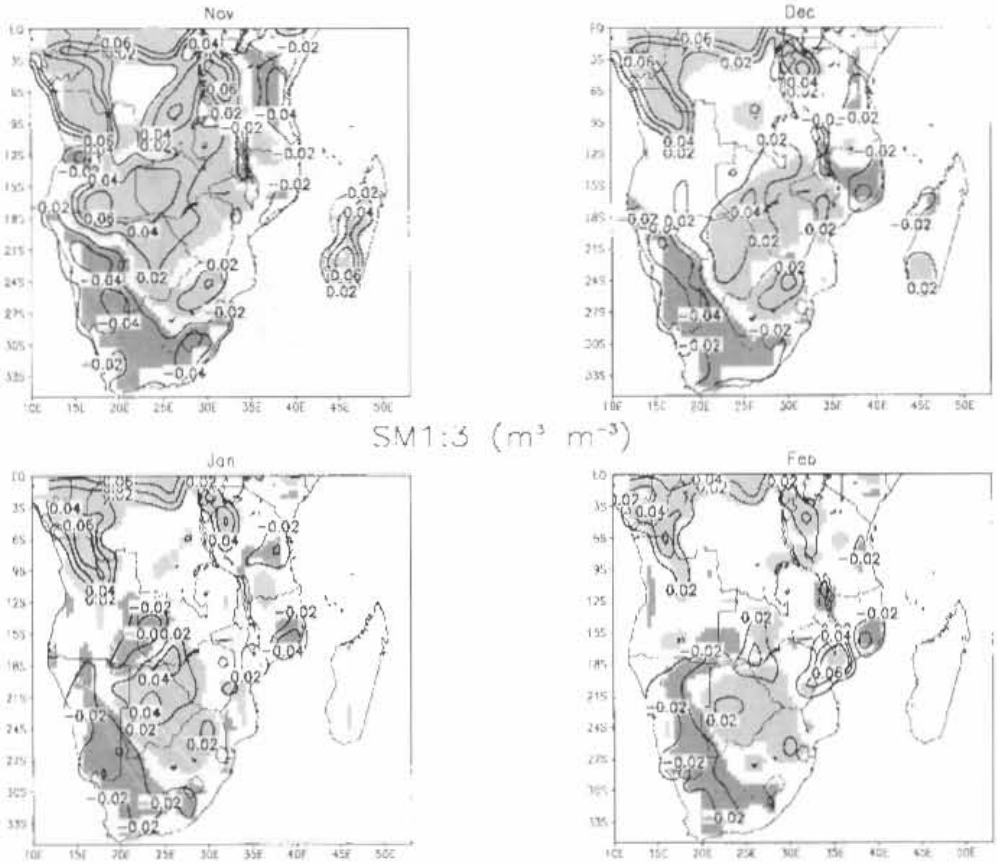

Figure 2.2: Monthly anomalies (NOV_SOIL_A ensemble mean minus NOV_SOIL_B ensemble mean) of soil moisture in layers 1:3. Light (dark) shading indicates positive (negative) anomalies significant at the 95% level.

The persistence of the soil moisture anomaly itself can be seen in Figure 2.2, which shows total volumetric soil water in the surface layer and the root zone (i.e. SM1:3). Nov anomalies closely match the initial perturbation, and strong persistence through the subsequent months is apparent south of 18 °S and in the north-western parts of the continental domain. The latter region is, however, close to the model boundary and is susceptible to spurious boundary effects in the RCM, such as rainfall being close to zero, which is clearly unrealistic for equatorial Africa. In the arid south-west, low rainfall rates ensure that insufficient water enters the soil to compensate for the initial deficit. The central parts of the continent see some persistence, but some large initial anomalies also dissipate very quickly. For example, initial increases of over 60% in

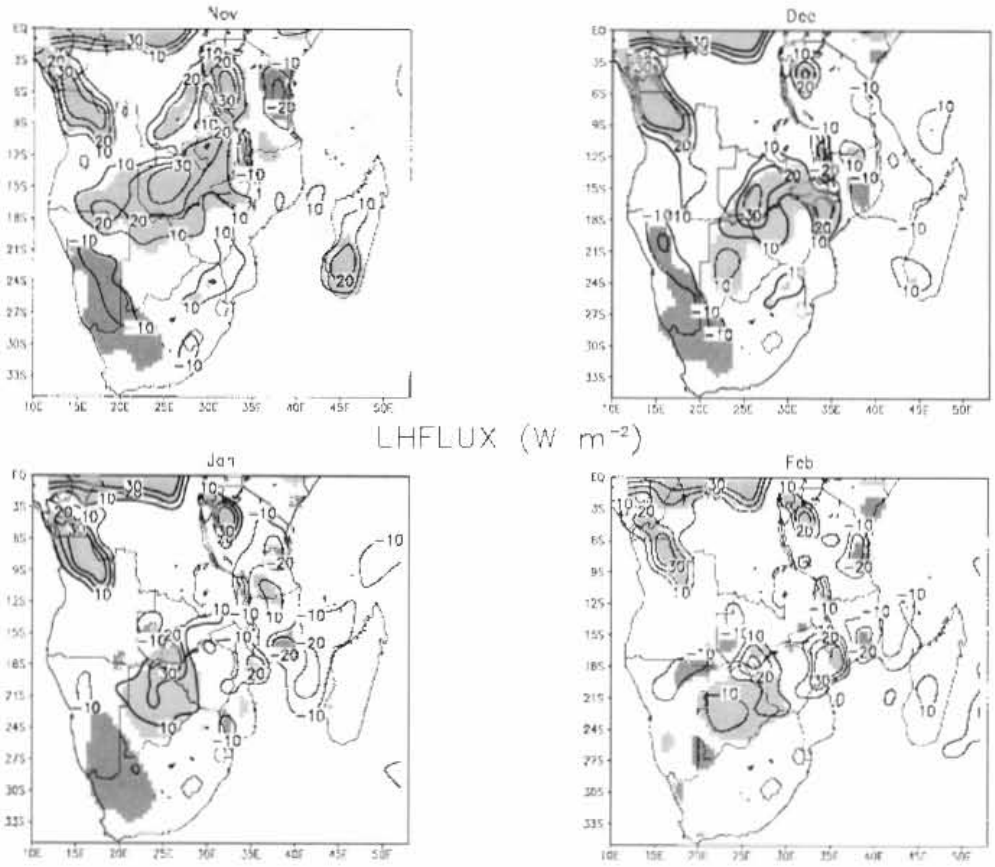

Figure 2.3: As per Figure 2.2, but for latent heat flux.

southern Angola are not evident in December. Madagascar also shows a rapid decrease in the strength of the anomaly.

Latent heat flux (Figure 2.3) significantly increases by more than 10 W m^{-2} in the centre of the continent during Nov. This is consistent with the SM1:3 anomalies and decreases in extent in the subsequent months. Significant negative anomalies occur in the south-west in Nov, Dec and Jan, but are not evident in Feb, which does not match the Feb SM1:3 conditions in this region. Since the vegetation here is predominantly shallow-rooted, the deeper soil layers do not contribute to transpiration and latent heat flux will be influenced by transpiration from the top soil layer and direct evaporation from the ground, rather than transpiration from sub-surface soil layers. The Feb moisture anomaly in the top soil layer (upper 10 cm) is in accordance with this, showing the initial deficit to have almost completely dissipated (not shown).

Despite the significant changes in latent heat, there is little significant change in sensible heat (not shown). Consequently, temperature at 2m (T2m; Figure 2.4) does not exhibit any significant anomalies aside from in the north-western extremities of the domain. Because of their proximity to the domain boundary and consequent susceptibility to boundary effects, these won't be discussed here. In Nov, decreases in T2m of over 0.5 °C in magnitude occur over parts of Angola, Zambia, the Democratic Republic of the Congo (DRC) and western Tanzania. This corresponds to the increased latent heat flux of over 10 W m^{-2} and decreased sensible heat flux of about 5 W m^{-2}. Latent (sensible) heat increases (decreases) of over 30 W m^{-2} (15 W m^{-2}) in western Zambia result in negative temperature anomalies greater than 1 °C in magnitude. As the latent heat flux anomalies weaken in the subsequent months, so the T2m response becomes more fragmented.

It is clear from the above that there is some relationship between the initial state of the soil and surface energy fluxes in subsequent months. For a further evaluation of the relative strength of this relationship we use r^2 as defined in Section 2.2.3. This gives a measure of the common variance shared by the spatial patterns of the initial SM1:3 anomaly and monthly mean anomalies of selected variables (Figure 2.5). Because of the spurious effects near the model boundary noted above, all grid cells north of 5 °S are discarded in the calculation of r^2. Of the variables shown, monthly SM1:3 anomalies, as expected, show the strongest relationship to their own initial state. The strength of the relationship decreases from r^2 >0.9 in Nov to <0.4 in Jan and Feb. Latent and sensible heat fluxes exhibit the next strongest correlation to the initial soil moisture disturbance, with r^2 decreasing from between 0.6 and 0.7 in Nov to <0.2 in Feb. T2m and the height of the PBL are linked to the initial soil moisture conditions via sensible heat flux and have r^2 values of ~0.5 for Nov, decreasing to ~0.2 in Dec. Changes in evaporation, as evident in latent heat flux, affect the humidity mixing ratio at 2m (Q2m). This has a relatively high sensitivity to the initial soil moisture in Nov (r^2 between 0.5 and 0.6), but the relationship rapidly weakens into Dec, most likely due to a higher proportion of Q2m being derived from moisture advection, rather that local evaporation, in the mid-summer months.

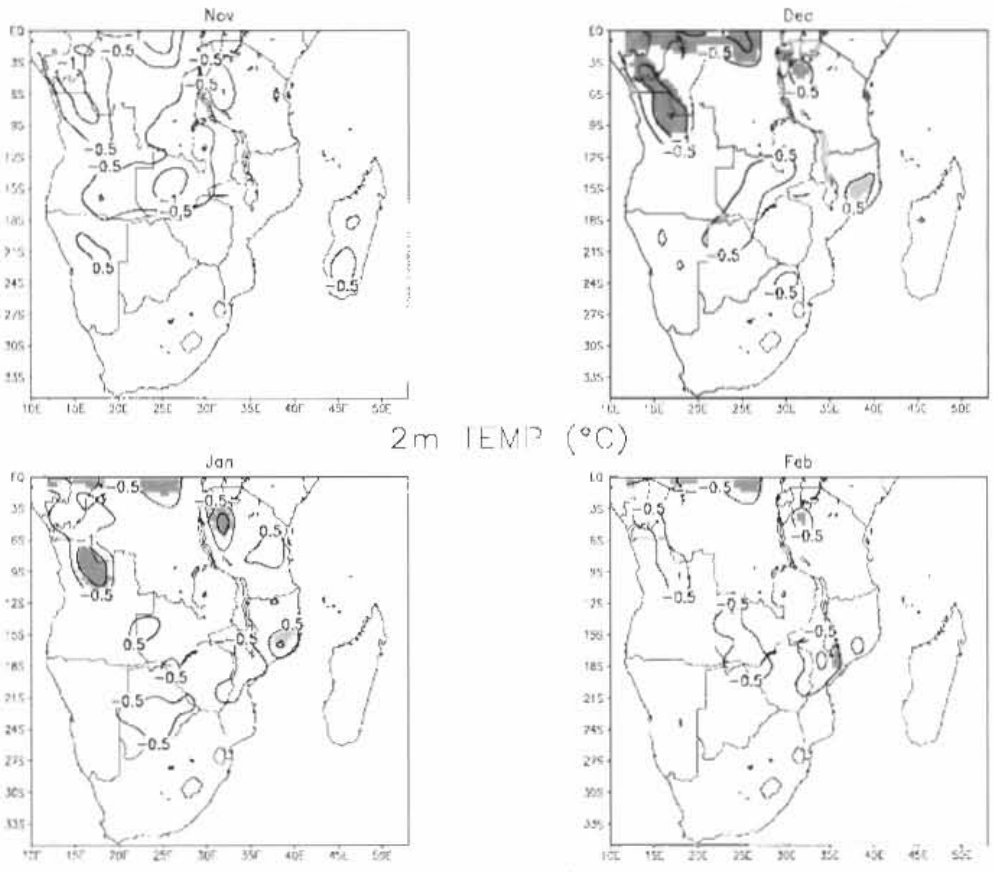

Figure 2.4: As per Figure 2.2, but for temperature at 2m.

The most notable result here is that there is no relationship between initial soil moisture and precipitation. This is a very important result which reveals that, for the full continental domain, there is little or no direct feedback between antecedent soil moisture and local precipitation. This is discussed further in the following sections.

2.3.2 Regional characteristics

Three areas have been selected to exemplify regional impacts of the soil moisture anomaly. These are denoted by the boxes in Figure 2.1 and represent a positive initial soil wetness perturbation in a humid region (CENT), a negative initial perturbation in an arid region (SW), and a positive perturbation in a climate strongly

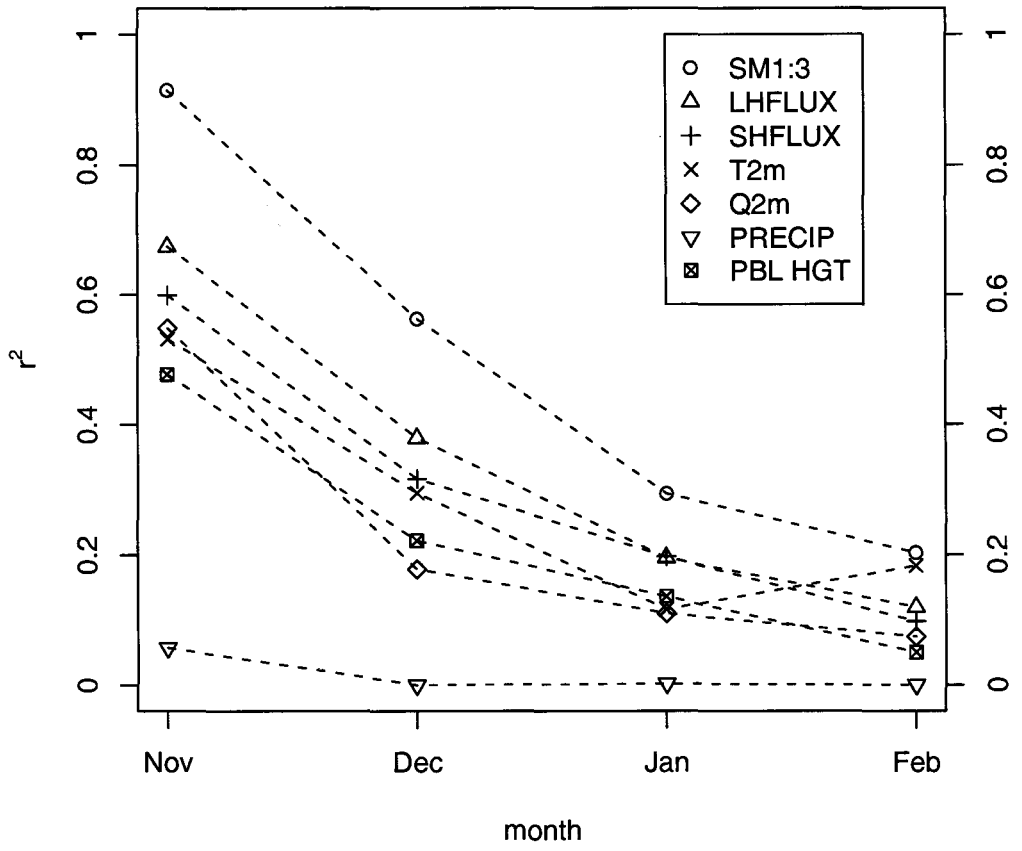

Figure 2.5: Common spatial variance between the initial soil moisture anomaly and monthly mean anomalies (NOV_SOIL_A ensemble mean minus NOV_SOIL_B ensemble mean) of soil moisture in layers 1 to 3 (circles), latent heat flux (triangle, apex up), sensible heat flux (+), temperature at 2m (×), humidity mixing ratio at 2m (◊), precipitation (triangle, apex down) and PBL height (box with cross).

influenced by moist maritime air (MAD). The daily evolution of selected area-averaged variables for these regions are presented in Figures 2.6-2.9. The broken lines are differences (NOV_A-NOV_B) for each of the three pairs of ensemble members and the solid line represents the ensemble mean anomaly.

The magnitude of the initial SM1:3 disturbances are similar for the three regions, but subsequent evolution is quite different (Figure 2.6). In CENT, the anomaly steadily

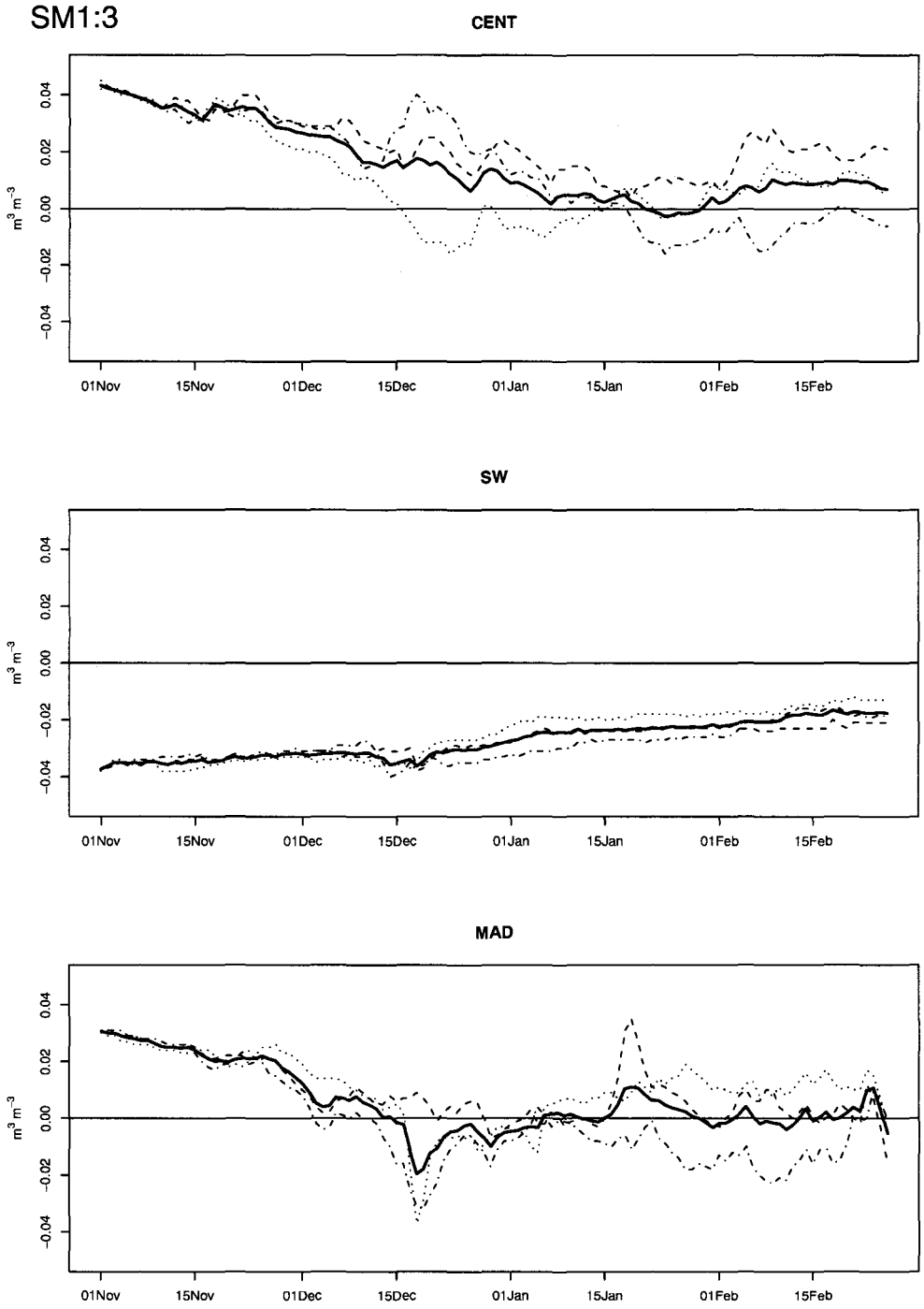

Figure 2.6: Area-averaged time-series of soil moisture in layers 1 to 3 for CENT, SW and MAD. Broken lines are differences (NOV_SOIL_A-NOV_SOIL_B) for each of the three pairs of ensemble members and the solid line represents the ensemble mean anomaly.

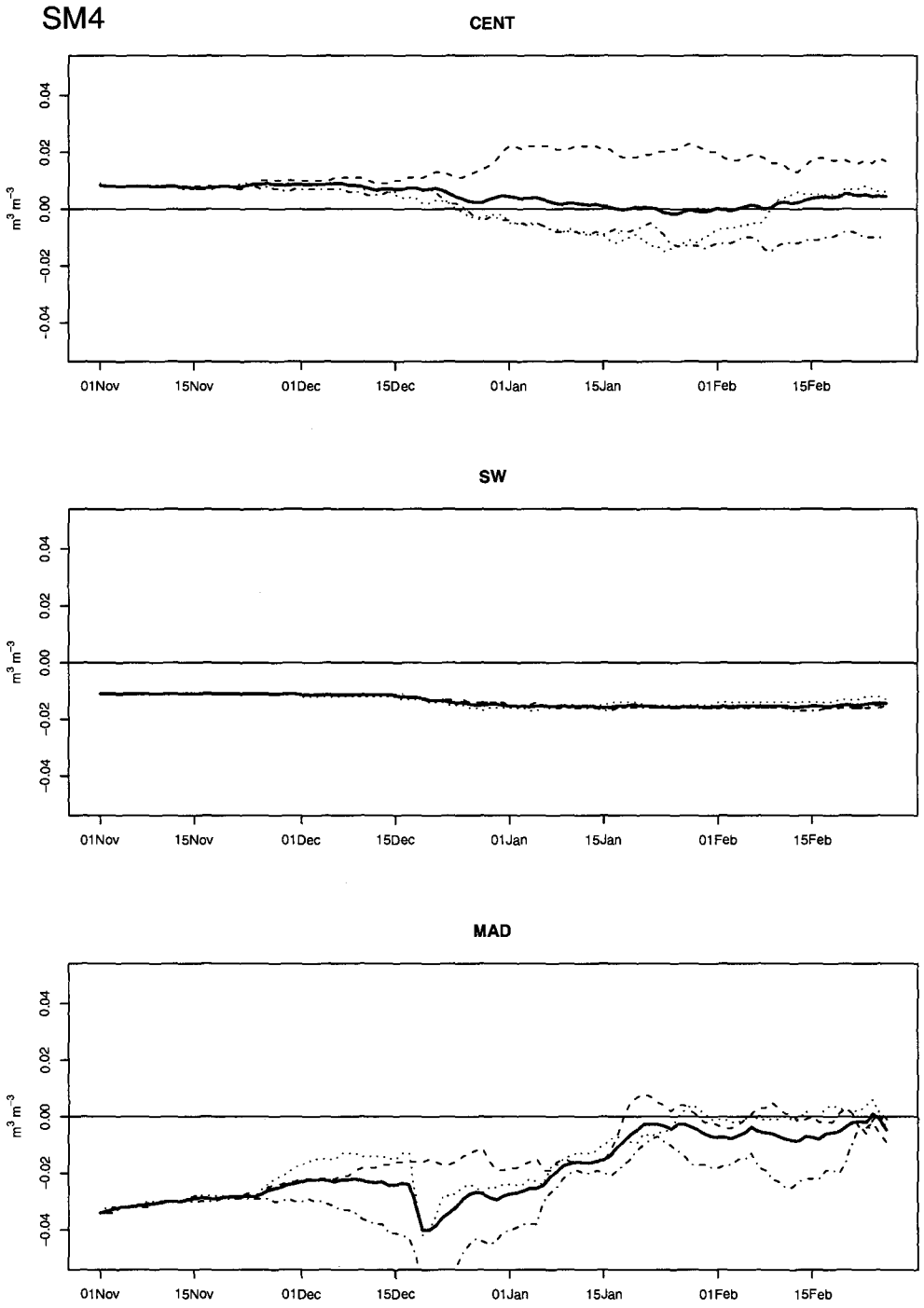

Figure 2.7: As per Figure 2.6, but for soil moisture in layer 4.

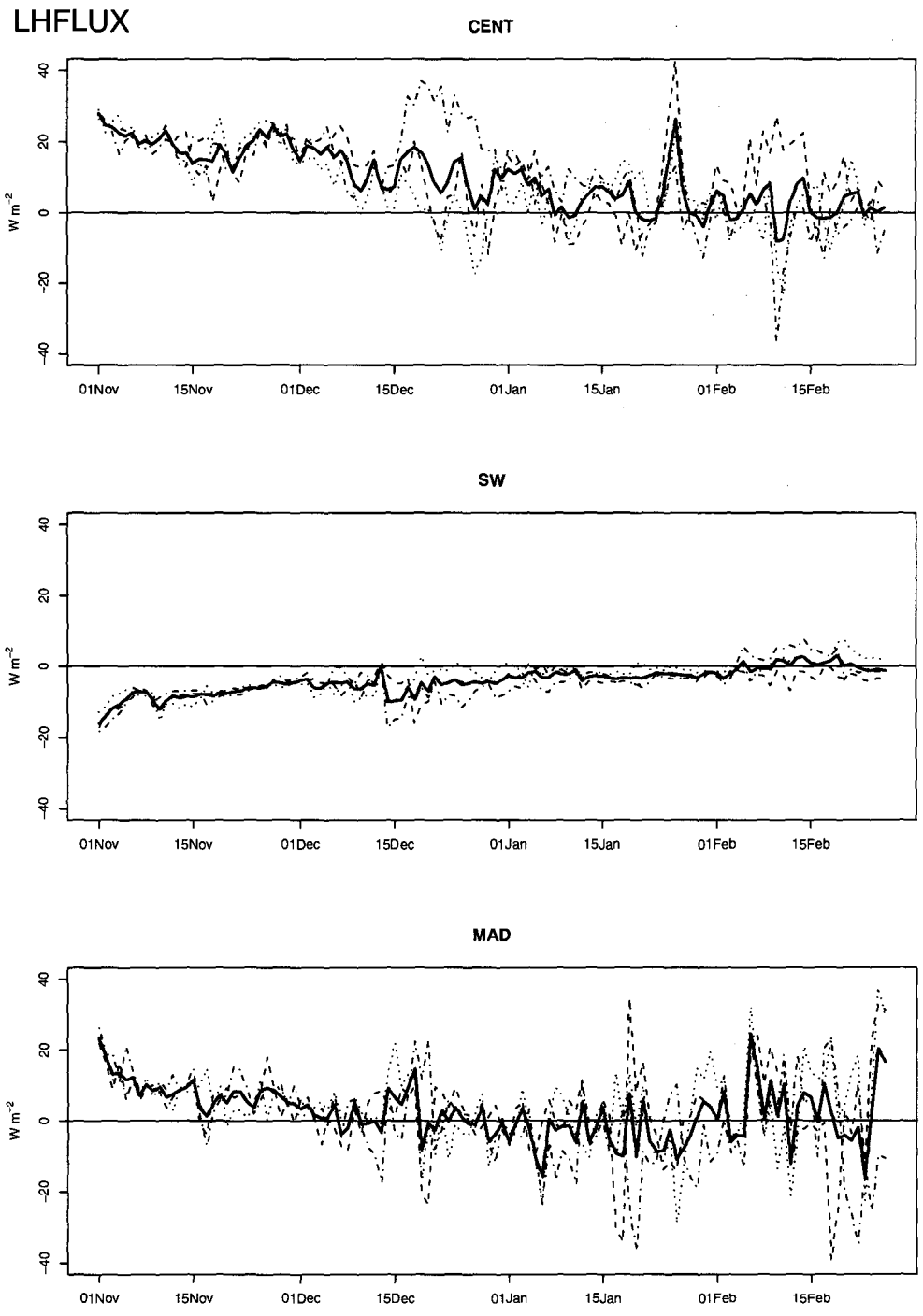

Figure 2.8: As per Figure 2.6, but for latent heat flux.

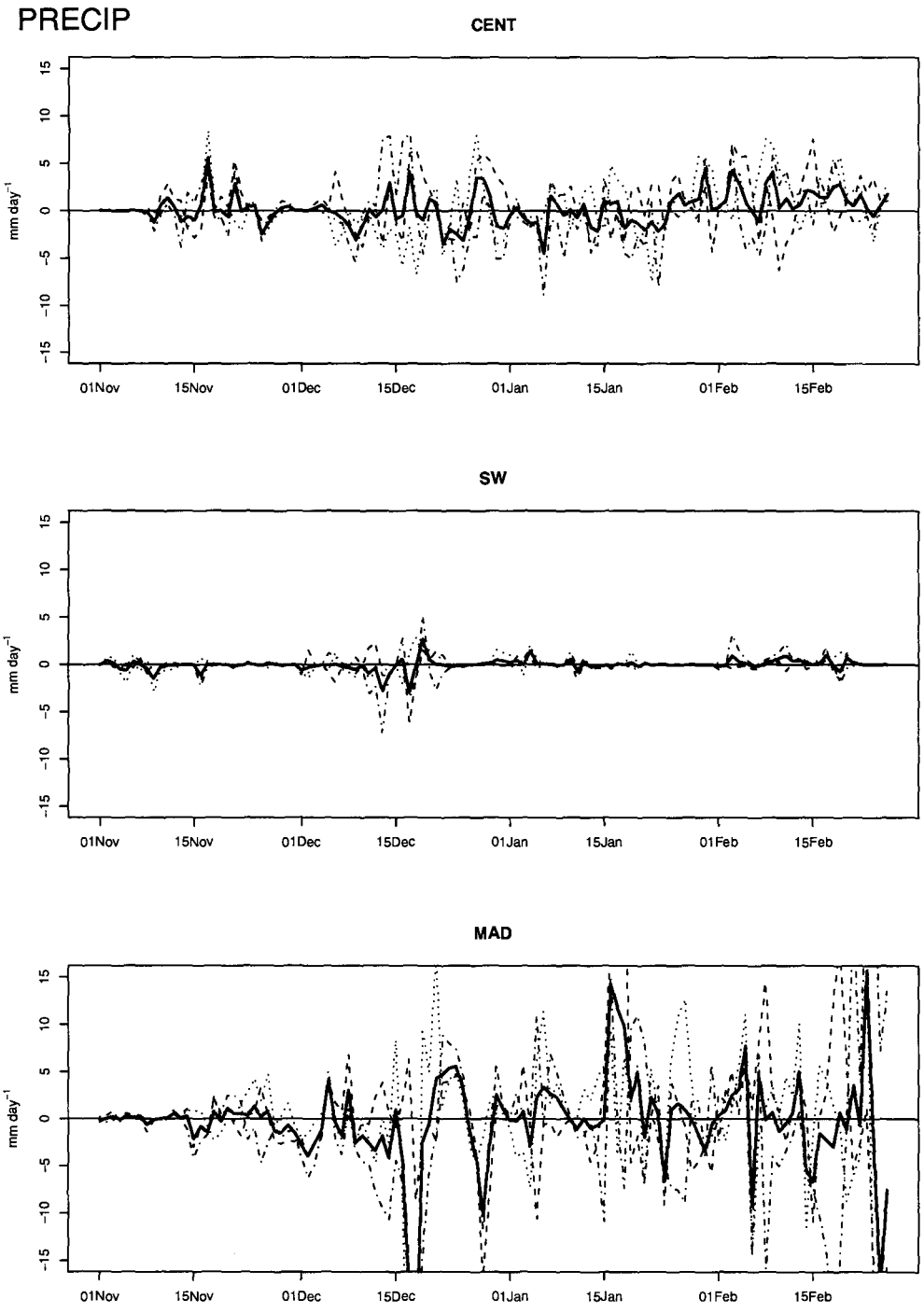

Figure 2.9: As per Figure 2.6, but for precipitation.

tends toward zero during Nov and Dec, after which no trend is apparent. From the beginning of Dec, however, variability between ensemble members begins to increase considerably. The RCM's internal variability is clearly as important (if not more) during the mid-summer months as the antecedent soil moisture perturbation applied here. A similar degree of intra-ensemble variability is seen in MAD, but the ensemble mean anomaly tends to zero more rapidly (by early Dec). In the arid region, SW, the initial anomaly is negative and there is a slow trend toward zero during the simulation, but the disturbance is not completely mitigated. Given the low input of water into the soil, both temporal and inter-ensemble variability are low.

Water storage in the deep soil layer (SM4; Figure 2.7) behaves very differently to SM1:3. In CENT, a small positive initial anomaly persists through to the middle of Dec, after which the signal is overwhelmed by intra-ensemble variability. In SW, the initial perturbation actually increases slightly. This could be due to either upward diffusion of water into layer 3, or a greater loss due to gravitational drainage at the bottom of the soil model than can be replaced by infiltration from above. Although MAD experiences a positive initial disturbance in SM1:3, the corresponding SM4 anomaly is negative. This initial difference is corrected for by the later part of Feb, largely through increased infiltration from the root zone.

Latent heat flux (Figure 2.8) follows the same general patterns as SM1:3, but variability is considerably higher. Although there is a persistent negative anomaly in SM1:3 in region SW, by Feb there is no latent heat anomaly. This is evident in the monthly mean plots discussed above (Figure 2.3) and can be explained by the top-layer soil moisture deficit being mitigated more rapidly than that in the layers beneath.

The spatial correlations in Section 2.3.1 reveal that, for the full land-surface domain, precipitation shows no response to the soil initialization. Accordingly, the regional precipitation anomalies (Figure 2.9) show very high temporal and intra-ensemble variability, with no apparent bias toward either positive or negative anomalies. The greatest variability occurs in MAD, which explains the rapid dissipation of the initial soil moisture anomaly. Since precipitation is linked to soil wetness via changes in MSE, a simple evaluation of the dry and moist energy terms comprising MSE was carried out, using MSE = $s + L_cQ$, where $s = gz + C_pT$ is dry static energy, L_c is latent

heat of condensation, Q is humidity mixing ratio, g is acceleration due to gravity, z is height, C_p is specific heat capacity of dry air at constant pressure, and T is temperature (Holton, 2004). For the three regions discussed here, both the dry and moist components of MSE show negligible change at all levels evaluated (900, 850, 800 and 700 hPa). The changes in energy flux at the surface are therefore insufficient to alter the energy structure of the atmosphere.

2.3.3 Effects across a dry-wet spatial gradient

Figure 2.1 shows a distinct gradient of anomalously dry conditions in the south-west becoming anomalously wet toward the centre of the continental domain. This gradient reflects the existing climatic conditions of the region, where a transition occurs from the arid or semi-arid conditions prevalent over most of Namibia and north-western South Africa to the more humid climates of north-eastern Namibia, eastern Angola and northern Botswana and Zambia. This climatic moisture gradient is therefore amplified by the soil moisture anomaly.

Georgescu *et al.* (2003) demonstrated how low-level circulation can be disrupted by an artificially imposed gradient in surface wetness. Resulting changes in moisture transport were found to act as a negative feedback mechanism and smooth out the gradient, thus restoring climatological conditions. Figure 2.10 illustrates how a similar process may operate in this experiment. Mean Nov SM1:3 anomaly is shown for the region of the moisture gradient, overlain by vectors indicating corresponding changes in 10 m wind. Anomalous divergent, anticyclonic flow is apparent over the wet soils of western Zambia and southern Angola. This results in a relatively strong increase (of the order of 1 m s^{-1}) in northerly winds in northern Namibia. Close to the transition between wet and dry soil is a distinct zone of convergence where the northerly flow meets weak south-westerly wind anomalies. The changes in low-level winds seen here can be attributed to air overlying the wet soils being cooled due to lower sensible heating, becoming negatively buoyant, thus sinking and causing divergence at the surface. Where the soil is anomalously dry, increased sensible heating results in positively buoyant air and hence surface convergence. This mechanism is similar to that responsible for the formation of a landscape breeze across a spatially heterogeneous land surface.

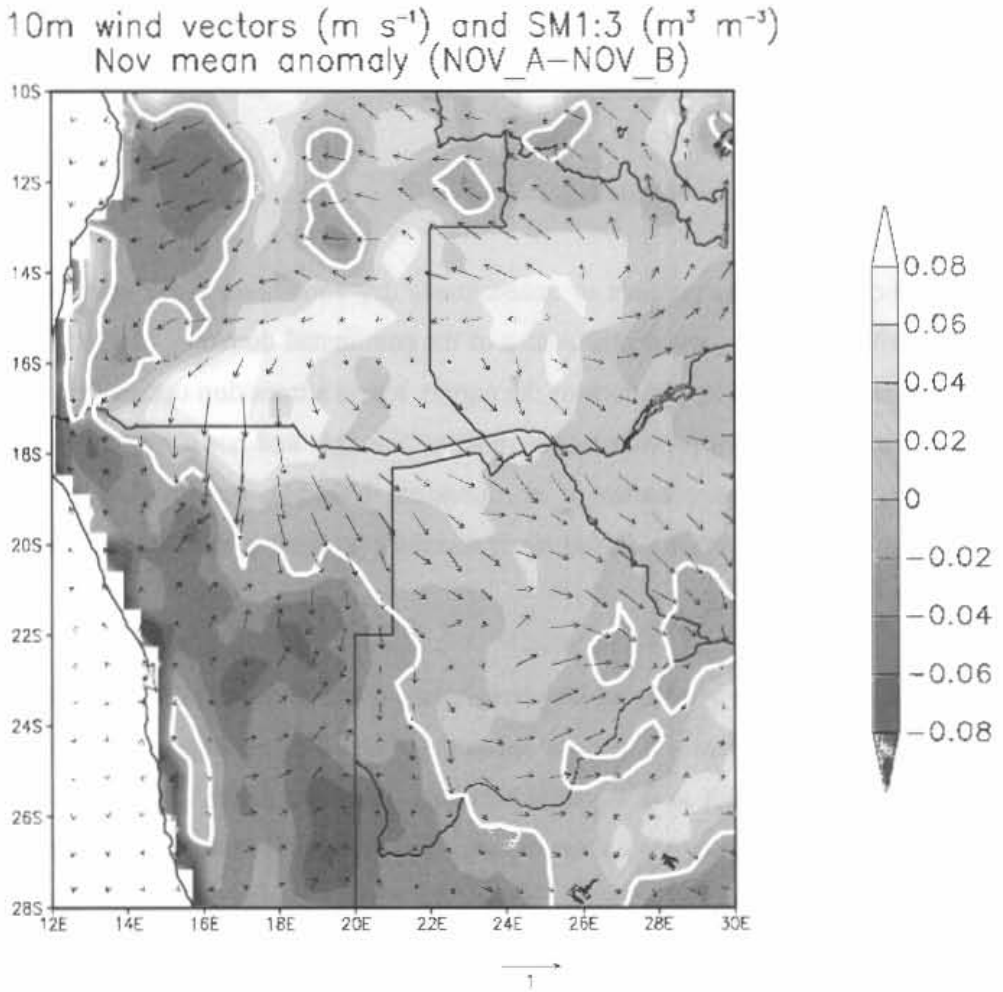

Figure 2.10: November difference (NOV_SOIL_A ensemble mean minus NOV_SOIL_B ensemble mean) in soil moisture in layers 1 to 3 (shading) and wind at 10m (vectors).

Although this circulation will assist in transporting relatively humid air into the region of dry soil, because there is no noticeable precipitation feedback it is unlikely that the enhanced gradient will be restored to climatology through this mechanism alone. However, the large positive soil moisture anomaly in southern Angola is not present in Dec (see Figure 2.2). It is therefore likely that the landscape breeze assists the

dissipation of this anomaly by transporting excess humidity from this location. This weakens the soil moisture gradient and from Dec onwards, the circulation changes are no longer apparent (not shown).

2.3.4 Differences due to time of year at initialization

Figure 2.11 displays r^2 for each month of the Aug-initialized simulations. The initial SM1:3 anomaly persists strongly through Aug and Sep, with r^2 >0.9, but from Oct the spatial relationship decays. Low rainfall rates during the early months of the simulation are largely responsible for the high values of r^2. Because of this persistence, latent and sensible heat fluxes show a much closer relationship to the initial soil moisture perturbations during the first four months than is seen in the Nov-initialized simulations (Figure 2.5). Interestingly, however, there is no relationship between initial SM1:3 and T2m for Aug and Sep, but a weak correlation (r^2 ~0.2) exists from Oct onwards. This suggests that T2m is determined more by radiative fluxes, rather than sensible heat fluxes, in the late-winter and early-summer months, and the influence of altered sensible heat fluxes on near-surface temperature only becomes apparent as the summer season develops. However, monthly mean anomalies of T2m are small in magnitude and not statistically significant (not shown). As is seen the Nov-initialized simulations, monthly mean rainfall shows no relationship with the initial soil moisture anomaly.

2.4 Discussion and conclusions

Simulations were carried out with the MM5 RCM coupled to the NOAH land-surface model to assess the impact of a specific perturbation in initial soil wetness over southern Africa. The applied perturbation represents the difference in volumetric soil moisture, at 1 November 1991, between the NCEP-NCAR reanalysis and an MM5-NOAH simulation initialised at 1 August 1991. The disturbance therefore represents the difference between two simulated representations of soil moisture: that of the NCEP-NCAR reanalysis and that represented within MM5.

Of primary interest to most studies of land-atmosphere interaction is the soil moisture-precipitation feedback mechanism. The results of this experiment reveal that either a) the magnitude of the initial perturbation is too small, or b) land-atmosphere coupling

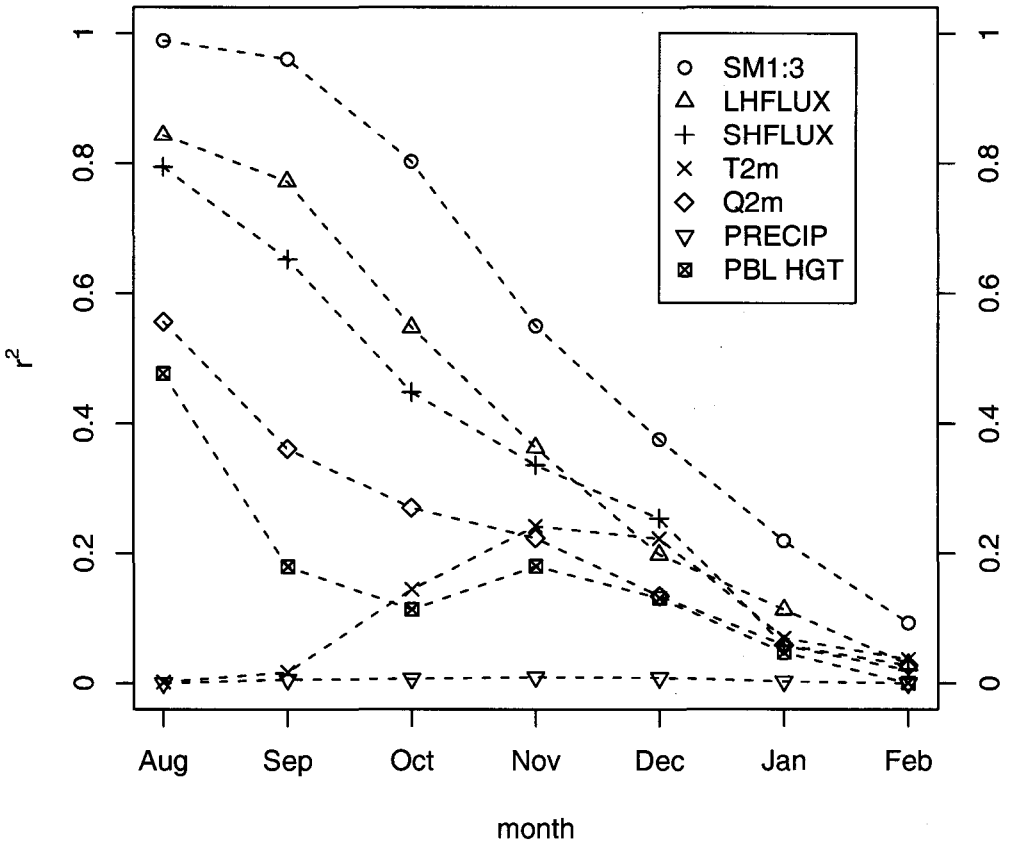

Figures 2.11: As per Figure 2.5, but for Aug-initialized simulations.

in the model used is too weak to result in any systematic change in local precipitation. Apart from local disruptions in circulation, such as that observed over an enhanced wet-dry soil gradient, no systematic changes in circulation are observed. Therefore, as well as having little direct effect on local precipitation, the initial soil moisture anomaly appears not to result in any indirect effects on rainfall through altered regional circulation.

Effects of the initial perturbation on other surface variables are more readily apparent. The anomalous soil wetness is shown to persist for longer in the sub-surface soil layers

of arid regions and for a shorter length of time in humid regions with rainfall high in both magnitude and variability. Latent heat flux is strongly related to the initial soil moisture anomaly in the first two to three months of the simulations. However, although monthly means of sensible heat and near-surface temperature show relatively high spatial correlations to the initial SM1:3 anomaly in the early months of the simulations, the magnitude of the temperature response is small. In the Nov-initialized simulations, spatial relationships between the initial SM1:3 anomaly and monthly mean surface climate are considerably weakened by the second month (Dec). For the Aug-initialized runs, however, a stronger relationship is maintained in the first two months of the simulations (Aug and Sep), due to low rainfall rates at this time of year, which allow the soil moisture anomaly to persist.

It is not clear to what extent the weak soil moisture-precipitation coupling shown in these experiments is due to the choice of RCM and its configuration. Koster *et al.* (2006) and Guo *et al.* (2006) demonstrate considerable variability in the strength of hydrological coupling between different general circulation models. It is therefore likely that a different RCM will yield notably different results for a similar experiment to that carried out here. Furthermore, the same RCM with a different choice of parameterization schemes may also produce different results. Tadross *et al.* (2006) compared MM5 simulations using the Betts-Miller (BM) and Kain-Fritch (KF) convective precipitation schemes and concluded that BM tended to simulate rainfall events with a lower frequency and higher intensity than observed, whereas KF simulated events at a higher frequency, but lower intensity. By favouring convective events of greater magnitude and spatial heterogeneity, it is likely that BM does not adequately account for weaker events that may be more sensitive to local land-surface processes and local circulation changes. On the other hand, Georgescu *et al.* (2003) and New *et al.* (2003) find that changing the convective scheme did not have any major consequences for their results. In the absence of a comprehensive evaluation of land-atmosphere coupling for different convective schemes in MM5, it can therefore be reasonably assumed that the results obtained here are for the large part independent of choice of convective parameterization.

A further consideration is the magnitude of the initial perturbation. The assumption made in this experiment is that the initial disturbance is within the range of uncertainty

of soil moisture representation for southern Africa. This order of magnitude is likely to be comparable to that applied in studies investigating the impact of "realistic" soil moisture initialization on model-predicted precipitation. For example, considering the impact of improved soil moisture initialization in different general circulation models, Dirmeyer (2006) found no gain in the predictability of precipitation and Koster and Suarez (2003) note only a very limited improvement in predicted rainfall. The results presented here are consistent with these findings and it can therefore be concluded that whilst the weak coupling between land-surface hydrology and precipitation in MM5 simulations for southern Africa may to some extent be a function of the model configuration, it is also likely to be a realistic feature of the region's climate.

PART III

CLIMATE RESPONSE TO VEGETATION CHANGE

Simulated effects of anthropogenic vegetation change on southern Africa's summer climate

Neil C. MacKellar, Mark A. Tadross and Bruce C. Hewitson

Abstract: A regional climate model is used to assess potential climatic impacts of altering the vegetation of southern Africa from an estimated natural state to present-day conditions. The Pennsylvania State University-National Center for Atmospheric Research Mesoscale Model (MM5) is integrated from 1 Aug to 28 Feb for 1988/89, 1991/92 and 1995/96 for two spatial vegetation representations: 1) potential natural vegetation as predicted by the Sheffield Dynamic Global Vegetation Model, and 2) current conditions given by the United States Geological Survey land-surface classification. Significant impacts on mean Sep-Nov (SON) and Dec-Feb (DJF) surface climate arise from the change in vegetation, the most notable of which is cooling over large parts of the continent in SON, which gives rise to increased large-scale subsidence and decreased moisture convergence. Resultant decreases in rainfall cause a hydrological feedback through reduced latent heat flux which mitigates the initial cooling and weakens the subsidence anomaly in DJF. The subsidence anomalies extend as high as 500 hPa, which has important implications for regional moisture transport over southern Africa.

3.1 Introduction

Numerous modelling studies have investigated the effect of vegetation change on climate. In particular, tropical deforestation has been the subject of many General Circulation Model (GCM) experiments (eg. Dickinson and Henderson-Sellers, 1988; Nobre *et al.*, 1991; Pitman *et al.*, 1993; Dirmeyer and Shukla, 1994; Hahmann and Dickinson, 1997; Semazzi and Song, 2001). Such experiments typically simulate the complete removal of all tropical forest, which is usually replaced by grassland or cropland. Although results vary, the experiments tend to agree that such extreme shifts in vegetation result in increased surface temperatures of as much as $4^{o}C$ (Dickinson and Henderson-Sellers, 1988) and reduced precipitation of up to 25% (Nobre *et al.*, 1991). Local changes in surface climate are primarily due to reduced evapotranspiration (ET) which causes reduced latent heat fluxes, resulting in warming, and reduced local recycling of moisture. In addition to these local effects on surface climate, vegetation change can also alter regional atmospheric circulation, which may enhance or mitigate the local responses. For example, in an Amazon deforestation study Zeng *et al.* (1996) proposed a weakening of the Walker cell over the Amazon-Atlantic region, analogous to the atmospheric disturbances caused by El Niño Southern Oscillation (ENSO). This disruption in circulation was attributed mainly to the radiative effects of increased albedo and consequent reductions in low-level moisture convergence – and hence decreased precipitation – over the Amazon. Furthermore, changes in the climate of regions not directly associated with a change in vegetation can occur through teleconnections. For example, Semazzi and Song (2001) ran a deforestation experiment for tropical Africa and proposed that changes in mid-tropospheric latent heating in the tropics could lead to changes in the trapped Rossby wave train that is initiated by this large-scale release of latent heat. Changes in the propagation of this wave were related to precipitation anomalies over southern Africa.

Sensitivity experiments such as those above give valuable insights into the dynamics of land-atmosphere interaction, but are limited in that the vegetation change they represent is an extreme scenario. Although the extent of tropical forests is reducing at a rapid rate through human activities, it is unlikely that they will be entirely destroyed and replaced with grassland. Furthermore, land use change is not limited to tropical forests and

within southern Africa the change from savanna to agricultural land is arguably as important. An approach to evaluating more accurately the effects of land-surface change on climate is therefore to consider a change in vegetation that is within the range of observed land-surface alteration. This reflects more complex spatial patterns of vegetation change than complete deforestation experiments, and resulting changes in climate can be expected to be similarly complex. Using such an approach, Marshall *et al.* (2004) undertook a regional climate model (RCM) experiment that simulated the effects of historical land-use change on the climate of the Florida peninsula. Changes in sensible and latent heat fluxes at the surface were found to affect the nature of the sea-breeze circulation, resulting in a general decrease in convective rainfall associated with sea-breeze fronts. Considering the conterminous United States, Baidya Roy *et al.* (2003) investigated the effect of a shift in vegetation from estimated pristine conditions to a present-day state. Significant decreases in average July temperature occurred over the Great Plains as a result of the conversion of natural vegetation to cropland. This agrees with similar experiments conducted by Bonan (1997) and Pan *et al.* (1999), but work by Copeland *et al.* (1996) indicates a slight warming in this region. Baidya Roy *et al.* (2003) point out that surface climate can be directly influenced by vegetation change through altered surface energy partitioning (ie. changes in the Bowen ratio), but there are cases where direct effects are not clearly evident. In these cases, other factors influencing the energy and water budgets – such as cloud cover and moisture advection, respectively – become more important.

Focusing on the African continent, Maynard and Royer (2004a) looked at the impact of a realistic deforestation scenario under increased greenhouse gas (GHG) forcing. They found that GHG forcing and land surface forcing tended to have the opposite effect on ET, such that increased ET caused by increased GHG concentrations was counteracted by reduced ET due to reduced forest cover. Changes in precipitation were thus of opposite sign, but the direction of temperature change was the same for the two forcing mechanisms. They also concluded that the vegetation changes were of insufficient magnitude to induce any significant changes in large-scale circulation.

These experiments suggest that changes in vegetation have appreciable effects on regional climate and whilst several sensitivity studies have been done for tropical and West Africa (eg. Charney, 1975; Charney *et al.*, 1977; Xue and Shukla, 1993; Xue,

1997; Hoffmann and Jackson, 2000; Semazzi and Song, 2001; Maynard and Royer, 2004a,b), little or no work has attempted to investigate the effect of a realistic historical shift in vegetation on the climate of the southern African region. This study aims to address this deficiency by using a Regional Climate Model (RCM) to simulate the atmospheric response to a plausible estimation of changing the vegetation of sub-equatorial Africa from a pristine natural state to one modified by human land-use practices.

3.2 Method

3.2.1 Model configuration

The atmospheric model used in this experiment is the fifth-generation Pennsylvania State University-National Center for Atmospheric Research Mesoscale Model (MM5; Grell *et al.*, 1994). The domain was set to cover approximately 0° – 40°S in latitude and 5° – 57°E in longitude (see Figure 3.2) at a grid resolution of 50 km and 23 vertical sigma levels.

Land surface processes are represented by the NOAH land surface scheme (Chen and Dudhia, 2001a). NOAH consists of 4 soil layers and a single plant canopy layer. Vegetation parameters such as albedo, roughness length and minimum stomatal resistance are defined according to the dominant vegetation class in each grid cell. Green vegetation fraction (f_G) – defined as the "grid-cell fraction for which midday downward solar insolation is intercepted by photosynthetically active green canopy" (Chen and Dudhia, 2001a) – is provided independently as a separate spatially continuous monthly climatology. Produced by Gutman and Ignatov (1998) from satellite-derived normalized difference vegetation index (NDVI), it assumes that the leaf area index (LAI) – the total area of leaves in all layers of a canopy divided by the area of the ground beneath the canopy – is fixed at a value of 4. It is clearly unrealistic to fix LAI to represent a dense canopy for all vegetation classes, but this is done because it is difficult to derive both LAI and f_G simultaneously from a single NDVI product (Gutman and Ignatov, 1998; Matsui *et al.*, 2005). It can be argued that natural variability in f_G is generally higher than for LAI (Chen and Dudhia, 2001a; Matsui *et al.*, 2005), so the assumption made in NOAH is to leave LAI fixed, but allow f_G to vary. Green

vegetation fraction is used as a weighting coefficient in the calculations of evaporation and transpiration, while LAI is a factor in the calculation of canopy resistance, and hence plant transpiration. All other vegetation parameters are independent of LAI and f_G. Soil data is provided by the United Nations Food and Agriculture Organization global classification. In the NOAH LSM, soil parameters determine hydrological properties such as field capacity and wilting point, which affect direct evaporation for the soil as well as plant transpiration. Surface albedo is defined according to land-use and is not altered by soil properties.

Planetary boundary layer (PBL) processes are computed using the MRF PBL scheme (Hong and Pan, 1996). The Betts-Miller convective adjustment scheme was chosen to represent moist convection and precipitation (Betts and Miller, 1993). This is a semi-empirical approach whereby profiles of temperature and moisture computed by the atmospheric model are relaxed toward predetermined reference profiles. In MM5 simulations for southern Africa, Tadross *et al.* (2006) found that the combination of the MRF PBL and Betts-Miller convection schemes tended to overestimate the magnitude of precipitation events, but better captured the phase of the diurnal cycle and interannual rainfall variability. Lateral boundary conditions, initial conditions and sea-surface temperatures are taken from the National Centers for Environmental Prediction-National Center for Atmospheric Research (NCEP-NCAR) reanalysis (Kalnay *et al.*, 1996).

3.2.2 Vegetation data

Two representations of spatial vegetation distribution are used. Present-day vegetation is given by the United States Geological Survey (USGS) global half-degree resolution classification, whereas an estimate of potential natural vegetation is simulated by the Sheffield Dynamic Global Vegetation Model (SDGVM; Woodward *et al.*, 1995; Woodward and Lomas 2004). SDGVM is designed to predict potential natural vegetation from estimates of precipitation, temperature, relative humidity and CO_2. The model includes subroutines for biomass, phenology, hydrology, carbon and nitrogen cycling, and dynamics (ie. transition between vegetation states). The

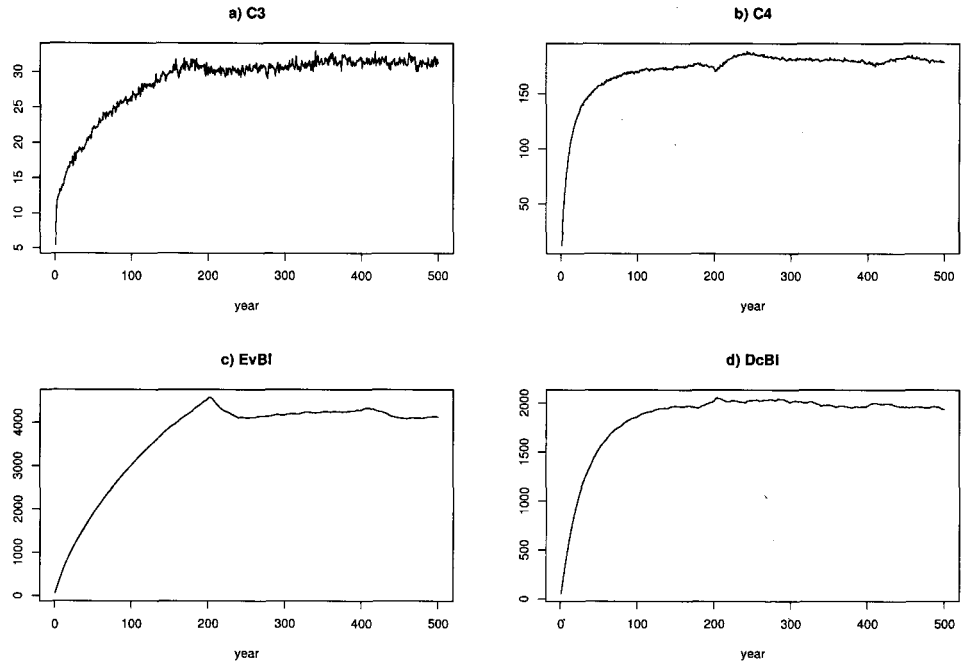

Figure 3.1: Domain-averaged biomass during SDGVM spin-up integration for a) C_3, b) C_4, c) evergreen broad-leaf and d) deciduous broad-leaf PFTs.

resulting vegetation is predicted in terms of six possible plant functional types (PFTs), namely C_3 and C_4 grasses, evergreen broad- and needle-leaf trees, and deciduous broad- and needle-leaf trees, as well as bare ground.

For this study, the input variables of monthly precipitation, surface temperature and relative humidity are provided by the University of East Anglia's Climatic Research Unit (CRU) land surface climatology (New *et al.*, 1999, 2000). Since the smallest time step in SDGVM is 1 day, the model uses a rainfall generator to create an artificial daily time series based on the CRU monthly total precipitation. Temperature is assumed to be constant throughout each month and minimum temperature is estimated from mean monthly temperature. Mean annual CO_2 concentration is taken from a time series produced by the Hadley Centre for the period 1830-2100. Initial estimates of soil carbon and nitrogen are derived by integrating a simplified version of the model, consisting of the carbon and nitrogen dynamics and net primary productivity (NPP) modules, under a constant climate until an equilibrium solution is reached. The

resulting conditions are then used to initialize a spin-up integration using the full SDGVM system. At the start of the spin-up, land cover is set to represent an even distribution of all PFTs. CRU climate data is taken from the period 1971-1990 and is cycled repeatedly to provide input for a 500-year integration. CO_2 is set at a constant partial pressure of 29 Pa for the duration of the spin-up. The spin-up allows for vegetation structure to tend toward a steady state that can then be used to initialize a subsequent SDGVM run. Figure 3.1 displays the evolution of domain-averaged biomass for the four PFTs relevant to the region (i.e. C_3 and C_4 grasses, evergreen broad- and needle-leaf trees). After 200 years, all types are at a near-stable state.

For the final simulation, SDGVM takes its initial state from the output of the spin-up and is run for a 30-year period (1971-2000) with observed climate and CO_2. The mean proportions of PFTs predicted for this period are then grouped to approximate the USGS natural vegetation classes. This is done so that the same set of vegetation parameters can be used for both the USGS and SDGVM representations. The difference between the two vegetation maps thus represents a spatial shift in land-surface parameters, rather than a change in the values of the parameters themselves.

Previous modelling studies have identified albedo as a primary controller of surface radiative fluxes (eg. Charney 1975; Charney *et al.*, 1977; Dickinson and Henderson-Sellers, 1988; Dirmeyer and Shukla, 1994), surface roughness length (Z_0) as a key parameter determining turbulent energy and moisture transfers in the boundary layer (Dickinson and Henderson-Sellers, 1988, Lean and Warrilow, 1989; Pitman *et al.*, 1993), and minimum stomatal resistance (R_{SMIN}) defining the capacity for plants to transfer water vapour from their leaves to the air. The latter has not been subjected to much research, but is a potentially important parameter for forest vegetation that is not limited by soil moisture availability (Maynard and Royer, 2004b). Green vegetation fraction is not specified according to vegetation type and LAI is given as a fixed value, so these are therefore not altered in this experiment. Since these are important parameters in the computation of evaporation and transpiration, the effect of vegetation change on surface moisture fluxes is likely to be underestimated.

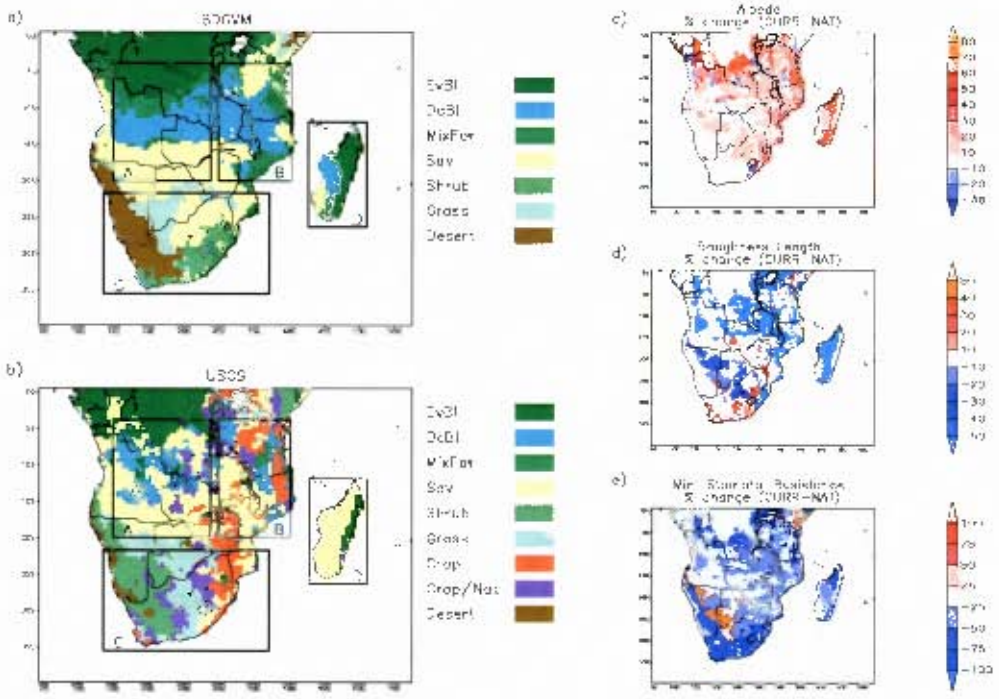

Figure 3.2: Vegetation maps for a) SDGVM (NAT) and b) USGS (CURR), with boxes denoting sub-regions CENT (A), EAST (B), SOUTH (C) and MAD (D). Differences in c) albedo, d) roughness length and e) minimum stomatal resistance between CURR and NAT.

Figure 3.2 shows the two vegetation maps (a and b) and illustrates how albedo (c), Z_0 (d) and R_{SMIN} (e) differ between the two classifications. The most obvious differences between the SDGVM and USGS maps are the presence of cropland along the eastern parts of the sub-continent and the fragmentation of tropical forests in the present-day representation. In terms of vegetation parameters, the effect of this is to increase albedo by over 50% in parts and to decrease Z_0 by over 50%. This is accompanied by reductions in R_{SMIN} of over 25%. Over South Africa and neighbouring countries, there are both increases and decreases in the three parameters – Z_0 in particular – but on average for the whole domain the shift from natural to present-day vegetation results in increased albedo, reduced Z_0 and reduced R_{SMIN}. A limitation of SDGVM is that it does not explicitly simulate a shrub PFT. The south-western parts of the region, although some C_3 grasses are present, are therefore classified as barren or sparsely vegetated, where in USGS this is shown as shrubland. Whilst this does not affect albedo or Z_0, R_{SMIN} is significantly reduced.

3.2.3 *Model simulations*

The MM5 configuration described in Section 3.2.1 is used to run a suite of simulations representing the early- and mid-summer period of southern Africa. Three years were selected in order to encompass a wide range of synoptic forcing conditions. Since El Niño Southern Oscillation (ENSO) exerts an influence on the regional circulation around southern Africa through atmospheric teleconnections, and other studies (e.g. Zeng and Neelin, 2000) have found land-atmosphere feedbacks to be modulated by interannual variability, the years were chosen to span this ENSO-induced variability. The years chosen are 1988/89, which was associated with a pronounced La Niña event and generally above-normal rainfall over much of the domain; 1991/92, which experienced strong El Niño conditions and widespread drought throughout southern Africa; and 1995/96, which represents a transition between ENSO phases. For each year a pair of model simulations was run: one using the USGS land-use map (hereafter CURR) and one in which the spatial distribution of land-use classes was replaced by the SDGVM simulation presented above (hereafter NAT). The magnitude of the change from NAT to CURR represents a plausible approximation of the impact of human activities on the vegetation of southern Africa. Each of the three pairs of simulations were initialized at 1 August and run through to 28 February of the following year. Although this is a small number of simulations, comparison of the results for each of the three individual periods shows that the response of atmospheric variables to the vegetation change is similar in each case (not shown). It is therefore felt that increasing the number of simulations will not qualitatively alter the results of this experiment.

Statistical significance of the difference between surface variables from the CURR and NAT simulations is given by the modified *t*-test of Zwiers and von Storch (1995). This method accounts for the occurrence of temporal autocorrelation in a time-series. A conventional *t*-test assumes observations to be independent of one another, but in a time-series of climate data, this assumption may not be valid. The method of Zwiers and von Storch (1995) estimates the number of samples that are independent of one-another by deriving an equivalent sample size n_e as a function of the lag-1 correlation coefficient. This equivalent sample size is then substituted for the actual sample size n when calculating the *t*-statistic. Since n_e is smaller than n, the modified *t*-statistic will

be smaller than a conventional *t*-statistic. The degrees of freedom are also reduced, so the critical *t* value is increased, thus giving a more conservative estimate of significance than the traditional method.

3.3 Results and discussion

3.3.1 Model performance

Precipitation given by the CURR simulations (i.e. present-day land surface) is compared to the Climate Prediction Center Merged Analysis of Precipitation (CMAP) rainfall climatology of Xie and Arkin (1996, 1997) as well as CRU precipitation for the same period (Figure 3.3). The average for Sep-Nov (SON) for the three years shows that the model simulates the position of rainfall maximum over the Democratic Republic of the Congo (DRC) and Angola reasonably well, but the peak magnitude in this region is much higher than observed. This can be expected given that the Betts-Miller convective scheme produces an amplified hydrological cycle (Tadross *et al.,* 2006). However, estimated error in the CMAP analysis for this region is high (Xie and Arkin, 1997), and station coverage in tropical Africa is particularly poor, so there is likely to be considerable uncertainty in the observations here. Rainfall over the eastern parts of South Africa is well represented in location, but its magnitude is too high. A major problem with the MM5 simulation is an extensive area of high rainfall over the Indian Ocean to the north of Madagascar. This is not present at all in the CMAP observations, but as this occurs over the ocean it should not affect the outcome of this experiment. For Dec-Feb (DJF), MM5 captures the spatial distribution of rainfall well, but once again overestimates its magnitude over DRC and Angola. The eastern parts of the continent and Madagascar show fairly good agreement with the CRU observations, but magnitudes are generally overestimated by MM5. It is likely these large biases in precipitation may have some effect on the results of this study, so this should be noted as an important caveat.

Simulated 2 m temperature is compared to the CRU land-surface temperature climatology (Figure 3.4). MM5 has positive biases of up to 4°C in places in SON. This is most evident in the tropics, whereas South Africa shows good agreement with observations. DJF temperatures are generally overestimated by MM5. Positive

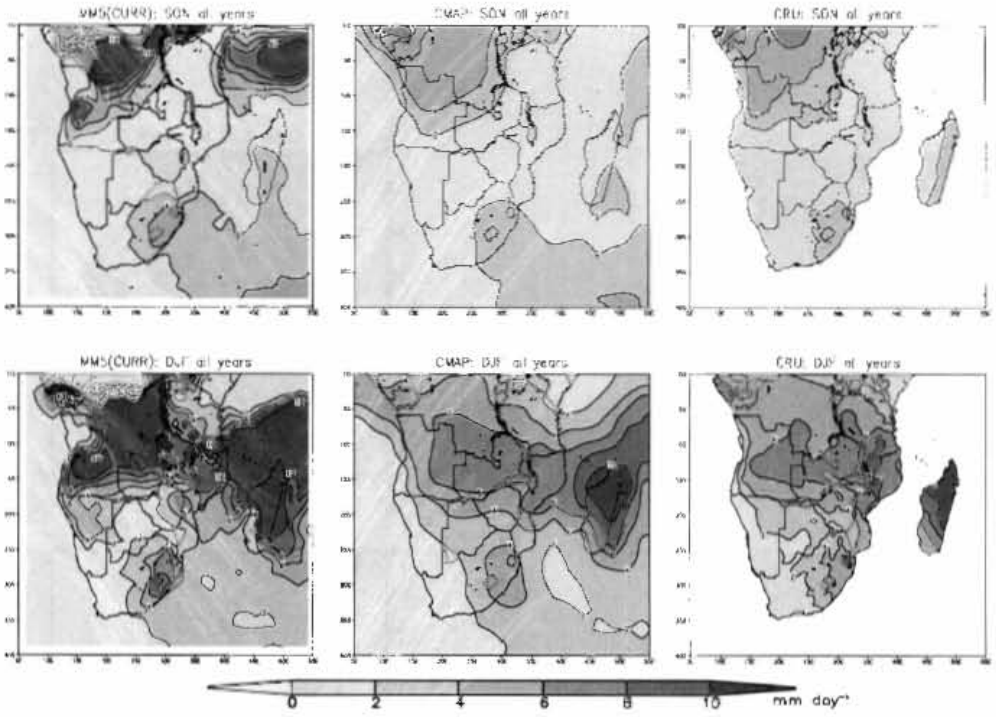

Figure 3.3: Comparison of MM5 simulated rainfall (left) to CMAP (middle) and CRU (right) observations. SON and DJF are averaged for all 3 simulated years (ie. 1988/89, 1991/92 and 1995/96).

temperature biases can be attributed to too few rain days which are accompanied by an increase in cloud-free days, greater solar radiation reaching the surface, and reduced latent cooling (Tadross *et al.*, 2006). MM5 also tends to simulate an optically thin atmosphere on cloud-free days (Chen and Dudhia, 2001b), further increasing the solar radiation bias. Because of this incoming radiation bias, the errors in surface temperature appear to be largely systematic and therefore should not greatly affect the outcome of the experiment. Negative temperature biases are likely to be a result of overestimated rainfall, perhaps topographically forced along the eastern escarpment of South Africa, resulting in increased latent cooling (Tadross, *et al.*, 2006).

3.3.2 Influence of vegetation change on surface climate

For selected surface variables, mean SON and DJF anomalies (CURR-NAT), averaged over the three simulated periods, are shown in Figures 3.5-3.7. Positive (negative)

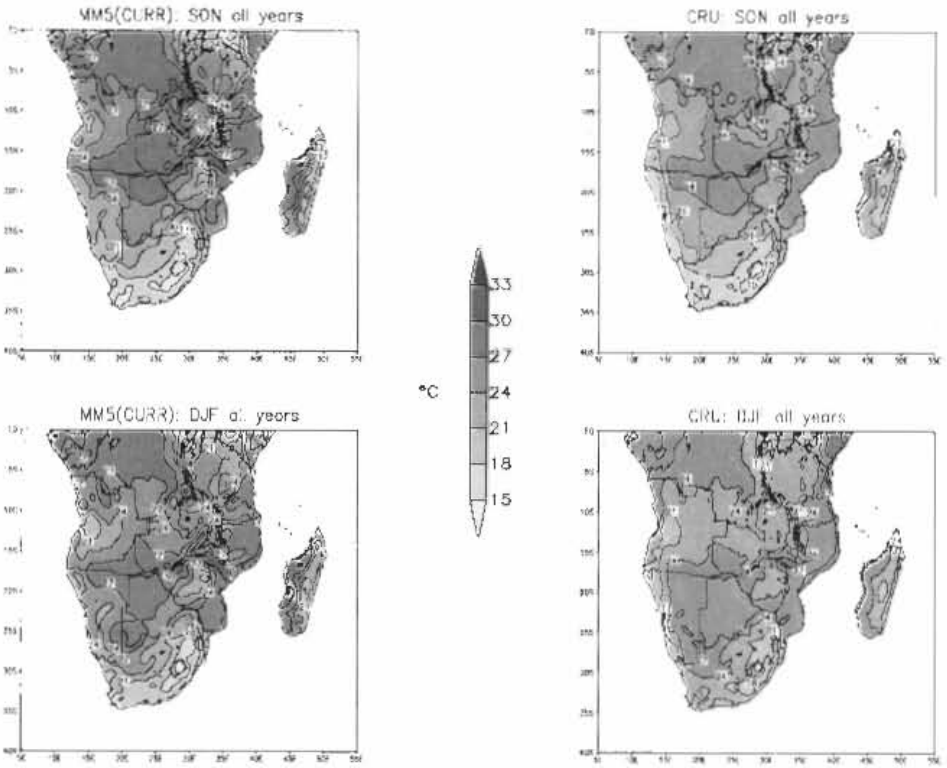

Figure 3.4: Comparison of MM5 simulated 2m temperature (left) to CRU observations (right). SON and DJF are averaged for all 3 simulated years (ie. 1988/89, 1991/92 and 1995/96).

differences that are significant at the 95% level are shaded in light (dark) grey. The surface energy fluxes of latent and sensible heat (Figure 3.5a,b) exhibit marked differences between early- (SON) and mid-summer (DJF). In SON, significant reductions in latent heat flux of over 5 W m^{-2} are seen over Zambia and parts of DRC, Angola, Mozambique and Madagascar. In terms of the land surface, these changes correspond to the expansion of savanna and cropland (CURR) at the expense of tropical forest (NAT). This equates to an increase in albedo of between 20 and 40% and a decrease in Z_0 from 50 m in NAT to 15 m in CURR (Figure 3.2c,d). The direct effects of this will be to reduce the amount of solar energy available for evaporation and surface heating and lower the turbulent transfer of energy and moisture from the surface. The decrease in R_{SMIN} of 25-50% (Figure 3.2e) will increase the potential for moisture to be transferred from the plant canopy to the atmosphere, but savanna and

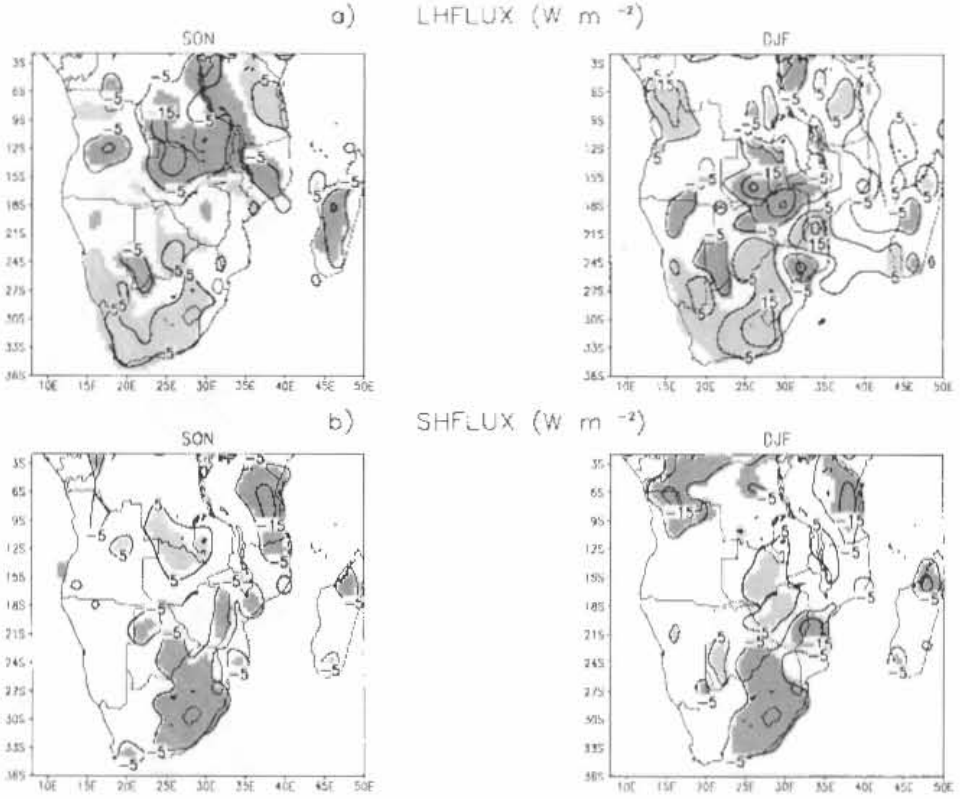

Figure 3.5: Mean SON and DJF differences (CURR-NAT) for a) latent heat flux and b) sensible heat flux. Light (dark) shading indicates positive (negative) anomalies significant at the 95% level.

cropland have a shallower rooting depth (soil layer 3, as opposed to layer 4 for forest), which will reduce the capacity of the vegetation to transfer moisture from lower soil layers to the atmosphere. In DJF the anomalies in these regions are less coherent and centred further south over the continent. A direct link to changes in the land surface is less evident, which implies that circulation changes are an important factor here.

Most of South Africa and the arid south-west experiences significant increases in latent heat flux of over 5 W m^{-2}. These changes are consistent with the reduced R_{SMIN} seen in this region, as well as increased Z_0 over parts of South Africa. The apparent influence of R_{SMIN} does, however, contradict the suggestion by Maynard and Royer (2004b) that this parameter will only be important where soil moisture is not a limiting factor, which is clearly not the case for an arid region. It must be noted that the changes in surface

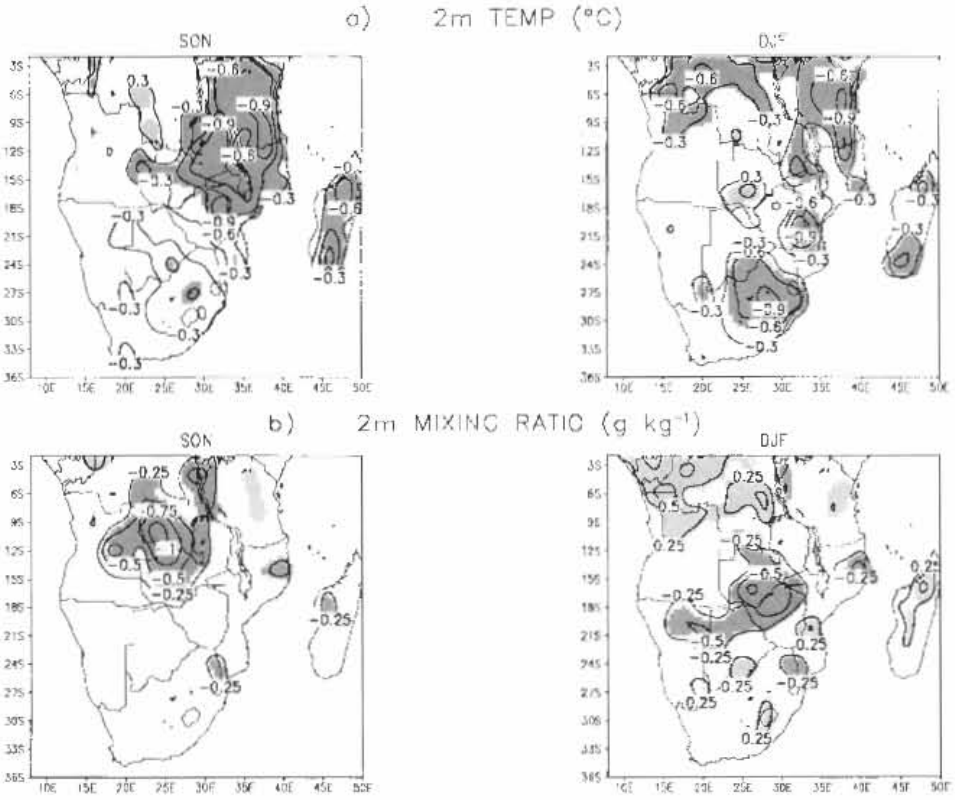

Figure 3.6: As per Figure 3.5, but for a) 2m temperature and b) 2m water vapour mixing ratio.

parameters over much of the south-west are due to SDGVM's inability to simulate shrubland, rather than a result of anthropogenic causes. Reduced LH over the Kalahari in south-western Botswana corresponds to decreased Z_0 and increased R_{SMIN} resulting from a shift from grassland in NAT to shrubland in CURR. This is also, however, a problematic region for SDGVM as the actual vegetation here has been described as arid shrub savanna (Weare and Yalala, 1971; Ringrose *et al.*, 1998), which is more closely matched by the USGS shrubland class than the grassland shown by SDGVM.

Unlike the tropical regions to the north, the anomalies seen in the south in SON persist through DJF, suggesting changes in dominant synoptic forcing plays less of a role in modulating land-surface feedback in this region. Patterns in the sensible heat flux anomalies (Figure 3.5b) generally mirror those for latent heat to reflect the changes in surface energy partitioning, but a notable exception is the south-west, where there is no

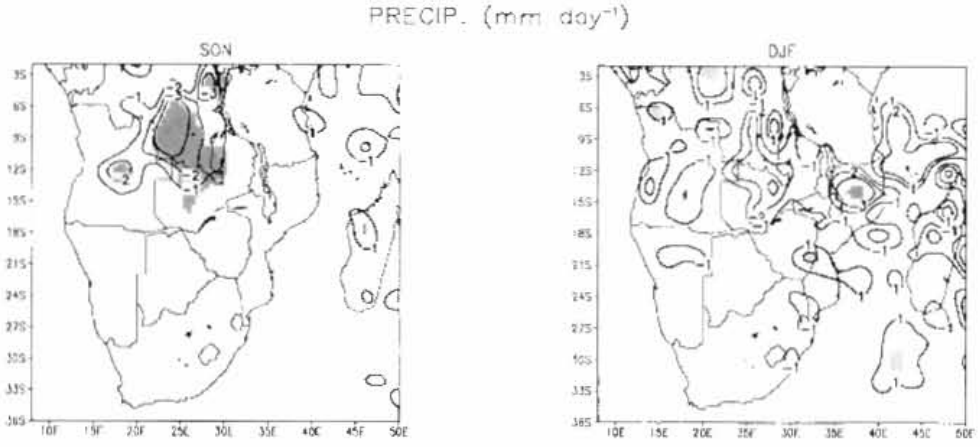

Figure 3.7: As per Figure 3.5 but for precipitation.

significant change in sensible heating. The only parameter to change in this region is R_{SMIN}, which decreases, thus reducing transpiration and latent heat flux. Given that SH shows little change here, the excess energy at the surface is probably balanced by an increase in emitted longwave radiation.

In SON, temperature at 2m above the surface (T2m; Figure 3.6a) experiences extensive reductions of over 0.5 °C in the central and eastern parts of the continent and most of Madagascar. This is consistent with radiative cooling resulting from increased albedo over these regions. In DJF, the decreases in T2m are more fragmented along the east coast when compared to SON, likely due to heterogeneous changes in mid-summer rainfall (see below) and consequent changes in the Bowen ratio. Small areas of increased T2m occur over southern DRC in SON and southern Zambia in DJF. Significant negative anomalies develop over eastern South Africa and in the far north-western parts of the domain in DJF as a result of reduced sensible heating.

The areas of increased T2m are generally associated with decreases in 2m water vapour mixing ratio (Q2m; Figure 3.6b). Extensive reductions in Q2m are seen over the centre of the continent in SON, shifting further south in DJF. These decreases in humidity

reflect a weakened hydrological cycle, which will raise surface temperature through reduced latent cooling and increased solar radiation. Decreases in Q2m correspond to the regions of large reductions in LH. These can therefore partly be due to changes in land surface parameters, but changes in low-level moisture advection or, more indirectly, changes in rainfall and the subsequent availability of moisture for local evaporation could also be determining factors. This is discussed further in Sections 3.3.3 and 3.3.4. Not illustrated here, but interesting to note, is the fact that the strongest mid-summer moisture anomaly occurs during the climatologically dry year (1991/92). Although by no means conclusive, this observation suggests the potential role of the land-surface in exacerbating drought conditions.

The response of precipitation (Figure 3.7) is generally noisy, but significant decreases of more than 2 mm day^{-1} are seen over the southern DRC in SON. This closely matches the reduced latent heat flux, increased surface temperatures and reduced humidity seen in this part of the domain. The only noticeable changes in DJF rainfall are seen over southern DRC and Zambia – where increases in surface temperature are experienced – and northern Mozambique, which mitigates the albedo-induced cooling in this area. The south-western parts of the continent do not experience any noticeable change in rainfall, so it appears that alteration of surface fluxes by the land surface in this region are not large enough to feed back to local precipitation processes.

3.3.3 Regional circulation

A cell of increased geopotential height at the 700 hPa level (H700; Figure 3.8a) is clearly evident over most of the sub-continent for both SON and DJF. The horizontal extent of this anomaly is greater in SON than DJF and its centre corresponds to anomalously dry and warm conditions at the surface. The increase in geopotential height implies anomalous subsidence and divergence, which is reflected by increased vertically integrated moisture flux divergence (MFD; Figure 3.8b) over southern DRC in SON and over parts of Angola, southern DRC, Zambia, Malawi and northern Mozambique in DJF. This reduction in moisture transport over the continent is the primary driver of the precipitation reductions seen in Figure 3.7, and is consistent with numerous studies that have shown increased albedo and decreased surface

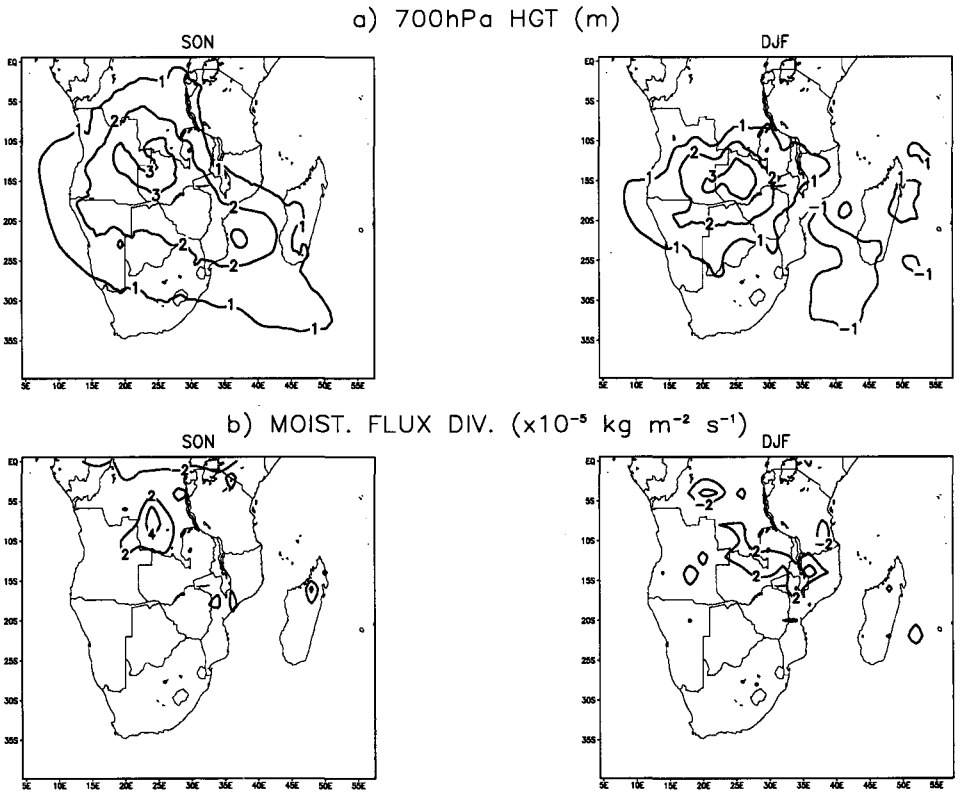

Figure 3.8: Mean SON and DJF differences (CURR-NAT) for a) 700 hPa geopotential height and b) vertically integrated moisture flux divergence.

roughness to result in reduced moisture convergence (Xue and Shukla, 1993; Zeng, *et al.*, 1996; Xue, 1997; Hoffmann and Jackson, 2000).

The vertical extent of geopotential height and water vapour mixing ratio anomalies are illustrated by meridionally-averaged transects taken between 10 and 25^{O} S (Figure 3.9). Increased subsidence over the continent is clearly shown by positive height anomalies extending to around the 600 hPa level in SON and 500 hPa in DJF (Figure 3.9a). The DJF anomalies have a smaller magnitude and horizontal extent than SON, further illustrating particularly strong early-summer sensitivity to land-surface processes. The greater vertical extent of the DJF anomaly is likely due to weaker subsidence during mid-summer, which will allow surface perturbations to influence higher layers.

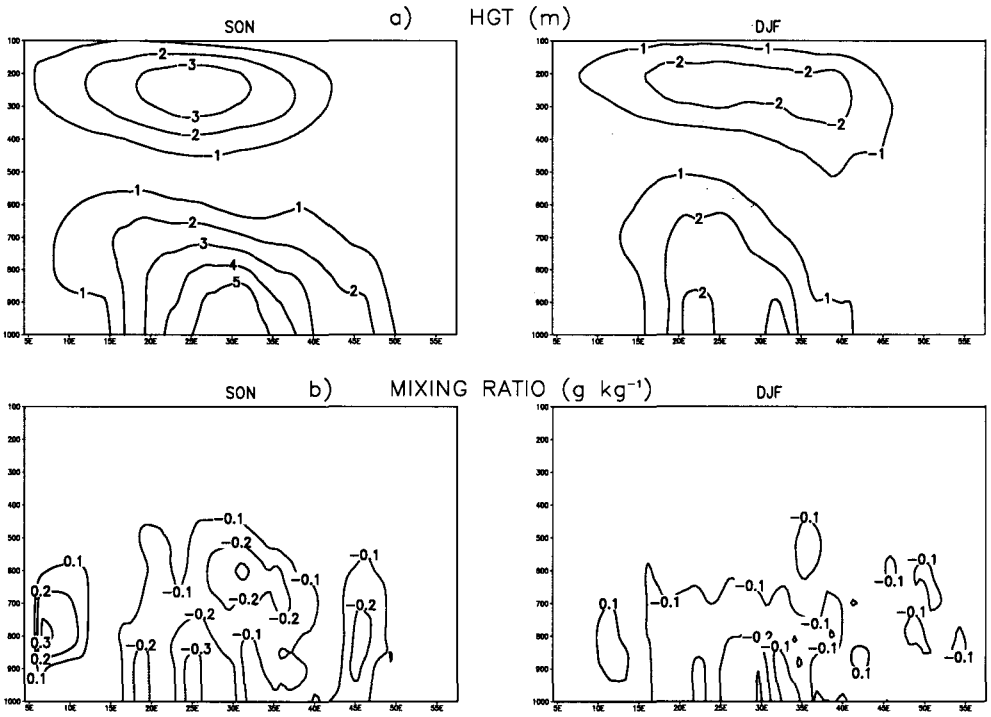

Figure 3.9: Vertical transects of mean SON and DJF differences (CURR-NAT) averaged between 10 and 25 °S for a) geopotential height and b) water vapour mixing ratio.

The vertical structure of water vapour mixing ratio (Figure 3.9b) shows negative anomalies extending as high as 500 hPa, with a maximum horizontal extent around 700 hPa. This decrease in atmospheric humidity reflects the increases in geopotential height and reductions in moisture convergence shown above.

3.3.4 Surface energy and moisture budgets

Four regions have been selected for a closer investigation of how the surface climate is affected by vegetation change: CENT (covering all land-surface grid cells between 4-20 °S and 15-28 °E), EAST (4-20 °S; 30-40 °E), SOUTH (22-36 °S; 13-38 °E) and MAD (Madagascar). These regions are illustrated by boxes A-D in Figure 3.2a and b. Figures 3.10 and 3.11 show monthly mean differences (CURR-NAT) for selected energy and moisture terms for each of the four regions. Although Aug is regarded as

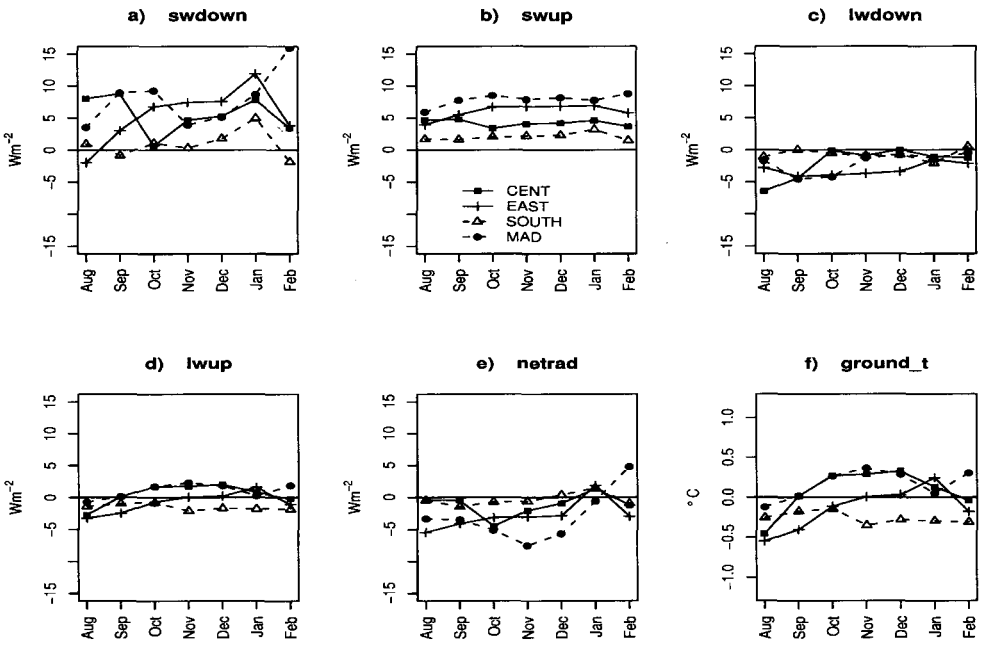

Figure 3.10: Mean monthly differences of a) downward shortwave, b) upward shortwave, c) downward longwave, d) upward longwave and e) net surface radiation, and f) ground surface temperature, averaged for each of the four sub-regions.

the spin-up month, it is included in the analysis for an idea of how the model evolves following initialization.

Downward shortwave radiation at the surface (SW↓; Figure 3.10a) shows considerable variability, but a general increase for all regions. The weakest response occurs in SOUTH, where only Jan sees an increase of notable magnitude. These reductions are linked to decreases in cloud liquid water (Figure 3.11f), and are consistent with other studies (Dirmeyer and Shukla, 1994; Xue, 1997; Maynard and Royer 2004a), which attribute increases in SW↓ to the effects of albedo change on cloudiness. A further consequence of reduced cloud cover is a reduction in downward longwave radiation (LW↓; Figure 3.10c), which partially offsets the increased SW↓. Reflected shortwave radiation (SW↑; Figure 3.10b) increases as a function of increased surface albedo, but is modulated by changes in SW↓. Consequently, the weakest response occurs in SOUTH, as this region experiences the smallest average albedo increase as well as

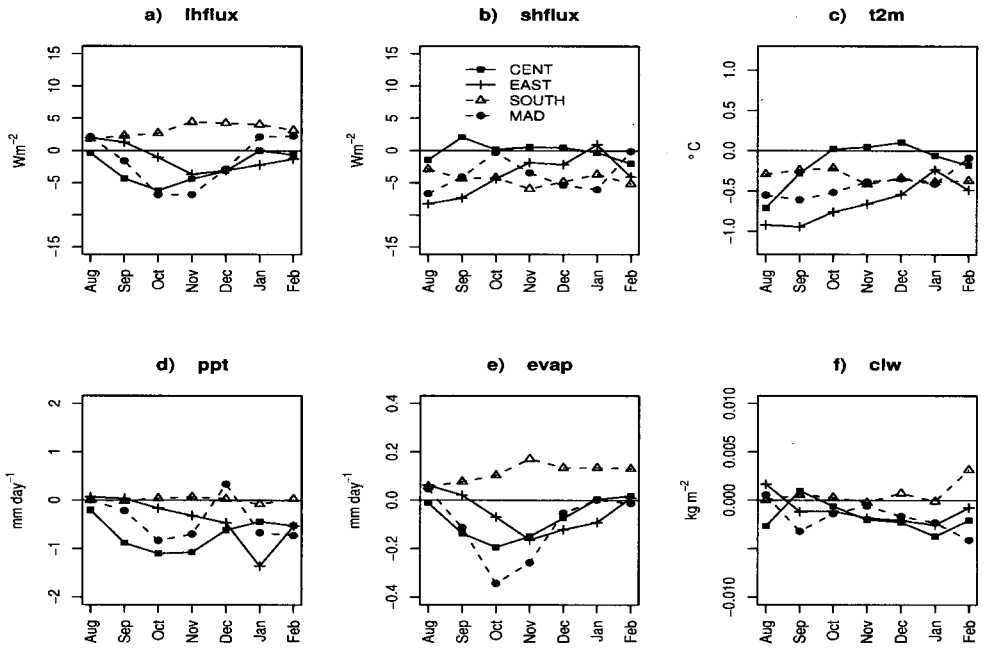

Figure 3.11: As per Figure 3.10, but for a) latent heat flux, b) sensible heat flux, c) 2m temperature, d) precipitation, e) evaporation and f) total column cloud liquid water.

little change in SW↓. Emitted black-body longwave radiation (LW↑; Figure 3.10d) varies as a function of the ground temperature difference (Figure 3.10f). The net effect on the radiation balance (Figure 3.10e) shows an overall decrease for all regions except SOUTH. These decreases are strongest from Aug to Dec, but are more variable in Jan and Feb due to changes in SW↓.

With the exception of SOUTH, latent heat flux from soil to atmosphere (LH; Figure 3.11a) shows an overall decrease from Sep-Dec, but a weaker and more varied response in Jan and Feb. Reduced LH in CENT, EAST and MAD is attributed to both a net radiation deficit and reduced precipitation, which, respectively, lowers the amount of energy and moisture available for evaporation. Although these three regions experience considerable decreases in rainfall for Jan and Feb, mixed changes in net radiation result in the varied LH and evaporation responses. SOUTH, by contrast, experiences increased LH and evaporation for all months, but little change in either net radiation or precipitation. In this region the changes in surface energy and moisture fluxes can therefore be directly linked to changes in vegetation parameters, in particular R_{SMIN}.

The increased evaporation causes cooling at the surface, but, as mentioned in Section 3.3.2, does not show any noticeable feedback to local precipitation processes.

Ground heat flux (not shown) has a negligible response, so the surface energy budget is balanced by predominantly negative sensible heat flux (SH) differences (Figure 3.11b), resulting in reduced 2m temperature (Figure 3.11c). From Oct-Jan in CENT and MAD, and in Dec and Jan in EAST, ground temperature increases while T2m decreases. The increased ground temperature can be explained by reduced LH, whereas the decreased T2m is caused by reduced SH. The reduction in both LH and SH is consistent with reduced turbulent transfer caused by decreased Z_0. In CENT, EAST and MAD, the largest reductions in T2m occur in Aug or Sep, with decreases of over 0.5 °C. Following this initial cooling, the magnitude of the difference steadily (or rapidly, in the case of CENT) decreases as the season progresses. As seen in the geopotential height field, which exhibits a greater response in SON compared to DJF, this initially large negative temperature difference in Aug and Sep will contribute toward a large-scale increase in subsidence over the sub-continent, which induces reduced moisture convergence over the continent. This leads to local reductions in rainfall, which mitigates the temperature reductions through decreases in latent heat flux. Because the extent of the reductions in surface temperature is reduced, the strength of the increased subsidence is weakened as the season progresses.

3.4 Conclusions

The aim of the model simulations presented here is to investigate the likely response of southern Africa's summer climate to a shift in vegetation from a potential natural distribution to present-day conditions. We used the MM5 RCM, run with two different vegetation distributions: a potential natural state as simulated by the SDGVM vegetation model and the present-day representation given by the USGS land-surface classification. Three separate 7-month periods (Aug-Feb) were simulated to incorporate a range of synoptic conditions associated with inter-annual variability.

The climate response to vegetation change shows marked differences between SON and DJF, with SON being characterized by the strongest atmospheric response. This implies that seasonal synoptic characteristics play a role in modulating land-surface

feedback. The mechanisms responsible for how the atmosphere responds to the land-surface change differs between early and mid-summer and can be summarized as follows. In the early part of the summer season, particularly before the onset of rain, direct local effects of land-surface change are readily apparent and cause surface cooling. The primary driver of this cooling is an increase in reflected solar radiation due to increased surface albedo. The cooling initiates a change in circulation through large-scale subsidence, as indicated by increased geopotential heights in the lower- to mid-troposphere. A consequence of this is a reduction in moisture convergence, which leads to reduced rainfall in some areas. Resultant decreases in evaporation and latent flux at the surface act to mask out the radiative effects of the land-surface change by promoting an increase in surface temperature. The changes in rainfall thus have a negative feedback on the albedo-induced circulation change by mitigating the surface cooling, and the circulation anomaly weakens. The direct effects of the vegetation change on latent heat flux will also assist in this mitigating effect.

The pronounced sensitivity of the early summer period (SON) to land-surface conditions has major implications for the seasonal onset of rainfall, as was found by Hoffmann and Jackson (2000) for the southern African savanna. Prevalent synoptic conditions are likely to be of primary importance in controlling the atmosphere's response to land-surface change in SON, but as the rainy season progresses the role of secondary feedback mechanisms – particularly in the hydrological cycle – become more apparent. Such secondary effects come about through changes in circulation and whilst these were not evident in the future deforestation scenario of Maynard and Royer (2004a), this study shows them to be very important. The change in vegetation prescribed by Maynard and Royer (2004a) was not as extensive as that applied here, which partly explains the difference in results.

A very important result for the sub-tropics is the vertical extent of the atmospheric response to land-surface change. Increased subsidence up to the 500 hPa level can have a marked impact on the dynamics of regional moisture transport dynamics. Further research is required for an improved understanding of these dynamics over southern Africa, and the results presented here provide a strong case that large-scale vegetation change, and other land-surface processes, should form an important part of such research.

PART IV

SYNOPTIC EVALUATION

Synoptic-based evaluation of climatic response to vegetation change over southern Africa

Neil MacKellar, Mark Tadross and Bruce Hewitson

Abstract: The results of regional climate model (RCM) simulations of the effects of vegetation change in southern Africa are analyzed to asses the role of synoptic forcing in land-atmosphere interactions. A self-organizing map (SOM) is used to identify the dominant large-scale features in the atmospheric boundary conditions used to force the RCM. The fields used to characterize the large-scale circulation are geopotential height at 850 and 500 hPa and total precipitable water between these two levels. For each of the patterns (nodes) identified in these variables by the SOM, the mean RCM-simulated response to vegetation change is evaluated. Notable differences are seen in the response of precipitation, near-surface temperature and geopotential heights to the land-surface change between different nodes. Conditions characterized by strong sub-tropical anticyclones and low atmospheric moisture show the greatest temperature and geopotential height changes and are most sensitive to changes in radiative fluxes, whereas precipitation and surface hydrological processes are more sensitive under conditions of weak subsidence and high levels of atmospheric moisture.

4.1 Introduction

Changes in vegetation can have a marked impact on local and regional climate (eg. Charney *et al.*, 1977; Lean and Warrilow, 1989; Zeng *et al.*, 1996; Bonan, 1997; Pielke, 2001; Narisma and Pitman, 2003; Marshall *et al.*, 2004). Most modelling experiments that investigate the effects of vegetation change on climate are concerned with the mean response of the atmosphere to land-surface perturbations over monthly or seasonal timescales. This is appropriate, as the seasonal cycle can modulate the effects of land-surface change by altering the radiation, moisture and circulation regimes under which surface processes operate. For example, Narisma and Pitman (2003) show large differences in mid-summer (January) and mid-winter (July) responses to land cover change over Australia. January experiences much larger reductions in latent heat flux (LE) than July, which leads to significant changes in temperature for the summer month. This is consistent with the suggestion of Koster *et al.* (2006) that coupling between hydrological land surface components and the atmosphere should be strongest in summer because evaporation rates are at a maximum. Observations by Rabin *et al.* (1990) reveal that influences of the land-surface on cumulus cloud formation are favoured under conditions of maximum incoming radiation and weak atmospheric forcing. Numerical simulations by Wang *et al.* (1996) indicate that a stable atmosphere and strong synoptic winds suppress mesoscale circulations induced by a thermally heterogeneous land surface. Similarly, Chen and Avissar (1994) note that large-scale background wind can inhibit landscape-driven convective precipitation. In contrast, Weaver and Avissar (2001) demonstrate that landscape-induced circulations are not necessarily dependent on synoptic winds, and can in fact be strengthened depending on the orientation of the large-scale flow. Findell and Eltahir (2003a) employed a 1-dimensional model to investigate how early morning temperature and humidity profiles are critical in determining the response of the boundary layer to altered land-surface fluxes. Findell and Eltahir (2003b) extend this to 3 dimensions to show that differences in low-level wind strength and wind shear can suppress or enhance soil moisture-precipitation feedbacks and Findell and Eltahir (2003c) describe how the strength and direction of these feedbacks vary according to climatic region. It was also noted in the latter study that inter-annual variability is an important factor in determining potential land-surface feedbacks. Studies of land-atmosphere coupling in general circulation models also reveal much regional variability in the strength of this coupling (Koster *et*

al., 2006; Guo *et al.*, 2006). Transitional zones between wet and dry regions (eg. the Sahel) are shown to be particularly prone to land-surface feedbacks. In addition to these spatial heterogeneities, Seneviratne *et al.* (2006) demonstrate that the strength of coupling between soil moisture and the atmosphere can be altered by a changing climate. They show that a northward shift of climate regimes over Europe under a future climate scenario causes a displacement of the zone of maximum land-atmosphere interaction. This is likely to be closely linked to changes in the synoptics associated with the climatic shift. It is therefore clear that prevailing synoptic conditions are important considerations for land-atmosphere sensitivity studies.

A particular season has a characteristic mean large-scale circulation, but deviations from this mean, in the form of transient systems, often define the most significant weather events in that season (Tyson, 1987). In the context of land-atmosphere feedback, there is likely to be a marked difference in how the land-surface influences the atmosphere under conditions typical of the mean circulation when compared to individual synoptic perturbations. Seasonal mean atmospheric anomalies induced by land-surface change may therefore not reveal these differences. To better understand this, one can classify the time-series into its dominant synoptic circulation patterns, and consider the mean response of the land-atmosphere system under each of these large-scale forcings, irrespective of at which point in the seasonal cycle they occur.

Synoptic classification methods have been widely used to characterize atmospheric circulation patterns and relate such patterns to local climatic features (see Hewitson and Crane, 2002), but are not commonly used in the analysis of atmospheric responses to land-surface change. A possible approach to utilizing synoptic classification in a land-atmosphere sensitivity study is to derive a number of circulation patterns that typify the simulated time period and then evaluate the mean atmospheric response to land-surface alteration for each synoptic type. The advantage this has over monthly or seasonal means is that much of the daily synoptic variability within each type is removed, which can reveal a stronger land-surface signal during particular circulation types and allow one to more accurately identify the dominant processes contributing to that signal.

A set of regional climate model experiments is described in MacKellar *et al.* (submitted; hereafter MS), which simulate the response of southern Africa's summer climate to a

change in vegetation from an estimated pristine state to present-day conditions. The present study extends the analysis of these experiments by employing a self-organizing map (SOM) to identify the dominant circulation types for the simulated time periods and evaluate the modelled response to the vegetation change based on these types. The aims are to 1) characterize the climate in terms of its synoptic circulation features, 2) investigate for each synoptic type the mean response of the atmosphere to the land-surface change, 3) establish what are the dominant land-atmosphere processes under different synoptic conditions, and 4) infer how these differences relate to inter-annual variability (ie. are climatic responses to land cover change greater in a dry or a wet year?).

4.2 Data and method

4.2.1 Land-surface sensitivity experiments

Simulations of the response of southern Africa's climate to a shift in vegetation from an estimated pristine state to present-day conditions were carried out in MS. A brief description of the experimental configuration is given here.

The fifth-generation Pennsylvania State University-National Center for Atmospheric Research Mesoscale Model (MM5; Grell *et al.*, 1994) was configured for a domain covering sub-equatorial Africa, including Madagascar, at a horizontal grid resolution of 50 km. Land-surface processes were simulated by the NOAH land-surface model (Chen and Dudhia, 2001), planetary boundary layer (PBL) physics by the MRF PBL scheme (Hong and Pan, 1996) and precipitation by the Betts-Miller convective adjustment scheme (Betts and Miller, 1993). The National Centers for Environmental Prediction-National Center for Atmospheric Research (NCEP-NCAR) reanalysis (Kalnay *et al.*, 1996) provided lateral boundary conditions and initial conditions to the RCM. Three 7-month periods (1 Aug to 28 Feb of 1988/89, 1991/92 and 1995/96) were chosen to incorporate a range of inter-annual variability. These years are representative of La Niña (1988/89), El Niño (1991/92) and neutral phases of the El Niño Southern Oscillation (ENSO). A pair of MM5 integrations was performed for each of these periods, one using an estimation of natural vegetation distribution simulated by the Sheffield Dynamic Global Vegetation Model (SDGVM; Woodward *et al.*, 1995;

Woodward and Lomas, 2004), and one using the present-day classification given by the United States Geological Survey (USGS).

The SDGVM output was classified so as to be comparable to the USGS natural vegetation classes. The two vegetation maps are shown in Figure 4.1; the difference between them can be interpreted as an approximation of land-use change due to human activities. In MM5, this vegetation shift translates into a change in parameters such as albedo, roughness length, minimum stomatal resistance and rooting depth. Leaf area index is given as a constant for all classes and green vegetation fraction is taken from a separate, spatially continuous monthly climatology, so these two parameters are not altered in the experiment. It is therefore likely that the effects of the vegetation change on evapotranspiration are underestimated.

4.2.2 SOM analysis

The Kohonen self-organizing map (SOM) algorithm (Kohonen, 1995) is becoming a popular tool in climate research, and has been used in the study of climate change and variability (Main, 1997; Cavazos, 1999, 2000; Cavazos *et al.*, 2002; Tennant and Hewitson, 2002; Hewitson and Crane, 2002; Tadross *et al.*, 2005; Tennant and Reason, 2005; Thomas *et al.*, 2007), identification of climatic regions (Malgrem and Winter, 1999) and both up- and downscaling of atmospheric data (Crane and Hewitson, 2003; Gutiérrez *et al.*, 2005; Hewitson and Crane, 2006). A SOM is a type of artificial neural network which identifies a user-defined number of nodes that represent commonly-occurring patterns in a multi-dimensional data set. A SOM does not make any assumptions about the statistical properties of the data and seeks to span the data space so that nodes tend to cluster where there is more data. A strength of SOMs is that they are able to recognize non-linear relationships within a data set. The map is trained in an iterative manner, such that each node or reference vector is weighted by the input data vectors that most closely match that node. Additionally, each node is also weighted by adjacent nodes in SOM space so that, rather than define discrete classes, a SOM treats the input data as a continuum (Hewitson and Crane, 2002). SOMs have proved to be an attractive alternative to other data-mining algorithms. For example, Reusch *et al.* (2005) compared the performance of principle component analysis (PCA)

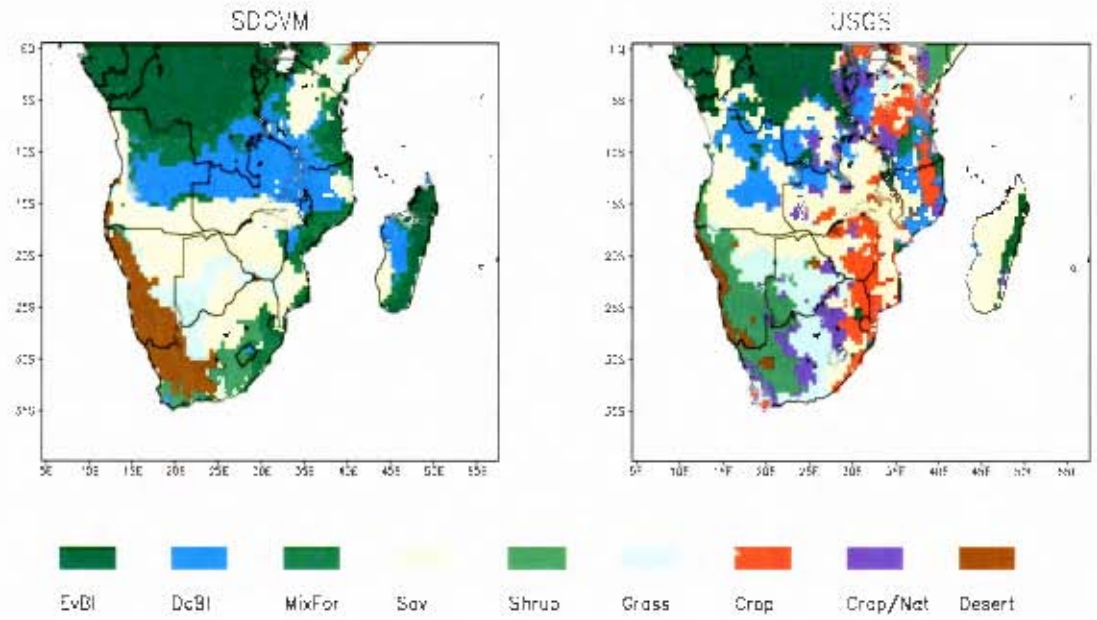

Figure 4.1: Natural (SDGVM) and present-day (USGS) land surface representations used by MacKellar *et al.* (submitted) in simulations of climatic response to vegetation change. Land cover classes are evergreen broad-leaf (EvBl), deciduous broad-leaf (DcBl), mixed forest (MixFor), savanna (Sav), shrubland (Shrub), grassland (Grass), cropland (Crop), mosaic of cropland and natural vegetation (Crop/Nat) and desert.

versus a SOM and concluded that the SOM more accurately identified underlying patterns in the input data.

For this study, a SOM is trained on daily averages of the NCEP-NCAR fields, for the full experimental domain, from which boundary conditions for the three time periods simulated by MM5 were taken. Each day is therefore mapped to a particular SOM node and is associated with the same day of the MM5 simulations for both the natural and present-day land surface classifications. In this way the mean response of atmospheric variables to the imposed vegetation change can be evaluated for each SOM node (i.e. each synoptic type). The variables selected for the training procedure are 850 and 500 hPa geopotential height and total precipitable water between 850 and 500 hPa. Geopotential heights at the two chosen levels are commonly used to characterize the circulation over southern Africa as they reflect baroclinic mid-latitude and barotropic sub-tropical and tropical systems well (eg. Tyson 1987). Precipitable water indicates the positioning of the inter-tropical convergence zone (ITCZ) and regional moisture

features over the continent, which are closely associated with adjacent oceanic conditions and the seasonal cycle. This minimal number of input variables adequately defines the important circulation and moisture features of the domain. For input to the SOM, each variable is standardized according to the variable's mean and standard deviation in space and time (i.e. for all grid points, through all timesteps). This preserves spatial patterns better than a grid-point by grid-point standardization.

The software package used is SOM_PAK version 3.2 (Kohonen *et al.*, 1996). The software allows for various parameters to be set by the user. One of the most important is the size of the SOM array, as this determines the degree of generalization within the SOM. Deciding on the size of the array is entirely subjective and depends on the level of detail that is desired in the definition of each archetype. Crane and Hewitson (2003) show that results are largely independent of SOM size, with only the degree of generalization being affected. A further consideration is the number of data samples that will map to each node, which decreases with a larger array size. If the number of samples is too small, interpretations for that particular node may not be robust. After testing 5x4, 4x3 and 3x3 rectangular array configurations, it was decided that the 4x3 array adequately captured the variability in the driving synoptic circulations without over-generalizing. An example of over-generalization would be a case where the nodes simply represent the seasonal cycle and do not reveal intra-seasonal synoptic perturbations. The procedure to train the SOM begins with a random initialization of the SOM array, followed by a two-step training process, with the second training run having a smaller learning rate and reduced update radius than the first. Test runs with different learning rates and update radii revealed that altering these parameters had very little effect on the both final SOM classification and the average error between each SOM reference vectors and its associated input data vectors.

4.3 Results

4.3.1 Circulation types

Figures 4.2-4.4 illustrate the patterns identified by the SOM in the three variables describing the synoptic conditions used as boundary conditions by MM5. The nodes are referenced by two numbers according to their position on the 2-dimensional SOM

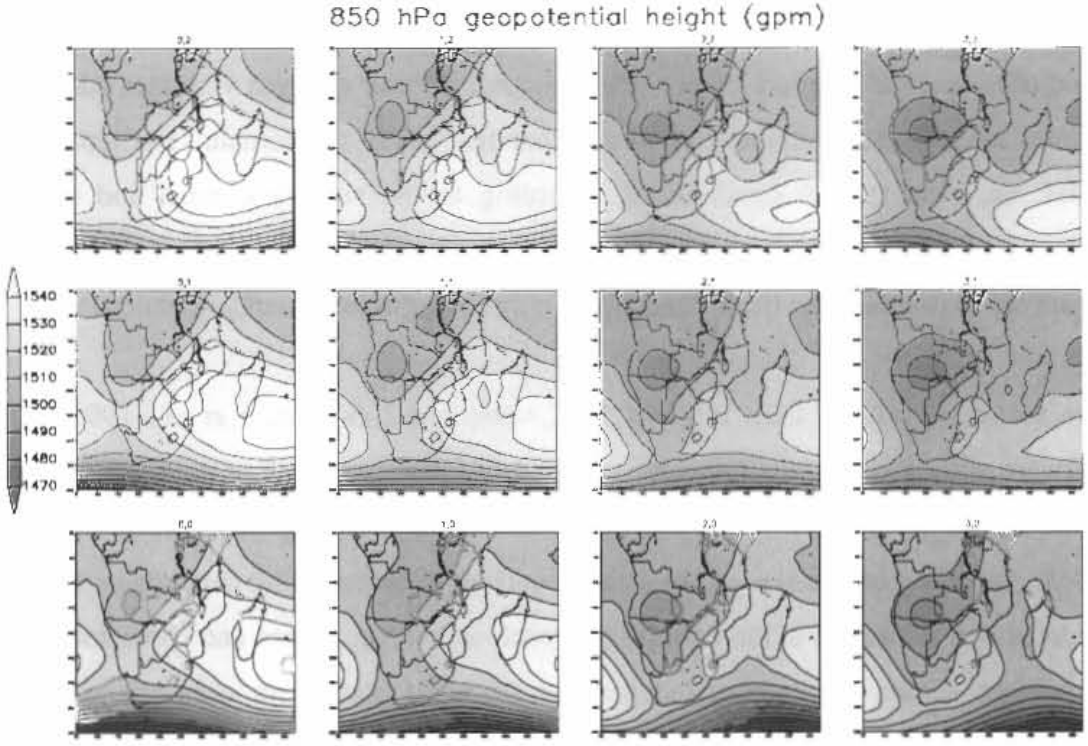

Figure 4.2: Patterns identified by the SOM for NCEP-NCAR 850 hPa geopotential height reanalysis. The SOM is trained on daily averages from 1 Aug to 28 Feb 1988/89, 1991/92 and 1995/96.

array. The first (second) number denotes column (row) position, beginning at 0, such that node [0,0] is positioned in the bottom left corner and node [3,2] is at the top right of the array. At 850 hPa (Figure 4.2), conditions representing the strongest subsidence in the sub-tropics occur on the left-hand side of the SOM array, as indicated by strong South Atlantic and South Indian anticyclones. The strength of this subsidence decreases from left to right and top to bottom across the SOM, such that at node [3,0] the sub-tropical anticyclones are weakest and low pressures dominate the centre of the continent. Mid-latitude depressions have a strong presence in the bottom row of the SOM, but shift southwards toward the top of the array. At 500 hPa (Figure 4.3), a similar shift in mid-latitude systems across the SOM array is seen. At this level a mid-latitude trough is positioned to the south-west of the continent in many nodes, two notable exceptions being nodes [2,0] and [3,0], where a trough is present towards the south-east. An extensive mid-tropospheric ridge occurs over the continent in the nodes on the left-hand side of the SOM space, which weakens toward the bottom right. The

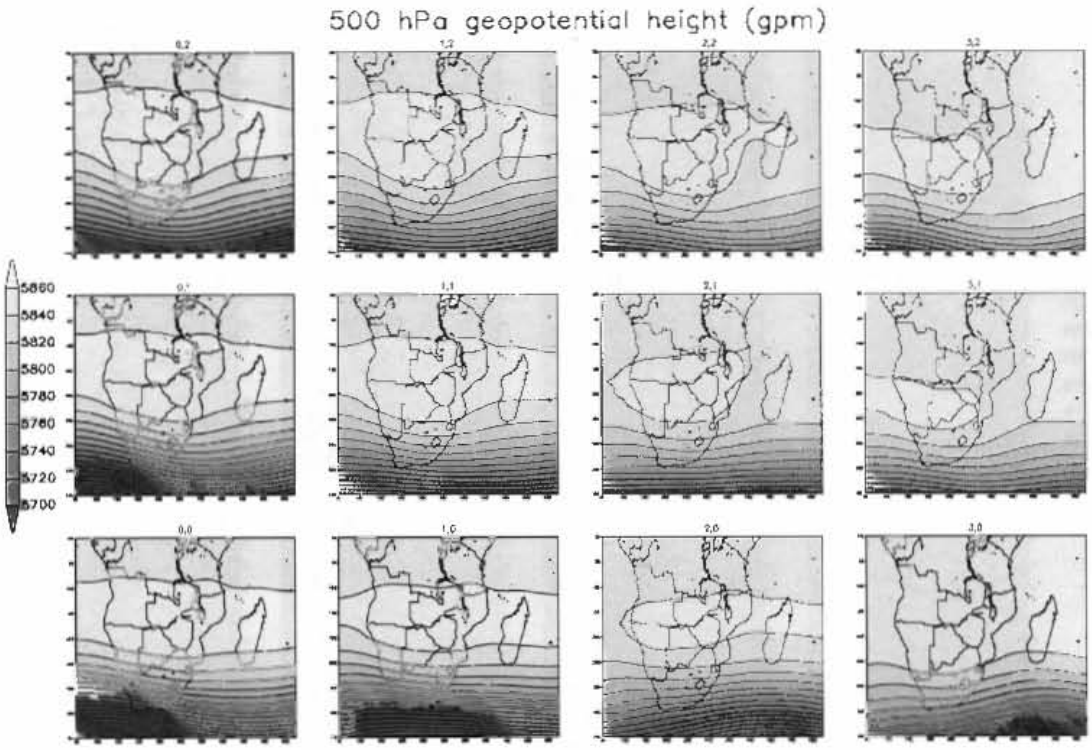

Figure 4.3: As per Figure 4.2 but for 500 hPa geopotential height.

associated moisture conditions (Figure 4.4) on the left of the SOM reflect dry conditions over most of the sub-continent, with maximum moisture occurring in the north-western parts of the domain. This pattern is consistent with a northerly displacement of the ITCZ, with the Congo Air Boundary (CAB) extending from central Angola to north eastern Democratic Republic of the Congo, which is typical of winter months (Van Heerden and Taljaard, 1998). Levels of precipitable water increase to the top-right of the SOM, where node [3,2] shows the highest moisture content over the continent. This reflects the more southerly positioning of the CAB and southward extension of the ITCZ over the eastern part of the continent, which occurs in summer (Van Heerden and Taljaard, 1998). Some regional variability is also evident in the different nodes. For example, the maximum precipitable water in node [3,2] is accompanied by a relatively strong South Indian Anticyclone. Moving down the array to nodes [3,1] and [3,0], this anticyclone weakens and the moisture over the continent is reduced slightly.

The patterns identified by the SOM generally indicate conditions typical of winter on the left-hand side, whereas the right-hand side represents summer-type patterns.

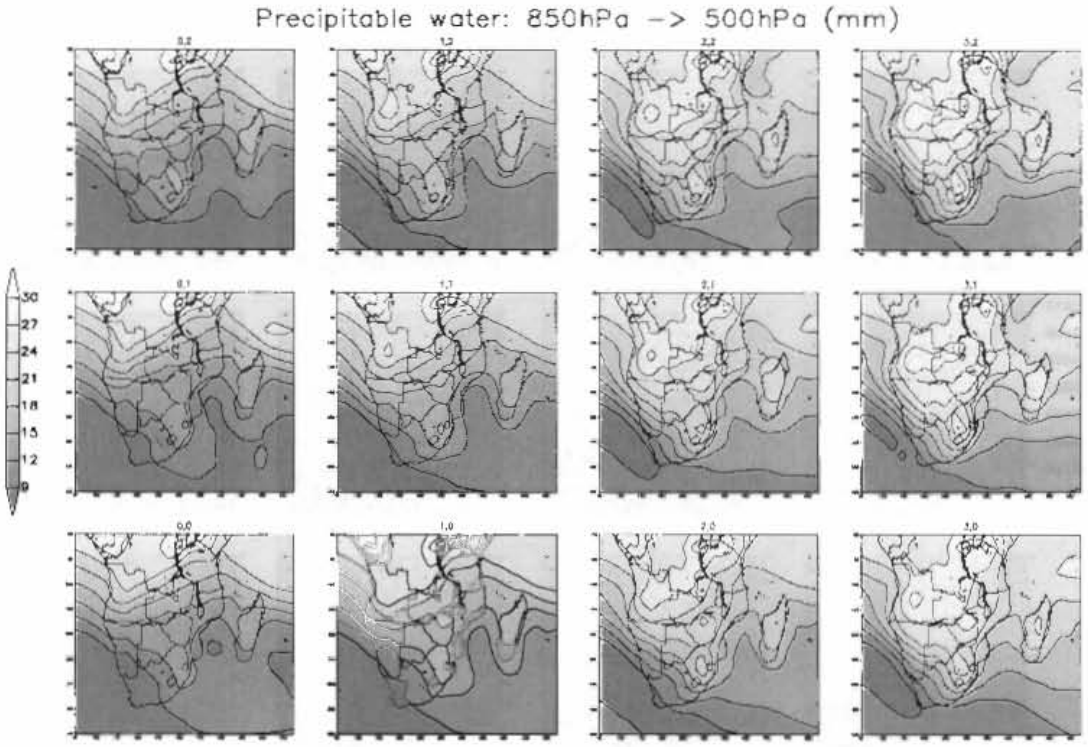

Figure 4.4: As per Figure 4.2, but for total precipitable water between 850 and 500 hPa.

Features such as the South Indian Anticyclone and mid-latitude westerly disturbances show variations from top to bottom in the array, and hence act to modulate the seasonal conditions. This pattern is more evident when one considers the time of year the nodes tend to occur, which is illustrated by the median date of occurrence for each node (Figure 4.5). Seasonal evolution is clearly evident for the three rows of the SOM. In the top row, for example, node [0,2] (furthest left on the SOM) occurs earliest in the time series and as one moves to the right of the SOM, nodes [1,2], [2,2] and [3,2] occur progressively later in the season. There is much less variation in median date of occurrence when moving from row to row in the same column.

Differences in the synoptic characteristics of the three simulated periods are illustrated by the frequency of occurrence of each SOM node during each period (Figure 4.6). Of particular interest is the contrast between the wet (1988/89) and dry (1991/92) years for certain nodes. Nodes [1,2] and [2,2] occur more frequently in 1991/92 and represent relatively strong anticyclonic circulation over the Indian Ocean

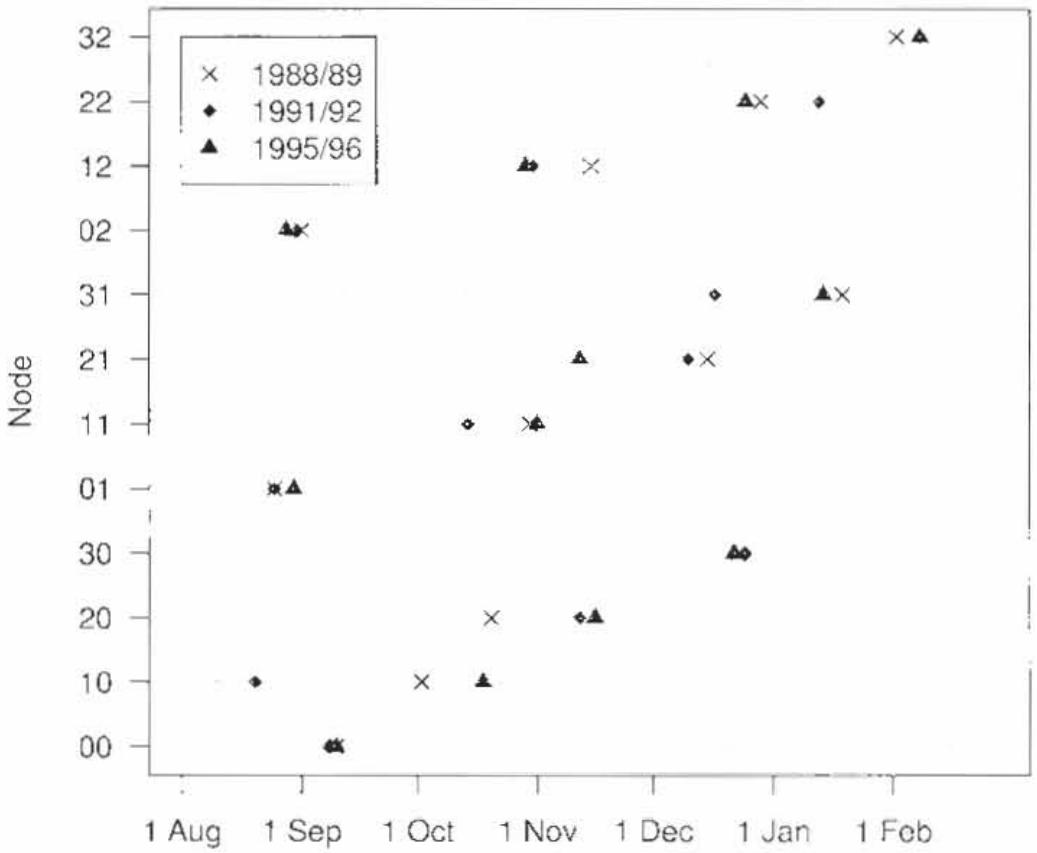

Figure 4.5: Median date of occurrence of each SOM node for each of the simulated periods.

and south-eastern parts of the continent, coupled with high geopotential heights over the centre of the continent at 500 hPa and relatively low precipitable water. The median dates at which these nodes occur (Figure 4.5) are in late October or early November for node [1,2] and late December or early January for node [2,2]. A high frequency of these circulation types during the early and middle part of the rainy season is likely to be an important contributor to below-average rainfall at these particular times. The most notable difference in frequencies is seen for node [3,1], where it occurs on 28 days in 1988/89, but only 7 times in 1991/92. The synoptic features associated with this node are high levels of precipitable water over the continent, weak

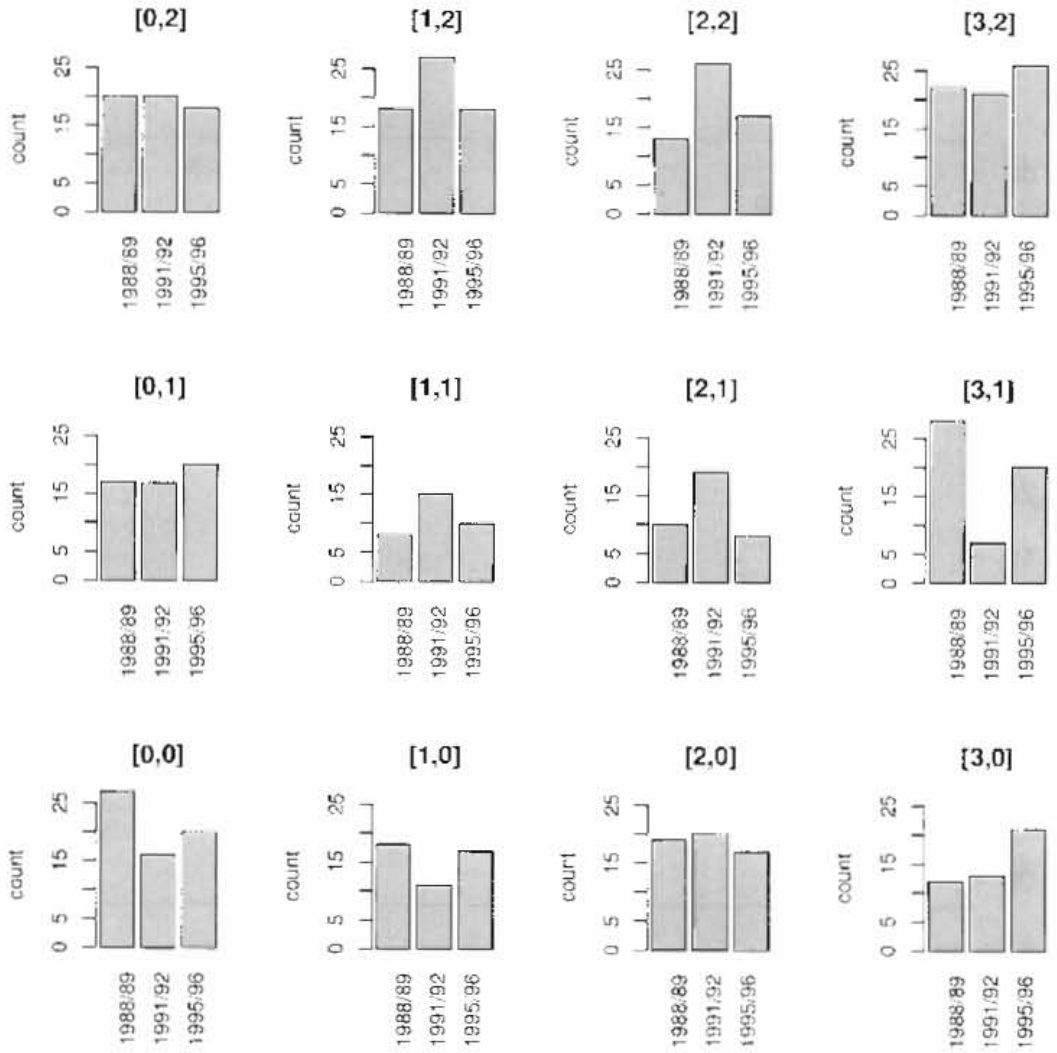

Figure 4.6: Frequency of occurrence of each SOM node in each of the three simulated periods.

sub-tropical anticyclones and a mid-latitude trough positioned to the south of the continent. Such conditions are conducive to the formation of tropical-temperate troughs (TTTs), which are responsible for much of South Africa's summer rainfall (Tyson 1987, Van Heerden & Taljaard 1998). The median date of occurrence for this node is in late Dec (1991/92) or late Jan (1988/89) and its low (high) frequency in 1991/92 (1988/89) is likely to be a major cause of below (above) average rainfall over the south-eastern parts of the continent.

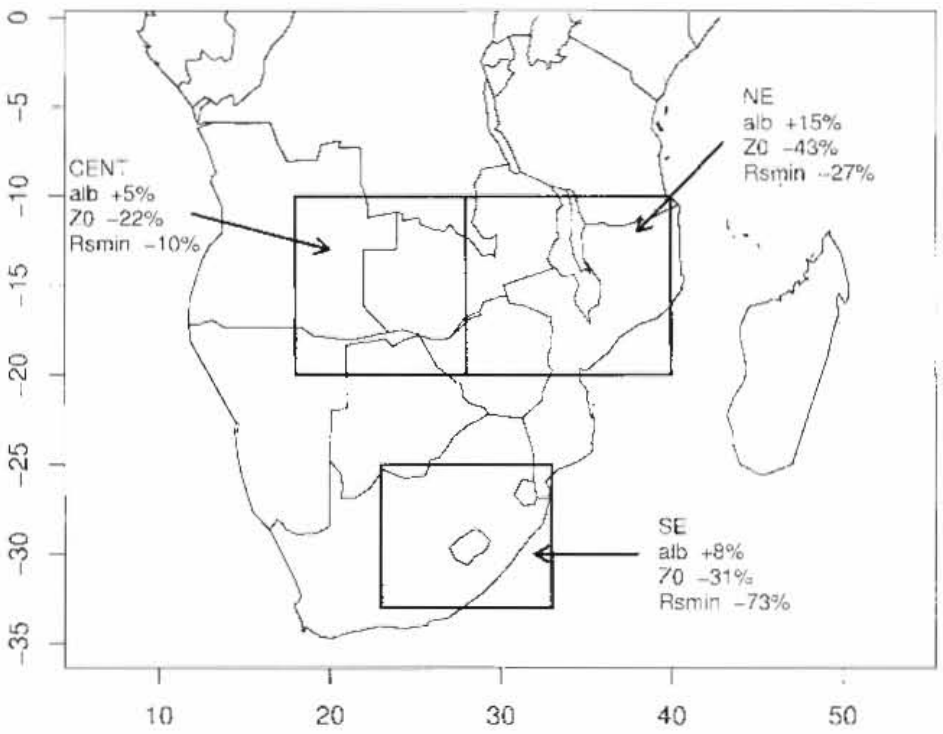

Figure 4.7: Regions selected for analysis, with corresponding changes in albedo (alb), roughness length (Z0) and minimum stomatal resistance (Rsmin).

4.3.2 Land-surface response

Having discussed the simulated time periods with respect to their dominant synoptic features, we now evaluate the atmospheric response to vegetation change under prevailing conditions described by each of these synoptic types. The mean difference of simulated MM5 fields using the current land surface, and MM5 fields using the natural land surface are computed for each SOM node. Since the SOM classification is performed for the atmospheric boundary forcing, rather than the MM5 output, the nodes represent the same days simulated by MM5 for both the natural and present-day vegetation. Three regions have been selected to best illustrate these differences, two being situated in the tropics and one in the sub-tropics. Each location is characterized by spatially coherent responses in surface variables such as 2 m temperature (not

shown). Their names and locations are defined as: CENT (10 – 20 °S, 18 – 28 °E), NE (10 – 20 °S, 28 – 40 °E) and SE (25 – 33 °S, 23 – 33 °E). The regions, as well as their corresponding average changes in albedo, roughness length (Z_0) and minimal stomatal resistance (R_{SMIN}) are shown in Figure 4.7. These three parameters have implications for radiative and turbulent fluxes at the surface (albedo and Z_0, respectively), and canopy transpiration (R_{SMIN}) and are referred to in the discussion on energy budgets below.

Anomalies of temperature at 2 m above the surface (T2m) averaged for each node are shown in Figure 4.8a. As a measure of the relative strength of the anomalies, a signal-to-noise ratio (SNR) has been computed as the absolute mean anomaly divided by the standard deviation of the anomalies for each node and region (Figure 4.8b). In region CENT, the nodes in the left-hand column of the SOM array show clear negative responses of greater than 0.5 °C in magnitude. The SNR shows the signal to be only just greater in magnitude than the noise component (i.e. SNR just over 1). For the other nodes the signal over this region is weak. The NE region also indicates a higher response within nodes on the left of the array, with differences approaching -1 °C and SNR close to 3. The signal weakens considerably towards the right of the array. Dry and stable conditions typical of winter and spring are therefore associated with the strongest response of T2m to changes in vegetation in these two regions. In contrast, the SE region has a relatively uniform negative response for all nodes, mostly between -0.4 and -0.6 °C, but less than -0.6 °C for nodes [2,2], [3,2] and [3,1]. SNR for these nodes is approximately 1.5. SE therefore exhibits the strongest response under conditions of high atmospheric moisture which typically occur during late summer.

The weakest response of precipitation to the vegetation changes (Figure 4.9a) occurs for the dry, stable synoptic states on the left-hand side of the SOM. As the nodes become representative of wetter conditions occurring later in the season, the precipitation changes increase in magnitude. Region NE displays the greatest variation in magnitude across the SOM, ranging from no change in the left-hand column to decreases of over 1.5 mm day^{-1} in the right-hand column. SE experiences little change in rainfall. SNR, however, is less than 0.8 for all regions across all nodes; even the large mean decreases seen in region NE on the left of the array are less than half of one standard deviation (Figure 4.9b).

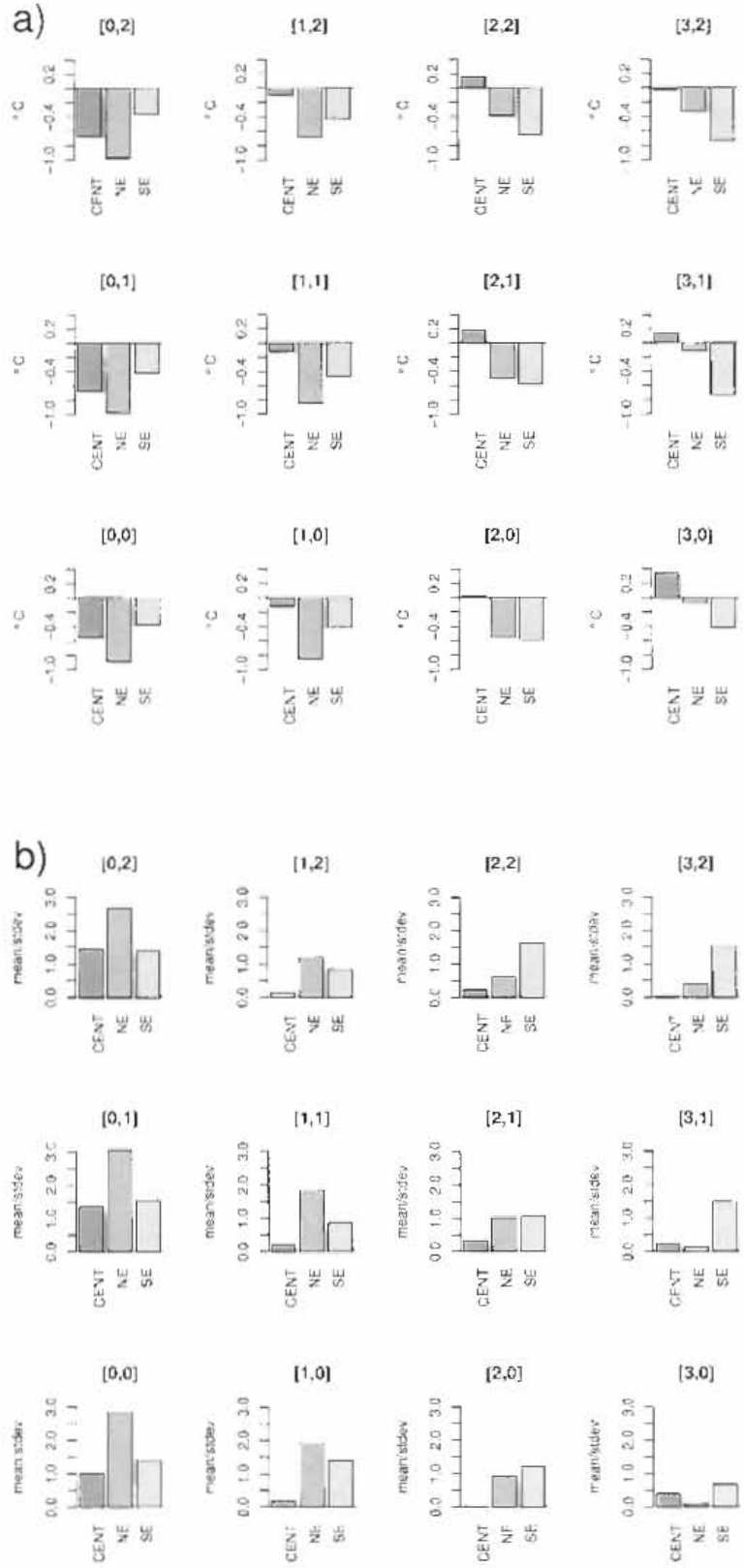

Figure 4.8: Response of 2m temperature (^{o}C) to land surface change under different synoptic forcing. (a) Differences between MM5 run with current land surface and MM5 run with natural land surface mapped to each SOM node, area-averaged for the three selected regions. (b) Signal to noise ratio calculated as absolute mean anomaly divided by standard deviation of anomalies for node.

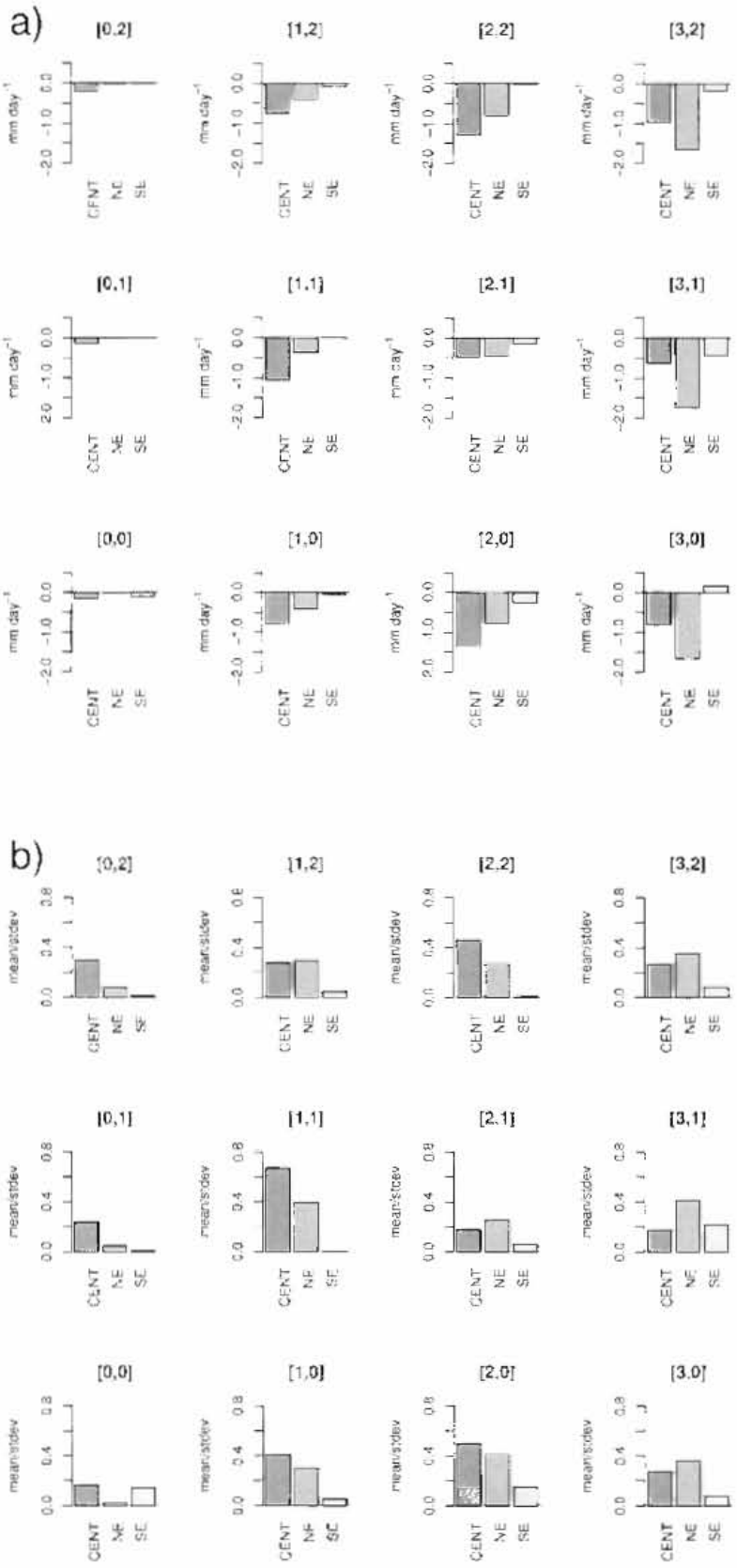

Figure 4.9: As per Figure 4.8, but for precipitation rate (mm day^{-1}).

The effects of the land-surface change on circulation is illustrated by 850 hPa geopotential height (z850) differences for each node (Figure 4.10). Positive anomalies occur in all nodes, but the strength and spatial coherence decreases from left to right across the SOM. This pattern corresponds to that shown by surface temperature in that the largest temperature decreases are associated with the most pronounced increases in z850. Relating these changes to the patterns shown in Figure 4.1 suggest that for the nodes in the left-hand half of the SOM, existing subsidence is enhanced in the south-eastern parts of the continent. The strongest increases in z850, however, occur over the centre of the domain and are therefore likely to cause reduced convergence over much of the subcontinent. The right-hand half of the array, despite experiencing a smaller change in z850, does suggest a weakening of the low pressure centred over southern Angola, which has important implications for moisture transport and precipitation in the sub-tropics. The vertical extent of these circulation anomalies is shown by a cross-section of geopotential height differences, meridionally averaged between 10 and 25 °S (Figure 4.11). The nodes in the left-hand column of the array (representing winter-type conditions), which experience the greatest temperature decreases, show the strongest and most vertically confined height anomaly over the continent. Strong mid-tropospheric subsidence characteristic of winter months confines the anomaly to below 700 hPa. The increases in geopotential height will act to enhance stability in the lower atmosphere. To the right of the SOM, the height anomalies progressively weaken in magnitude, but increase in vertical extent. The decrease in magnitude corresponds to weaker negative T2m anomalies (i.e. less surface cooling). So as synoptic conditions further promote vertical mixing, the surface perturbation extends to higher levels but weakens in magnitude.

4.3.3 Surface energy and moisture balances

The changes in T2m, rainfall and geopotential height are a result of changes in the energy and moisture budgets at the surface. To illustrate how these relate to synoptic conditions we have selected two nodes ([0,2] and [3,0]) that are most dissimilar in terms of both their synoptics and the response of the surface energy balance to the vegetation change. Node [0,2] represents dry conditions with strong anticyclonic circulation in the sub-tropics, whereas node [3,0] is characterized by humid conditions and weak sub-tropical anticyclones. Figures 4.12 and 4.13 show the surface energy

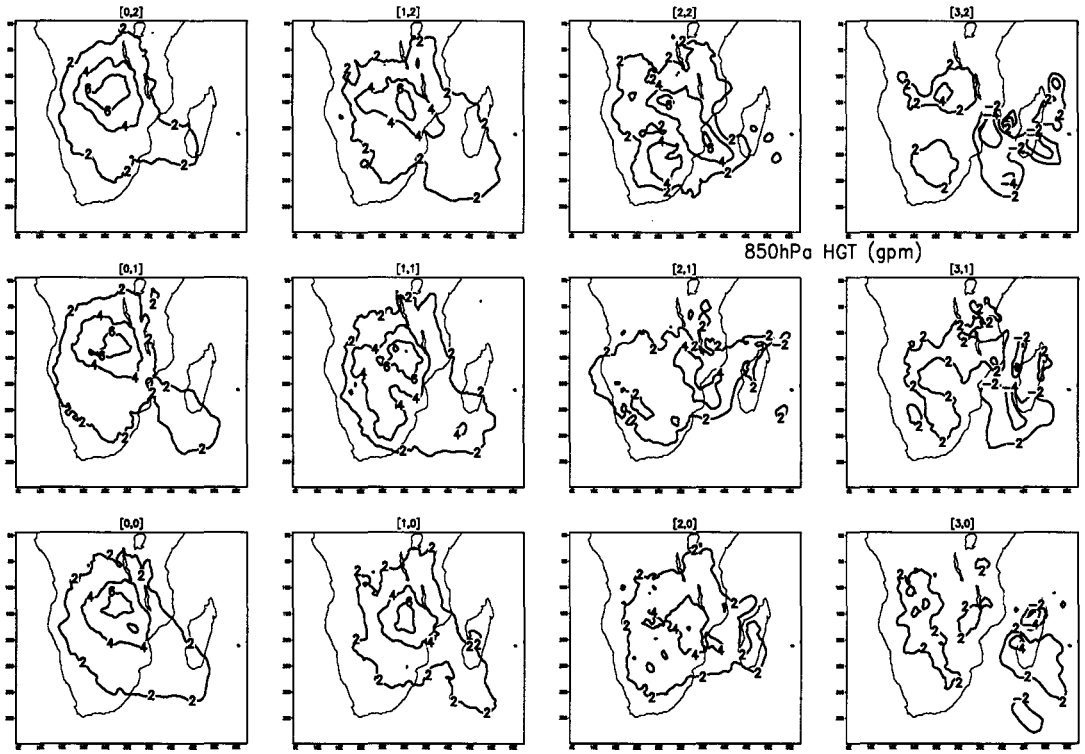

Figure 4.10: Differences, for each node, in MM5-simulated 850 hPa geopotential height between MM5 run with current land surface and MM5 run with natural land surface.

terms for the three regions defined above. Ground heat flux, which is the final component of the surface energy balance, shows negligible change, so is not shown. Hydrological terms are not explicitly illustrated, but are discussed where appropriate.

Of the four radiation terms in node [0,2] (Figure 4.12), the most consistent change is an increase in upward shortwave radiation (SW↑) because of increases in albedo in all three regions. However, net radiation is influenced by changes in the other radiation terms that are small as a percentage, but are of similar magnitude to the increased SW↑. Region CENT experiences a considerable increase in downward shortwave (SW↓), which can be largely attributed to a 6% reduction in cloud liquid water (CLW; not shown). This is in turn primarily due to a 27% increase in vertically integrated moisture flux divergence (MFD; not shown), which is consistent with the strong subsidence anomaly seen in Figures 4.10 and 4.11. The decrease in downward longwave radiation (LW↓) in this region is partly due to reduced atmospheric

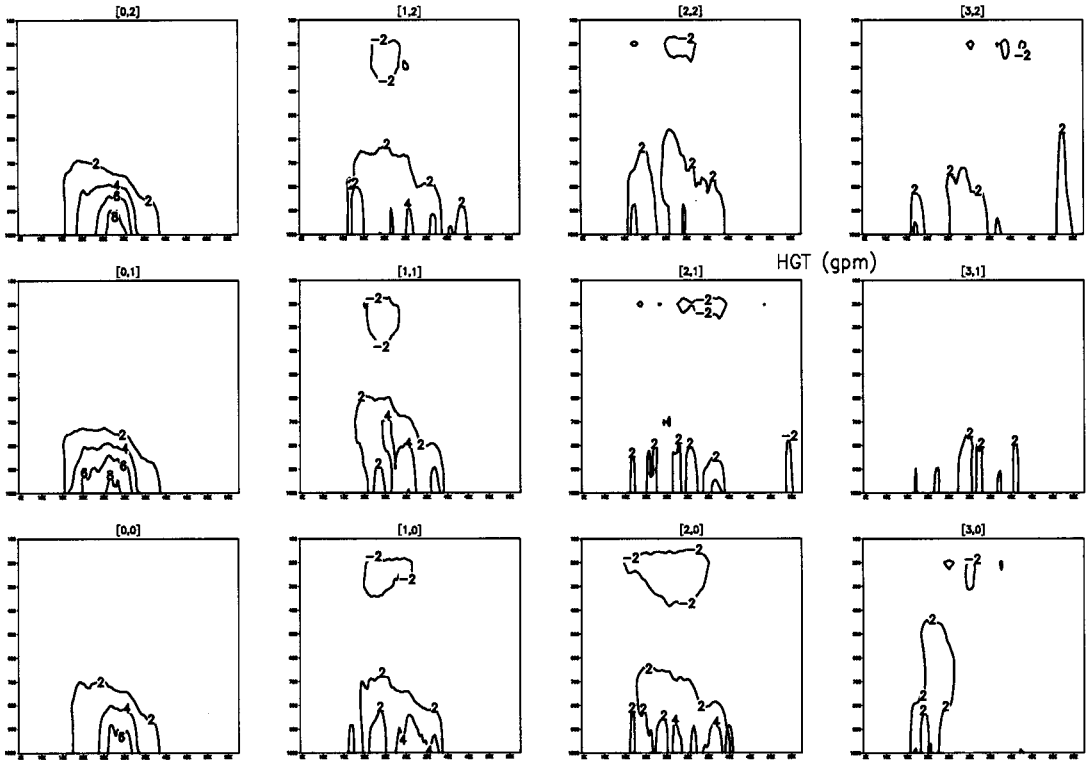

Figure 4.11: Latitudinal profiles of MM5-simulated geopotential height, averaged between 10 and 25 ^{o}S. Values are differences between MM5 run with current land surface and MM5 run with natural land surface. Vertical coordinate is pressure (hPa).

moisture content, but is also linked to cooler temperatures in the lower troposphere (not shown), both of which contribute to reduced atmospheric longwave emission. Although the effect of increased albedo on SW↑ is the primary forcing mechanism on the radiation budget, secondary feedbacks affecting the other radiative terms mask this and net radiation received at the surface consequently increases by a very small amount (<1%). A small precipitation deficit (0.2 mm day^{-1}) results in a small reduction in latent heat (LH) and small increase in sensible heat (SH) fluxes.

Region NE is affected least by changes in atmospheric moisture. CLW increases by <1% and MFD decreases by 3%, which results in a negligible change in SW↓. Differences in LW↓ and outgoing longwave radiation (LW↑) mostly balance, so the decrease in net radiation is primarily due to the increase in reflected solar radiation. This results in a net radiation deficit of nearly 5 W m^{-2}, a negligible change in LH, a

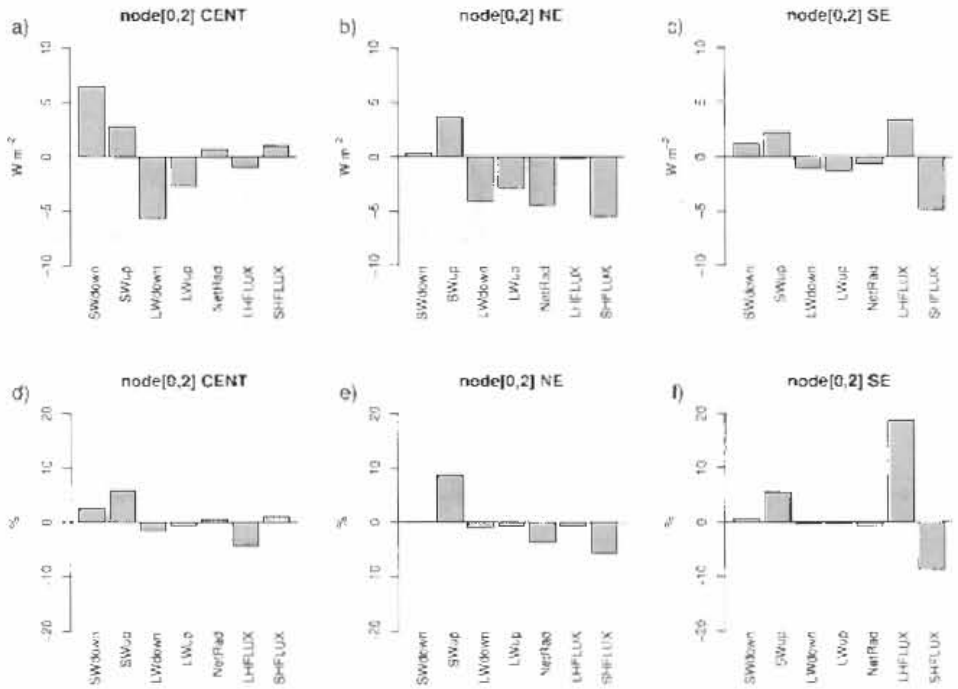

Figure 4.12: Differences in surface energy terms for node [0,2] (MM5: current vegetation minus MM5: natural vegetation). Anomalies in W m^{-2} are shown for regions CENT (a), NE (b) and SE (c). Percentage differences are also shown (d, e and f).

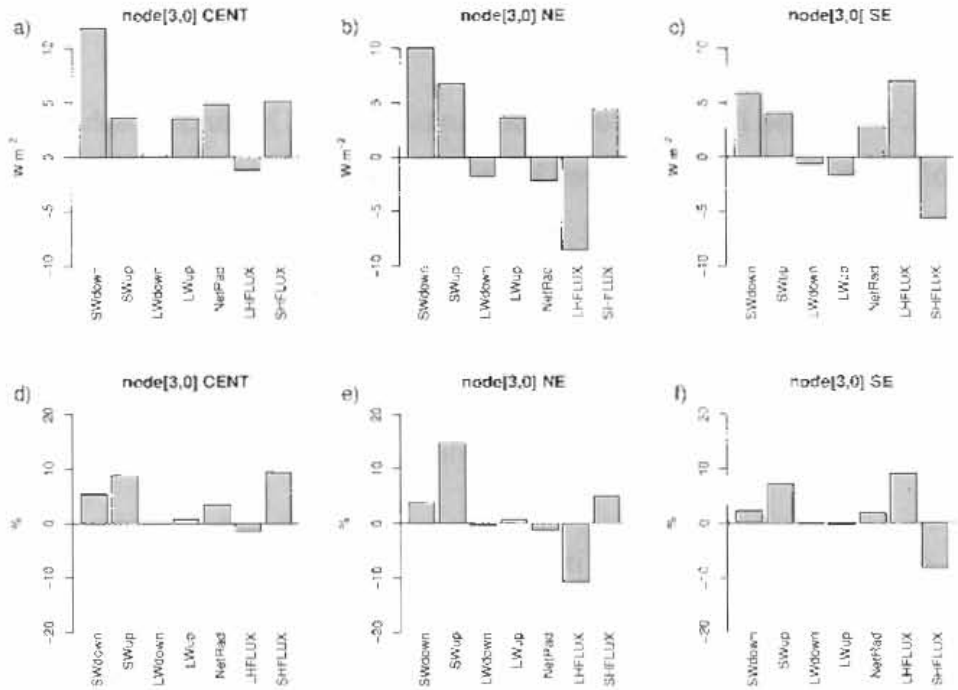

Figure 4.13: As per Figure 4.9, but for node [3,0].

6% reduction in SH and a 1 °C decrease in T2m (see Figure 4.8).

Despite a negligible change in rainfall (Figure 4.9), region SE shows a large increase in LH (19%). This is consistent with the 73% reduction in R_{SMIN} in this region (Figure 4.7), which leads to increased canopy transpiration. Changes in radiative fluxes in this region are small, so control of vegetation on evapotranspiration is of primary importance to the energy budget in this region and under these synoptic conditions.

For node [3,0] (Figure 4.13), SW↑ again increases in all regions as a function of increased albedo, but by a larger amount than is seen for node [0,2]. This is due to greater increases in SW↓ across all regions. In region CENT, SW↓ increases by 12 W m^{-2}, which is caused by a large increase in MFD (15%) resulting in reduced CLW (-18%). This results in a net increase of radiation received at the surface. Although rainfall decreases by 9%, the surplus of energy available for evaporation ensures that LH does not reduce drastically. Furthermore, the 10% reduction in R_{SMIN} in this region allows for enhanced transpiration, which will promote a higher LH. Region NE experiences a 20% reduction in precipitation, but a small decrease in net radiation received at the surface. LH therefore shows an 11% reduction, but the resulting change in T2m is small. Ground temperature (Ts), however, increases by 0.5 °C. This is consistent with the large (43%) reduction in Z_0 for the region, which, by reducing turbulent fluxes, will confine the anomaly to the surface. Region SE shows a similar response to node [0,2]: little change in net radiation and negligible change in rainfall, but a large increase in LH, thus demonstrating the importance of reduced canopy resistance in this region regardless of synoptic forcing.

4.4 Discussion and conclusions

The analysis performed here evaluates the role of synoptic forcing in simulations of climatic response to vegetation change. The method aggregates, according to large-scale circulation regime, the differences between RCM simulations using alternate land-surface maps. The synoptic-based approach has a theoretical advantage over seasonal aggregation as it accounts for unseasonal synoptic features that could influence the mean climate response to land-surface change for that season. The method therefore represents both the seasonal cycle as well as important intra-seasonal variations in large-

scale circulation. The results presented here show the most obvious differences in atmospheric response to land-surface change to be most strongly related to the seasonal cycle, whereas intra-seasonal differences are more subtle.

For the same set of RCM experiments, MS indicate that the average climatic response to the imposed vegetation change in Sep-Nov (SON) is a general cooling over the continent due primarily to the radiative effects of increased surface albedo, which causes increased subsidence in the lower troposphere. This results in reduced moisture convergence over parts of the continent and in Dec-Feb (DJF) some areas of decreased rainfall are evident. The hydrological cycle is thus weakened, which causes a reduction in latent heat flux and hence an increase in surface temperatures. This has a mitigating effect on the cooling seen in SON, and the circulation anomaly associated with increased subsidence is thus weakened. There are therefore two important controlling factors here: 1) the direct effects of land surface change, as manifested by changes in response to parameters such as albedo, Z_0 and R_{SMIN}, and 2) internal hydrological feedbacks that are a secondary effect of the land-surface change and act to mitigate (or possibly enhance) the direct response. The monthly evaluation of MS indicates that the direct effects are more evident in the early part of the summer season, but secondary hydrological feedbacks become more important towards the middle of summer, when atmospheric moisture content and precipitation are at a maximum. This is corroborated by the synoptic evaluation presented here: circulation types prevalent in late winter and spring show the strongest cooling and most pronounced subsidence anomalies in response to increased albedo, while typical mid-summer patterns have the greatest rainfall anomalies and a less coherent temperature and geopotential height response.

The synoptics typical of late winter and early summer are characterized by low atmospheric moisture and widespread subsidence over the continent. Wang *et al.* (1996) indicate that stable atmospheric conditions tend to suppress turbulent heat transfers at the land surface, but Rabin *et al.* (1990) note that clear skies and weak pressure gradients can promote land-atmosphere feedbacks. The conditions referred to in both of these studies are typical of winter-type conditions over sub-tropical southern Africa, so it is not immediately apparent how the climate will respond to land-surface change under such synoptic forcing. The results here show winter-type conditions are, in fact, associated with the greatest changes in near-surface temperature, and

consequently act to strengthen subsidence in the lower troposphere. This is consistent with the observations of Rabin *et al.* (1990) because the temperature decrease is due primarily to the radiative effects of increased albedo, rather than changes in turbulent fluxes. This can be expected, as coupling between land and atmosphere components of the hydrological cycle is strongest during the summer months (Dirmeyer, 2006; Koster *et al.*, 2006). Furthermore, because levels of atmospheric moisture are highest in summer, a small percentage increase in MFD and consequent decrease in cloud cover can be large enough in magnitude to cause enough of an increase in incoming solar radiation to compensate for an albedo-induced radiative loss at the surface.

Regional differences in atmospheric response to land-surface changes are apparent. These are partly due to the specific nature of the imposed vegetation change and its resultant effect on land surface parameters, but will also be dependant on regional climatic regime, as was shown by Findell and Eltahir (2003c). Of the three areas investigated, CENT and NE show more pronounced changes in T2m in winter-type conditions, whereas region SE exhibits a slightly larger temperature change under summer-type conditions. An important factor determining the temperature response in SE is the large reduction in R_{SMIN}, and consequent increase in transpiration. Precipitation shows the opposite response to temperature: synoptics typical of summer experience the greatest rainfall anomalies, but the signal is very noisy. Increases in lower tropospheric geopotential heights and consequent reductions in moisture convergence suggest that reductions in rainfall are the result of circulation changes rather than direct local feedbacks. This is in agreement with previous studies, which have demonstrated increased MFD resulting from increased surface albedo (eg. Charney *et al.*, 1977; Dirmeyer and Shukla, 1994; Maynard and Royer, 2004).

For the three periods considered here, differences in the frequency of occurrence of synoptic states are evident, particularly when comparing the wet (1988/89) and dry (1991/92) years. Given that we have shown temperature, rainfall and circulation to respond differently to land-surface change under different synoptic conditions, it can be inferred that interannual variability in land-atmosphere coupling may result from year-to-year differences in the frequency of synoptic patterns. Findell and Eltahir (2003c) observe significant interannual variability in feedback potential over the contiguous United States, but do not explore in detail the causes of this variability. They do

suggest, however, that interannual shifts in the positioning of dominant large-scale circulation features are an important factor determining regional land-atmosphere coupling. Further insight into this question could be gained from a synoptically-based analysis such as that presented in this paper.

In conclusion, the synoptic-based approach used here presents a useful method for evaluating the results of an RCM experiment that investigates climatic impacts of vegetation change. Notable differences in the response of near-surface temperature, rainfall and geopotential height to the imposed land-surface change are evident between synoptic states, which confirms that large-scale circulation is important in modulating land-atmosphere feedback.

PART V

SYNTHESIS

5.1 Summary

This thesis presents a Regional Climate Model (RCM) study investigating the response of southern Africa's summer climate to changes in land surface conditions. The aims of the study are to:

- evaluate the sensitivity of an RCM to initial soil moisture and consequent hydrological feedbacks;
- produce an estimate of pristine vegetation using a dynamic vegetation model and incorporate this into the RCM;
- compare RCM simulations for the natural vegetation and for present-day vegetation to establish a) whether or not this change in land surface has a noticeable impact on southern Africa's climate and b) if so, what are the dominant mechanisms responsible for this;
- compare atmospheric response to the land-surface change under different synoptic conditions to establish how climate sensitivity to land-surface change differs under different large-scale circulation.

To address these aims the coupled land-atmosphere system over southern Africa is simulated by the MM5 RCM, incorporating the NOAH land-surface model. MM5 is configured for a domain covering sub-equatorial Africa at a horizontal grid resolution of 50 km, and forced at its lateral boundaries by National Centers for Environmental Prediction-National Center for atmospheric Research (NCEP-NCAR) reanalysis data.

Given the important role of soil moisture in modifying near-surface climate and contributing to internal variability in an RCM, MM5 simulations are undertaken to gain insight into how sensitive the model configuration is to perturbations in initial soil moisture. A perturbation in soil moisture of a magnitude and spatial variability that is within the bounds of uncertainty in soil moisture representation for the region is applied to the initial conditions of a series of MM5 simulations. It is found that latent heat fluxes in subsequent months are significantly affected in certain regions, but there is little effect on sensible heat flux and near-surface temperature and no noticeable impact on regional circulation or precipitation. This implies that soil moisture-rainfall coupling

in the model is weak. The persistence of the initial soil moisture anomaly and its associated impacts on surface climate differ according to location, and time of year at initialization, but the anomalies typically dissipate within the first one to two months of the simulations.

The Sheffield Dynamic Global Vegetation Model (SDGVM) is used to simulate potential natural vegetation for southern Africa. Following a spin-up sequence allowing for vegetation structure to reach a stable state, the model is forced with observations of CO_2, temperature, humidity and rainfall and run for a 30-year period to derive a mean vegetation "climatology". In order for this information to be used by MM5, the proportions of plant functional types (PFTs) simulated by SDGVM for each grid point are classified to approximate the natural vegetation classes given by MM5's default land-use map. The latter is the present-day land-use classification of the United States Geological Survey (USGS). A major limitation of SDGVM is that it does not explicitly represent a shrub PFT. This is problematic for the semi-arid regions of the domain.

To simulate the climatic effects of shifting vegetation, two sets of MM5 runs are carried out: one incorporating the simulated natural vegetation as its land-surface map, and one where vegetation is given by the USGS classification. The difference in the two vegetation representations provides a plausible estimate of anthropogenic land-surface alteration. Three 7-month periods are simulated, representing 1 August to 28 February of 1988/89, 1991/92 and 1995/96. These years account for a range of inter-annual variability.

The results show significant changes in surface latent and sensible heat fluxes, and near-surface temperature and humidity. The most prominent feature is widespread cooling over the north-eastern parts of the sub-continent in Sep-Nov (SON), caused primarily by an increase in surface albedo. This is still present in Dec-Feb (DJF), but the pattern is less coherent. The reduced surface temperature results in increased subsidence in the lower troposphere, as indicated by positive geopotential height anomalies over most of the continent, extending upwards to 500 hPa. As the temperature anomaly weakens in DJF, so does the height anomaly. A consequence of the increased subsidence is an increase in horizontal moisture flux divergence. This is not as widespread as the

temperature or height anomalies, but nevertheless results in areas of decreased precipitation, hence promoting a weaker hydrological cycle and reduced latent heat flux. Furthermore, reduced cloud cover acts to increase incident shortwave radiation at the surface. The effect of these two factors is to mitigate the albedo-induced cooling at the surface. The circulation changes induced by the land-surface alteration therefore act as a negative feedback mechanism.

To further analyse the experimental results, a self-organizing map (SOM) is employed to characterize the simulated time periods according to dominant large-scale circulation features. The SOM analysis is performed on the NCEP-NCAR boundary fields used by the RCM. Geopotential height at 850 and 500 hPa and total precipitable water between these levels are the variables selected to define the large-scale circulation. The synoptic types identified show a clear seasonal signal, but also account for some intra-seasonal variability.

Evaluating the results of the MM5 vegetation change simulations under each synoptic type indicates some notable differences. Conditions characterized by strong sub-tropical anticyclones and low atmospheric moisture are most sensitive to changes in radiative fluxes, whereas hydrological processes at the land surface are more sensitive under conditions of weak subsidence and high levels of atmospheric moisture. This corresponds closely to seasonality and emphasises the suggestion given by the seasonal mean analysis that synoptic types prevalent in late winter or spring experience the greatest temperature and geopotential height response, whereas types typical of summer show the greatest rainfall change. There is some variation between types occurring at similar times of year, but these are relatively small.

Considering these findings in the context of the aims of the thesis, it can be concluded that:

- the RCM configuration exhibits weak soil moisture-precipitation coupling and, depending on region, the effects of perturbed soil moisture on near-surface climate generally dissipate within the first one to three months of the simulations;
- the dynamic vegetation model used presents a valid method of representing

natural vegetation, but does not simulate shrub-type vegetation, which is problematic in semi-arid regions;

- the climate of southern Africa is sensitive to a change in vegetation of the magnitude applied in this study, and this change has major implications for both near-surface climate and regional circulation;
- the atmosphere responds differently to land-surface change under different synoptic conditions, with radiative effects being dominant under winter-type conditions, but hydrological effects being more important under summer-type conditions.

5.2 Discussion

The experiments carried out here are a first step towards quantifying the impact of human land-use on southern Africa's climate. As with any modelling study, this work is limited by a number of assumptions and caveats that should be considered when interpreting how the results relate to the real world.

Numerous uncertainties are introduced from the spatial representation of vegetation distribution. Although satellite observations enable the production of global land cover data sets for the present day, different classification algorithms often yield quite different results at regional and local scales. This is illustrated by inconsistencies between the USGS classification and other land-cover products over southern Africa. For example, USGS indicates far more extensive cropland over eastern and south-eastern Africa than the University of Maryland global land cover classification (Hansen *et al.*, 2000), despite being sourced from the same satellite data. The Global International Geosphere-Biosphere Programme land cover classification (Friedl *et al.*, 2002), based on data from the Moderate Resolution Imaging Spectroradiometer, shows even less cropland. It is therefore likely that USGS overestimates the extent of cultivated land over southern Africa. This is a very important consideration as a large portion of the cooling simulated in the vegetation change experiments results from the conversion of forest and savanna to cropland.

Estimation of undisturbed natural vegetation poses further difficulties. Global representations of potential natural vegetation exist (eg. Ramankutty and Foley, 1999), but for this study a mechanistic vegetation model in the form of SDGVM was used. A major shortcoming of SDGVM is that it does not simulate a functional type representative of shrubland. This is problematic for the semi-arid south-western parts of the continent. Furthermore, comparing the model's representation of forests with that of Ramankutty and Foley (1999) shows the latter to be more fragmented, with a less smooth transition between biomes. It is unclear which representation is more realistic, but it is possible that SDGVM does not adequately represent local-scale disturbances such as fire and grazing. Given this, and the overestimation of cropland in the present-day land-use map, the vegetation change applied in this experiment is therefore likely to be greater than the true extent of anthropogenic influences.

Inter-model variability is a major factor influencing the results of land-surface sensitivity studies. A robust method to address this problem is to repeat the same experiment using a selection of different models, or the same model with different combinations of parameterization options, or both. The drawback of this is that is a computationally demanding exercise. Given the hardware resources available for this study, it was decided to utilize a single model configuration that has been shown to adequately simulate the climate of the chosen domain. This does limit the experiment, but the results nevertheless give a physically plausible insight into the land-atmosphere system of southern Africa. Tadross *et al.* (2006) tested the performance of MM5 over southern Africa using different combinations of planetary boundary layer and convective precipitation schemes and found that the Betts-Miller convective scheme overestimated rainfall intensity, but best captured the phase of the diurnal cycle. Using this convection scheme in the present study shows that, for the present-day land surface, the model simulates the spatial distribution of seasonal (SON and DJF) rainfall adequately for the domain, but peak magnitudes, particularly in the tropics, are too high. This is problematic as it may affect the outcome of the vegetation change experiments. A hydrological cycle that is too intense could mask out changes in evaporation and precipitation resulting from the land-surface change that may in fact be significant. The precipitation response indicated by the vegetation change experiments is very noisy, so it is possible that a more conservative parameterization scheme will simulate a more

coherent change in rainfall. However, taking these biases into account and considering the evaluation of Tadross *et al.* (2006), it is felt that the model does an adequate job in simulating the climate of the chosen domain. Furthermore New *et al.* (2003) and Georgescu *et al.* (2003) note that employing different convection schemes did not significantly alter the results of their experiments.

The degree to which the model configuration is sensitive to land-atmosphere coupling is an important consideration. Koster *et al.* (2006) demonstrate considerable variations in how strongly the land and atmosphere components of a number of General Circulation Models are coupled. A model in which this coupling is weak is likely to underestimate the atmosphere's response to land-surface change. No comprehensive evaluation of land-atmosphere coupling in MM5 has been undertaken for the southern African domain, but the present study does provide some insight into this issue. It is found that although perturbed initial soil moisture has a significant impact on subsequent latent and sensible heat fluxes, its effect on near-surface temperature is small and there is no apparent feedback on precipitation. This result implies a weak coupling between surface turbulent heat fluxes and precipitation processes in the model configuration. If this is model-specific, then it can be inferred that the effects of land-surface change on precipitation through local cycling of energy and moisture are underestimated by this experiment. If, however, the weak coupling is indeed a real feature of the land-atmosphere system in southern Africa, this has negative implications for the use of antecedent land-surface moisture as a predictor in seasonal forecasting. In the Southern African Development Community (SADC), collaborative seasonal forecasting efforts currently include both statistical and dynamical models that utilize sea-surface temperature indices and fields as predictors and boundary conditions. To the best knowledge of the author, the incorporation of antecedent land-surface conditions into operational long-range forecasts has not yet been explored for the region.

Although the impacts of altered latent and sensible heat fluxes appear to be small, changes in radiative fluxes have important implications. The strongest signal resulting from the vegetation change is widespread cooling over the continent in early summer, driven by increased surface albedo. The synoptic evaluation confirms that such

radiative effects are strongest under dry and stable conditions typical of late-winter and early summer. This raises the question that if weak soil moisture-rainfall coupling mean that antecedent moisture conditions are unlikely to have a major impact on subsequent rainfall, can variability in the radiative properties of the land surface be used as an alternative predictor for seasonal forecasts? An unusually dry antecedent land surface will be manifested not only by low soil moisture, but also a degraded vegetation state associated with late green-up. This will be characterized by above-average albedo, which, as has been shown in this and other studies, can result in surface cooling, increased subsidence, decreased moisture convergence and reduced rainfall. The implications of this in early summer could be a delayed onset of the summer rainfall season, which will have a critical impact on agriculture in southern Africa. The effects of a delayed onset would be further amplified by a persistence of synoptic conditions favourable for the albedo feedback mechanism. Changes in large-scale circulation regimes driven by both inter-annual variability and long term climate change are therefore likely to be key determinants of the extent to which early summer land-atmosphere feedbacks manifest themselves.

5.3 Recommendations

There is much scope for further research into land-atmosphere interactions over southern Africa. Since this study is limited to a single model configuration and has a relatively small temporal coverage, much benefit will be gained from the use of different models and longer, multi-year simulations. Longer simulations will enable further evaluation of the connections between inter-annual synoptic variability and land-atmosphere feedbacks. The use of different models, and a comprehensive evaluation of the strength of land-atmosphere coupling between them, will reduce uncertainties introduced by choice of model.

A more accurate definition of African vegetation classes and their associated structural, physiological and phenological parameters would be a great asset to climate modelling in the region. Not only will this reduce model biases arising from inaccuracies in land-

surface representation, but will also provide a baseline against which to compare estimates of undisturbed vegetation state. The true extent of land-use change can thus be better quantified. The near-surface cooling and reduced precipitation resulting from the simulated vegetation change in this study suggest that land-use change may be an important contributor to climatic trends observed over the past few centuries. This study has not attempted to relate the simulated changes in climate to any historical records, but with a more realistic account of observed land-use change, this would be feasible.

The present study has identified a mechanism through which the land surface can alter regional atmospheric circulation over southern Africa. This has major implications for further understanding of the processes responsible for moisture transport in the region, which has particular relevance for seasonal forecasting and projections of long-term climate change. While the effect of antecedent soil moisture on summer rainfall has previously been identified as potentially important, the results of this study suggest an alternative avenue to explore. The effects of antecedent land-surface albedo could be a critical factor in controlling the onset of summer precipitation. Continuous satellite observations provide measurements of surface albedo and can monitor inter-annual variations in springtime vegetation green-up. There is therefore scope to evaluate the effects the timing of this green-up may have on regional moisture convergence and the timing of rainfall onset.

REFERENCES

Atlas R, Wolfson N, Terry J. 1993. The effect of SST and soil moisture anomalies on GLA model simulations of the 1988 U.S. summer drought *Journal of Climate*, 6(11): 2034-2048.

Baidya Roy S, Hurtt GC, Weaver CP, Pacala SW. 2003. Impact of historical land cover change on the July climate of the United States. *Journal of Geophysical Research* 108(D24): 4793.

Betts AK, Miller MJ. 1993. The Betts-Miller scheme. Chapter in *The representation of cumulus convection in numerical models of the atmosphere*. Eds. Emanuel KA, Raymond DJ. American Meteorological Society.

Bonan GB. 1997. Effects of land use on the climate of the United States. *Climatic Change* 37: 449-486.

Cavazos T. 1999. Large-scale circulation anomalies conducive to extreme precipitation events and derivation of daily rainfall in northeastern Mexico and southeastern Texas. *Journal of Climate* 12: 1506-1523.

Cavazos T. 2000. Using self-organizing maps to investigate extreme climate events: an application to wintertime precipitation in the Balkans. *Journal of Climate* 13: 1718-1732.

Cavazos T, Comrie AC, Liverman DM. 2002: Intraseasonal variability associated with wet monsoons in southeast Arizona. *Journal of Climate* 15: 2477-2490.

Caya D, Biner S. 2004. Internal variability of RCM simulations over an annual cycle. *Climate Dynamics* 22: 33-46.

Charney JG. 1975. Dynamics of deserts and drought in the Sahel. *Quarterly Journal of the Royal Meteorological Society* 101: 193-202.

Charney JG, Quirk WJ, Chow S, Kornfield J. 1977. A comparative study of the effects of albedo change on drought in semi-arid regions. *Journal of the Atmospheric Sciences* 34: 1366-1385.

Chen F, Avissar R. 1994. Impact of land-surface moisture variability on local shallow convective cumulus ans precipitation in large-scale models. *Journal of applied Meteorology* 33: 1382-1401.

Chen F, Dudhia J. 2001a. Coupling an advanced land surface-hydrology model with the Penn State-NCAR MM5 modeling system. Part I: Model implementation and

sensitivity. *Monthly Weather Review* 129: 569-585.

Chen F, Dudhia J. 2001b. Coupling an advanced land surface-hydrology model with the Penn State-NCAR MM5 modeling system. Part II: Preliminary model validation. *Monthly Weather Review* 129: 587-604.

Christensen OB, Gaertner MA, Prego JA, Polcher J. 2001. Internal variability of regional climate models. *Climate Dynamics* 17: 875-887.

Claussen M. 1997. Modelling bio-geophysical feedback in the African and Indian monsoon region. *Climate Dynamics* 13: 247-257.

Cook BI, Bonan GB, Levis S. 2006. Soil moisture feedbacks to precipitation in southern Africa. *Journal of Climate* 19: 4198-4206.

Copeland JH, Pielke RA, Kittel TGF. 1996. Potential climatic impacts of vegetation change: A regional modeling study. *Journal of Geophysical Research* 101(D3): 7409-7418.

Crane RG, Hewitson BC. 2003. Clustering and upscaling of station precipitation records to regional patterns using self-organizing maps (SOMs). *Climate Research* 25: 95-107.

Dickinson RE, Henderson-Sellers A. 1988. Modeling tropical deforestation: A study of GCM land-surface parameterizations. *Quarterly Journal of the Royal Meteorological Society* 114: 439-462.

Dirmeyer PA. 2005. Land surface contribution to the potential predictability of boreal summer season climate. *Journal of Hydrometeorology* 6: 618-632.

Dirmeyer PA. 2006. The hydrologic feedback pathway for land-climate coupling. *Journal of Hydrometeorology* 7: 857-867.

Dirmeyer PA, Shukla J. 1994. Albedo as a modulator of climate response to tropical deforestation. *Journal of Geophysical Research* 99(D10): 20,863-20,877.

Douville H, Chauvin F, Broqua H. 2001. Influence of soil moisture on the Asian and African monsoons. Part I: Mean monsoon and daily precipitation. *Journal of Climate* 14: 2381-2403.

Eltahir EAB. 1998. A soil moisture-rainfall feedback mechanism 1. Theory and observations. *Water Resources Research* 34(4): 765-776.

Ferranti L, Viterbo P. 2006. The European summer of 2003: Sensitivity to soil water initial conditions. *Journal of Climate* 19: 3659-3680.

Findell K, Eltahir EAB. 1997. An analysis of the soil moisture-rainfall feedback, based on direct observations from Illinois. *Water Resources Research* 33(4): 725-735.

Findell KL, Eltahir EAB. 2003a. Atmospheric controls on soil moisture-boundary layer interactions. Part I: Framework development. *Journal of Hydrometeorology* 4: 552-569.

Findell KL, Eltahir EAB. 2003b. Atmospheric controls on soil moisture-boundary layer interactions: Three-dimensional wind effects. *Journal of Geophysical Research* 108(D8): 8385.

Findell KL, Eltahir EAB. 2003c. Atmospheric controls on soil moisture-boundary layer interactions. Part II: Feedbacks within the continental United States. *Journal of Hydrometeorology* 4: 570-583.

Fischer EM, Seneviratne SI, Vidale PL, Lüthi D, Schär C. 2007. Soil moisture-atmosphere interactions during the 2003 European summer heatwave. *Journal of Climate* 20: 5081-5099.

Friedl MA, McIver DK, Hodges JCF, Zhang XY, Muchoney D, Strahler AH, Woodcock CE, Gopal S, Schneider A, Cooper A, Baccini A, Gao F, Schaaf C. 2002. Global land cover mapping from MODIS: Algorithms and early results. *Remote Sensing of Environment* 83(1-2): 287-302.

Fuller DO, Ottke C. 2002. Land cover, rainfall and land-surface albedo in west Africa. *Climatic Change* 54: 181-204.

Georgescu M, Weaver CP, Avissar R, Walko RL, Miguez-Macho G. 2003. Sensitivity of model-simulated summertime precipitation over the Mississippi River Basin to the spatial distribution of soil moisture. *Journal of Geophysical Research* 108(D22): 8855.

Giorgi F, Bi X. 2000. A study of internal variability of a regional climate model. *Journal of Geophysical Research* 105(D24): 29,503-29,521.

Giorgi F, Mearns LO, Shields C, Mayer L. 1996. A regional model study of the importance of local versus remote controls of the 1988 drought and the 1993 flood over the central United States. *Journal of Climate* 9: 1150-1162.

Grell GA, Dudhia J, Stauffer DR. 1994. A description of the fifth-generation Penn State/NCAR Mesoscale Model (MM5). NCAR Technical Note NCAR/TN-3981STR, 117 pp.

Guo Z & 25 co-authors. 2006. GLACE: The Global Land–Atmosphere Coupling Experiment. Part II: Analysis. *Journal of Hydrometeorology* 7: 611-625.

Gutiérrez JM, Cano R, Cofiño AS, Sordo C. 2005. Analysis and downscaling multi-model seasonal forecasts in Peru using self-organizing maps. *Tellus* 57A: 435-

447.

Gutman G, Ignatov A. 1998. The derivation of the green vegetation fraction from NOAA/AVHRR data for use in numerical weather prediction models. *International Journal of Remote Sensing* 19: 1533–1543.

Hahmann AN, Dickinson RE. 1997. RCCM2-BATS model over tropical South America: applications to tropical deforestation. *Journal of Climate* 10: 1944-1964.

Hewitson BC, Crane RG. 2002. Self-organizing maps: applications to synoptic climatology. *Climate Research* 22: 13-26.

Hewtson BC, Crane RG. 2006. Consensus between GCM climate change projections with empirical downscaling: precipitation downscaling over South Africa. *International Journal of Climatology* 26(10): 1315-1337.

Hansen MC, DeFries RS, Townshend JRG, Sohlberg R. 2000. Global land cover classification at 1km spatial resolution using a classification tree approach. *International Journal of Remote Sensing* 21: 1331-1364.

Hoffmann WA, Jackson RB. 2000. Vegetation-climate feedbacks in the conversion of tropical savanna to grassland. *Journal of Climate* 13: 1593-1602.

Holton JR. 2004. *An introduction to dynamic meteorology, fourth edition*. Elsevier Academic Press. 535pp.

Hong S-Y, Kalnay E. 2000. Role of sea surface temperature and soil-moisture feedback in the 1998 Oklahoma-Texas drought. *Nature* 408: 842-844.

Hong S-Y, Pan H-L. 1996. Nonlocal boundary layer vertical diffusion in a medium-range forecast model. *Monthly Weather Review* 124: 2322-2339.

Kalnay E & 21 co-authors. 1996. The NCEP/NCAR 40-year reanalysis project. *Bulletin of the American Meteorological Society* 77(3): 437–471.

Kanae S, Hirabayashi Y, Yamada T, Oki T. 2006. Influence of "realistic" land surface wetness on predictability of seasonal precipitation in boreal summer. *Journal of Climate* 19: 1450-1460.

Kim Y, Wang G. 2007. Impact of initial soil moisture anomalies on subsequent precipitation over North America in the coupled land-atmosphere model CAM3-CLM3. *Journal of Hydrometeorology* 8:513-533.

Kohonen T. 1995. *Self-organizing maps*. Vol. 30, Springer series in Information Sciences. Springer-Verlag, 362 pp.

Kohonen T, Hynninen J, Kangas J, Laaksonen J. 1996. SOM_PAK: The self-organizing map program package. Report A31, Laboratory of Computer and Information

Science, Helsinki University of Technology, 24 pp.

Koster RD & 25 co-authors. 2006. GLACE: The Global Land–Atmosphere Coupling Experiment. Part I: Overview. *Journal of Hydrometeorology* 7: 590-610.

Koster RD, Suarez MJ. 2003. Impact of Land Surface Initialization on Seasonal Precipitation and Temperature Prediction. *Journal of Hydrometeorology* 4: 408–423.

Laval K, Picon L. 1986. Effect of a change of the surface albedo of the Sahel on climate. *Journal of the Atmospheric Sciences* 43(21): 2418-2429.

Lean J, Rowntree P. 1993. A GCM simulation of the impact of Amazonian deforestation on climate using an improved canopy representation. *Quarterly Journal of the Royal Meteorological Society* 119: 509-530.

Lean J, Warrilow DA. 1989. Simulation of the regional climatic impact of Amazon deforestation. *Nature* 342: 411-413.

MacKellar NC, Tadross MA, Hewitson BC. Simulated effects of anthropogenic vegetation change on southern Africa's summer climate. Submitted to *International Journal of Climatology.*

Main JPL. 1997. Seasonality of circulation in southern Africa using the Kohonen self organizing map. MSc thesis, University of Cape Town, 84 pp.

Malgrem BA, Winter A. 1999. Climate zonation in Puerto Rico based on principal components analysis and an artificial neural network. *Journal of Climate* 12: 977-985.

Marshall CH, Pielke, RA, Steyaert LT, Willard DA. 2004. The impact of anthropogenic land-cover change on the Florida Peninsula sea breezes and warm season sensible weather. *Monthly Weather Review* 132: 28-52.

Matsui T, Lakshmi V, Small E. 2005. The effects of satellite-derived vegetation cover variability on simulated land–atmosphere interactions in the NAMS. *Journal of Climate* 18: 21-40.

Maynard K, Royer J-F. 2004a. Effects of "realistic" land-cover change on a greenhouse-warmed African climate. *Climate Dynamics* 22: 343-358.

Maynard K, Royer J-F. 2004b. Sensitivity of a general circulation model to land surface parameters in African tropical deforestation experiments. *Climate Dynamics* 22: 555-572.

Meehl GA. 1994. Influence of the land surface in the Asian summer monsoon: external conditions versus internal feedbacks. *Journal of Climate* 7: 1033-1049.

Narisma GT, Pitman AJ. 2003. The impact of 200 years of land-cover change on the Australian near-surface climate. *Journal of Hydrometeorology* 4: 424-436.

Narisma GT, Pitman AJ, Eastman J, Watterson IG, Pielke R Sr, Beltrán-Prezekurat A. 2003. The role of biospheric feedbacks in the simulation of the impact of historical land cover change on the Australian January climate. *Geophysical Research Letters* 30(22): 2168.

New MG, Hulme M, Jones PD. 1999. Representing twentieth century space-time climate variability. Part I: Development of a 1961-1990 mean monthly terrestrial climatology. *Journal of Climate* 12: 829-856.

New MG, Hulme M, Jones PD. 2000: Representing twentieth century space-time climate variability. Part II: development of 1901-96 monthly grids of terrestrial surface climate. *Journal of Climate* 13: 2217-2238.

New M, Washington R, Jack C, Hewitson B. 2003. Sensitivity of southern African climate to soil moisture, *Clivar Exchanges* 27, 45-47.

Nobre C, Sellers P, Shukla J. 1991. Amazonian deforestation and the regional climate change. *Journal of Climate* 4: 957-988.

Paegle J, Mo KC, Noguéz-Peagle J. 1996. Dependence of simulated precipitation on surface evaporation during the 1993 United States summer floods. *Monthly Weather Review* 124: 345-361.

Pal JS, Eltahir EAB. 2001. Pathways relating soil moisture conditions to future summer rainfall within a model of the land-atmosphere system. *Journal of Climate* 14: 1227-1242.

Pan Z, Takle E, Segal M, Aritt R. 1999. Simulation of potential impacts of man -made land use changes on U.S. summer climate under various synoptic regimes. *Journal of Geophysical Research* 104: 6515 – 6528.

Pielke R. 2001. Influence of the spatial distribution of vegetation and soils on the prediction of cumulus convective rainfall. *Reviews of Geophysics* 39: 151-177.

Pielke RA, Zeng X. 1989. Influence on severe storm development of irrigated land. *National Weather Digest* 14: 16-17.

Pitman AJ, Durbidge TB, Henderson-Sellers A, McGuffie K. 1993. Assessing climate model sensitivity to prescribed deforested landscapes. *International Journal of Climatology* 13: 879-898.

Polcher J, Laval K. 1994. The impact of African and Amazonian deforestation on tropical climate. *Journal of Hydrology* 155: 389-405.

Rabin RM, Stadler S, Wetzel P, Stensrud DJ, Gregory M. 1990. Observed effects of landscape variability on convective clouds. *Bulletin of the American Meteorological Society* 71: 272-280.

Ramankutty N, Foley JA. 1999. Estimating historical changes in global land cover: croplands from 1700 to 1992. *Global Biogeochemical Cycles* 13: 997-1027.

Reusch DB, Alley RB, Hewitson BC. 2005. Relative performance of self-organizing maps and principle component analysis in pattern extraction from synthetic climatological data. *Polar Geography* 29: 188-212.

Rind D. 1982. The influence of ground moisture conditions in North America on summer climate as modeled in the GISS GCM. *Monthly Weather Review* 110: 1487-1494.

Ringrose S, Matheson W, Vanderpost C. 1998. Analysis of soil organic carbon and vegetation cover trends along the Botswana Kalahari Transect. *Journal of Arid Environments* 38: 379–396.

Schär C, Lüthi D, Beyerle U, Heise E. 1999. The soil-precipitation feedback: a process study with a regional climate model. *Journal of Climate*, 12: 722-741.

Semazzi FHM, Song Y. 2001. A GCM study of climate change induced by deforestation in Africa. *Climate Research* 17: 93-103.

Seneviratne SI, Lüthi D, Litschi M, Schär C. 2006. Land-atmosphere coupling and climate change in Europe. *Nature* 443: 205-209.

Shukla J, Mintz Y. 1982. Influence of land-surface evapotranspiration on the earth's climate. *Science* 215(4539): 1498-1501.

Shukla J, Nobre C, Sellers P. 1990. Amazon deforestation and climate change. *Science* 247(4948): 1322-1325.

Sud Y-C, Fennessey M. 1982. A study of the influence of surface albedo and July circulation in semi-arid regions, using the GLAS GCM. *Journal of Climatology* 2: 105–125.

Tadross MA, Gutowski WJ, Hewitson BC, Jack C, New M. 2006. MM5 simulations of interannual change and the diurnal cycle of southern African regional climate. *Theoretical and Applied Climatology* 86: 63-80.

Taylor CM, Saïd F, Lebel T. 1997. Interactions between the land surface and mesoscale rainfall variability during the HAPEX-Sahel. *Monthly Weather Review* 125: 2211-2227.

Taylor CM, Lambin EF, Stephenne N, Harding RJ, Essery RLH. 2002. The influence of

land use change on climate in the Sahel. *Journal of Climate* 15: 3615-3629.

Tennant WJ, Hewitson BC. 2002. Intra-seasonal rainfall characteristics and their importance to the seasonal prediction problem. *International Journal of Climatology* 22: 1033-1048.

Tennant WJ, Reason CJ. 2005. Associations between the global energy cycle and regional rainfall in South Africa and Southwest Australia. *Journal of Climate* 18: 3032-3047.

Thomas DSG, Twyman C, Osbahr H, Hewitson BC. 2007. Adaptation to climate change and variability: farmer responses to intra-seasonal precipitation trends in South Africa. *Climatic Change* 83: 301-322.

Tyson PD. 1987. *Climatic change and variability over southern Africa.* Oxford University Press, Cape Town 220pp.

Van Heerden J, Taljaard JJ. 1998. Africa and surrounding waters. Chapter 3D in *Meteorology of the Southern Hemisphere.* American Meteorological Society, Boston. 410pp.

Voloire A, Royer JF. 2004. Tropical deforestation and climate variability. *Climate Dynamics* 22: 857-874.

Wang G, Eltahir EAB. 2000a. Biosphere-atmosphere interactions over West Africa. I: Development and validation of a coupled dynamic model. *Quarterly Journal of the Royal Meteorological Society* 126: 1239-1260.

Wang G, Eltahir EAB. 2000b. Biosphere-atmosphere interactions over West Africa. I: Multiple climate equilibria. *Quarterly Journal of the Royal Meteorological Society* 126: 1261-1280.

Wang J, Bras RL, Eltahir EAB. 1996. A stochastic linear theory of mesoscale circulation induced by the thermal heterogeneity of the land surface. *Journal of the Atmospheric Sciences* 53(22): 3349-3366.

Weare F, Yalala P. 1971. Provisional vegetation map of Botswana. Botswana Notes and Records, The Botswana Society, Gaborone, Botswana, 3: 131–152.

Weaver CP, Avissar R. 2001. Atmospheric disturbances caused by human modification of the landscape. *Bulletin of the American Meteorological Society* 82(2): 269-281.

Woodward FI, Smith TM, Emanuel WR. 1995. A global land primary productivity and phytogeography model. *Global Biogeochemical Cycles* 9: 471-490.

Woodward FI, Lomas MR. 2004. Vegetation dynamics – simulating responses to climatic change. *Biological Reviews* 79: 643-670.

Xie P, Arkin PA. 1996. Analyses of global monthly precipitation using gauge observations, satellite estimates, and numerical model predictions. *Journal of Climate* 9: 840-858.

Xie P, Arkin PA. 1997. Global Precipitation: A 17-year monthly analysis based on gauge observations, satellite estimates, and numerical model outputs. *Bulletin of the American Meteorological Society* 78: 2539-2558.

Xue Y. 1997. Biosphere feedback on regional climate in tropical north Africa. *Quarterly Journal of the Royal Meteorological Society* 123: 1483-1515.

Xue Y, Shukla J. 1993. The influence on land surface properties on Sahel climate. Part 1: Desertification. *Journal of Climate* 6: 2232-2245.

Yeh T-C, Wetherald RT, Manabe S. 1984. The effect of soil moisture on the short-term climate and hydrology change – a numerical experiment. *Monthly Weather Review* 112: 474-490.

Zeng N, Dickinson RE, Zeng X. 1996. Climatic impact of Amazon deforestation – a mechanistic model study. *Journal of Climate* 9: 859-883.

Zeng N, Neelin JD. 2000. The role of vegetation–climate interaction and inter-annual variability in shaping the African savanna. *Journal of Climate* 13: 2665-2670.

Zwiers FW, Von Storch H. 1995. Taking serial correlation into account in tests of the mean. *Journal of Climate* 8: 336-351.